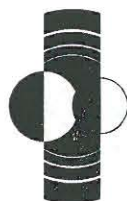


WORKSHOP PROGRAM AND ABSTRACTS



LPI Contribution No. 1213

HEMISPHERES APART: THE ORIGIN AND MODIFICATION OF THE MARTIAN CRUSTAL DICHOTOMY

September 30–October 1, 2004

Houston, Texas

SPONSORED BY

Lunar and Planetary Institute
National Aeronautics and Space Administration

CONVENERS

Thomas R. Watters, *Smithsonian Institution*
Patrick J. McGovern, *Lunar and Planetary Institute*

SCIENTIFIC ORGANIZING COMMITTEE

Herbert V. Frey, *NASA Goddard Space Flight Center*
James W. Head III, *Brown University*
Adrian Lenardic, *Rice University*
George E. McGill, *University of Massachusetts*
Francis Nimmo, *University of California, Los Angeles*
Norman H. Sleep, *Stanford University*
Sean C. Solomon, *Carnegie Institution of Washington*
Kenneth L. Tanaka, *U.S. Geological Survey*

Lunar and Planetary Institute 3600 Bay Area Boulevard Houston TX 77058-1113

LPI Contribution No. 1213

Compiled in 2004 by
LUNAR AND PLANETARY INSTITUTE

The Institute is operated by the Universities Space Research Association under Agreement No. NCC5-679 issued through the Solar System Exploration Division of the National Aeronautics and Space Administration.

Any opinions, findings, and conclusions or recommendations expressed in this volume are those of the author(s) and do not necessarily reflect the views of the National Aeronautics and Space Administration.

Material in this volume may be copied without restraint for library, abstract service, education, or personal research purposes; however, republication of any paper or portion thereof requires the written permission of the authors as well as the appropriate acknowledgment of this publication.

Abstracts in this volume may be cited as

Author A. B. (2004) Title of abstract. In *Workshop on Hemispheres Apart: The Origin and Modification of the Martian Crustal Dichotomy*, p. XX. LPI Contribution No. 1203, Lunar and Planetary Institute, Houston.

This volume is distributed by

ORDER DEPARTMENT
Lunar and Planetary Institute
3600 Bay Area Boulevard
Houston TX 77058-1113, USA
Phone: 281-486-2172
Fax: 281-486-2186
E-mail: order@lpi.usra.edu

Mail order requestors will be invoiced for the cost of shipping and handling.

ISSN No. 0161-5297

PREFACE

This volume contains abstracts that have been accepted for presentation at the Workshop on Hemispheres Apart: The Origin and Modification of the Martian Crustal Dichotomy, September 30–October 1, 2004, Houston, Texas.

Administration and publications support for this meeting were provided by the staff of the Publications and Program Services Department at the Lunar and Planetary Institute.

CONTENTS

Program	1
Geomorphic Analyses of Debris Aprons Along the Martian Dichotomy Boundary, Tempe Terra/Mareotis Fossae Region, Mars <i>F. C. Chuang and D. A. Crown</i>	7
Mars Crustal Dichotomy and World Maps with Constant Scale Natural Boundaries (CSNB) — “A Creative Approach to Visualizing Subtle Points of Geodesy” <i>C. S. Clark</i>	9
A Magnetic Perspective on the Martian Crustal Dichotomy <i>J. E. P. Connerney, M. H. Acuna, N. F. Ness, D. L. Mitchell, R. P. Lin, and H. Reme</i>	11
Ancient Giant Basin/Aquifer System in the Arabia Region, Mars, and Its Influence on the Evolution of the Highland-Lowland Boundary <i>J. M. Dohm, N. G. Barlow, J. P. Williams, J. C. Ferris, H. Miyamoto, V. R. Baker, W. V. Boynton, R. G. Strom, A. Rodríguez, A. G. Fairén, T. M. Hare, R. C. Anderson, J. Keller, and K. Kerry</i>	13
Martian Early Magnetic Field as a Result of Magma Ocean Cumulate Overturn <i>L. T. Elkins-Tanton, S. Zaranek, and E. M. Parmentier</i>	15
Magnetic Anomalies North of the Dichotomy Boundary: Possible Evidence for Dichotomy Retreat? <i>C. I. Fassett and J. W. Head III</i>	17
Impact Constraints on the Age and Origin of the Crustal Dichotomy on Mars <i>H. V. Frey</i>	19
Constraints on Early Mars Evolution and Dichotomy Origin from Relaxation Modeling of Dichotomy Boundary in the Ismenius Region <i>A. Guest and S. E. Smrekar</i>	21
Application of Recent Mission Results to the Origin and Evolution of the Dichotomy <i>J. W. Head III</i>	23
Mars Dichotomy Boundary Degradational Processes: Evidence for Extensive Amazonian Glaciation <i>J. W. Head III, M. C. Agnew, C. I. Fassett, D. R. Marchant, and M. A. Kreslavsky</i>	25
Mars Dichotomy Boundary Degradational Processes: Model of the Noachian-Hesperian Hydrological Cycle <i>J. W. Head III, M. H. Carr, C. I. Fassett, and P. S. Russell</i>	27
Mars Dichotomy Boundary Degradational Processes in Space and Time: Clues to Global Climate Evolution <i>J. W. Head III and C. I. Fassett</i>	29
Crustal Dichotomy Boundary and Fretted Terrain Development at Aeolis Mensae, Mars <i>R. P. Irwin III and T. R. Watters</i>	31

Gravity Modeling of the Isidis/Syrtis Major Region of Mars: Implications for Lithospheric Properties and for the Origin and Evolution of the Dichotomy Boundary <i>W. S. Kiefer</i>	33
The Crustal Dichotomy as a Trigger for Edge Driven Convection: A Possible Mechanism for Tharsis Rise Volcanism? <i>S. D. King and H. L. Redmond</i>	35
Mars and Earth: Two Dichotomies — One Cause <i>G. G. Kochemasov</i>	37
Depth-dependent Rheology and the Wavelength of Mantle Convection with Application to Mars <i>A. Lenardic, M. A. Richards, F. H. Busse, and S. J. S. Morris</i>	39
The Martian Relief's Dichotomy and Planetary Axial Structural Symmetry <i>G. F. Makarenko</i>	41
Crustal Evolution of the Protonilus Mensae Area, Mars <i>G. E. McGill, S. E. Smrekar, A. M. Dimitriou, and C. A. Raymond</i>	42
Loading-induced Stresses and Topography Near the Martian Hemispheric Dichotomy Boundary <i>P. J. McGovern and T. R. Watters</i>	44
Topographic Change of the Dichotomy Boundary Suggested by Crustal Inversion <i>G. A. Neumann</i>	46
Tectonic Consequences of Dichotomy Modification by Lower Crustal Flow and Erosion <i>F. Nimmo</i>	48
Glacial Modification of the Martian Crust in Aeolis Region, Mars <i>J. Nussbaumer</i>	50
Degree-1 Mantle Convection as a Process for Generating the Martian Hemispheric Dichotomy <i>J. H. Roberts and S. Zhong</i>	52
Control of Exposed and Buried Impact Craters and Related Fracture Systems on Hydrogeology, Ground Subsidence/Collapse, and Chaotic Terrain Formation, Mars <i>J. A. P. Rodriguez, S. Sasaki, J. M. Dohm, K. L. Tanaka, H. Miyamoto, V. Baker, J. A. Skinner Jr., G. Komatsu, A. G. Fairén, and J. C. Ferris</i>	54
Outflow Channel Sources, Reactivation and Chaos Formation, Xanthe Terra, Mars <i>J. A. P. Rodriguez, S. Sasaki, J. M. Dohm, K. L. Tanaka, H. Miyamoto, V. Baker, J. A. Skinner Jr., G. Komatsu, A. G. Fairén, and J. C. Ferris</i>	56
Mass-Wasting of the Circum-Utopia Highland/Lowland Boundary: Processes and Controls <i>J. A. Skinner Jr., K. L. Tanaka, T. M. Hare, J. Kargel, G. Neukum, S. C. Werner, and J. A. P. Rodriguez</i>	58
Subsurface Structure of the Ismenius Area and Implications for Evolution of the Martian Dichotomy and Magnetic Field <i>S. E. Smrekar, C. A. Raymond, and G. E. McGill</i>	60

Endogenic Mechanisms for the Formation of the Martian Crustal Dichotomy: Hypotheses and Constraints <i>S. C. Solomon</i>	62
Triggering the End of Plate Tectonics by Forced Climate Changes <i>M. G. Spagnuolo and J. Dohm</i>	64
Mars Impact Energy Analysis in Support of the Origin of the Crustal Dichotomy and Other Anomalies <i>G. R. Spexarth</i>	66
Topographic and Geomorphic Modification History of the Highland/Lowland Dichotomy Boundary of Mars: I. Noachian Period <i>K. L. Tanaka</i>	68
Topographic and Geomorphic Modification History of the Highland/Lowland Dichotomy Boundary of Mars: II. Hesperian and Amazonian Periods <i>K. L. Tanaka</i>	70
Long Wavelength Topography of the Dichotomy Boundary in Northern Terra Cimmeria: Evidence for Flexure of the Southern Highlands <i>T. R. Watters, P. J. McGovern, and R. P. Irwin III</i>	72
Effect of the Dichotomy on Mantle Plume Locations <i>M. J. Wenzel, M. Manga, and A. M. Jellinek</i>	74
On the Dynamic Origin of the Crustal Dichotomy and Its Implications for Early Mars Evolution <i>S. J. Zhong, J. H. Roberts, and A. McNamara</i>	76

PROGRAM

Thursday, September 30, 2004

INTRODUCTION

9:00 a.m. Lecture Hall

Watters T. R. McGovern P. J.
Welcome and Announcements

OVERVIEWS

9:15 a.m. Lecture Hall

**Chairs: T. R. Watters
P. J. McGovern**

- 9:15 a.m. Solomon S. C. *
Endogenic Mechanisms for the Formation of the Martian Crustal Dichotomy: Hypotheses and Constraints [#4024]
- 9:45 a.m. Frey H. V. *
Impact Constraints on the Age and Origin of the Crustal Dichotomy on Mars [#4012]
- 10:15 a.m. Tanaka K. L. *
Topographic and Geomorphic Modification History of the Highland/Lowland Dichotomy Boundary of Mars: I. Noachian Period [#4023]
- 10:30 a.m. Tanaka K. L. *
Topographic and Geomorphic Modification History of the Highland/Lowland Dichotomy Boundary of Mars: II. Hesperian and Amazonian Periods [#4030]
- 10:45 a.m. Head J. W. III*
Application of Recent Mission Results to the Origin and Evolution of the Dichotomy [#4038]
- 11:15 – 11:30 a.m. Break**
- 11:30 a.m. McGovern P. J.
Discussion of Overviews
- 12:00 – 1:30 p.m. Lunch**

Thursday, September 30, 2004 (continued)

EARLY DICHOTOMY

1:30 p.m. Lecture Hall

Chairs: N. H. Sleep
S. C. Solomon

- 1:30 p.m. Connerney J. E. P. * Acuna M. H. Ness N. F. Mitchell D. L. Lin R. P. Reme H.
A Magnetic Perspective on the Martian Crustal Dichotomy [#4005]
- 1:45 p.m. Elkins-Tanton L. T. Zaranek S. Parmentier E. M. *
Martian Early Magnetic Field as a Result of Magma Ocean Cumulate Overturn [#4009]
- 2:00 p.m. Zhong S. J. * Roberts J. H. McNamara A.
On the Dynamic Origin of the Crustal Dichotomy and Its Implications for Early Mars Evolution [#4019]
- 2:15 p.m. Wenzel M. J. * Manga M. Jellinek A. M.
Effect of the Dichotomy on Mantle Plume Locations [#4035]
- 2:30 p.m. King S. D. * Redmond H. L.
The Crustal Dichotomy as a Trigger for Edge Driven Convection: A Possible Mechanism for Tharsis Rise Volcanism? [#4010]
- 2:45 p.m. Lenardic A. * Richards M. A. Busse F. H. Morris S. J. S.
Depth-dependent Rheology and the Wavelength of Mantle Convection with Application to Mars [#4037]
- 3:00 – 3:15 p.m. Break

Thursday, September 30, 2004 (continued)

THINK LOCALLY
3:15 p.m. Lecture Hall

Chairs: G. E. McGill
K. L. Tanaka

- 3:15 p.m. Head J. W. III Carr M. H. Fassett C. I. * Russell P. S.
Mars Dichotomy Boundary Degradational Processes: Model of the Noachian-Hesperian Hydrological Cycle [#4022]
- 3:30 p.m. Head J. W. III Agnew M. C. * Fassett C. I. Marchant D. R. Kreslavsky M. A.
Mars Dichotomy Boundary Degradational Processes: Evidence for Extensive Amazonian Glaciation [#4026]
- 3:45 p.m. Head J. W. III* Fassett C. I.
Mars Dichotomy Boundary Degradational Processes in Space and Time: Clues to Global Climate Evolution [#4027]
- 4:00 p.m. Irwin R. P. III* Watters T. R.
Crustal Dichotomy Boundary and Fretted Terrain Development at Aeolis Mensae, Mars [#4025]
- 4:15 p.m. Rodriguez J. A. P. * Sasaki S. Dohm J. M. Tanaka K. L. Miyamoto H. Baker V.
 Skinner J. A. Jr. Komatsu G. Fairén A. G. Ferris J. C.
Control of Exposed and Buried Impact Craters and Related Fracture Systems on Hydrogeology, Ground Subsidence/Collapse, and Chaotic Terrain Formation, Mars [#4015]
- 4:30 p.m. Dohm J. M. * Barlow N. G. Williams J. P. Ferris J. C. Miyamoto H. Baker V. R.
 Boynton W. V. Strom R. G. Rodríguez A. Fairén A. G. Hare T. M.
 Anderson R. C. Keller J. Kerry K.
Ancient Giant Basin/Aquifer System in the Arabia Region, Mars, and Its Influence on the Evolution of the Highland-Lowland Boundary [#4007]
- 4:45 p.m. Skinner J. A. Jr.* Tanaka K. L. Hare T. M. Kargel J. Neukum G.
 Werner S. C. Rodriguez J. A. P.
Mass-Wasting of the Circum-Utopia Highland/Lowland Boundary: Processes and Controls [#4031]
- 5:00 – 5:15 p.m. Break**
- 5:15 p.m. Solomon S. C.
Discussion
- 5:45 – 8:00 p.m. Dinner Reception and Poster Session**

Thursday, September 30, 2004 (continued)

POSTER SESSION
6:00 – 8:00 p.m. Great Room

Chuang F. C. Crown D. A.

Geomorphic Analyses of Debris Aprons Along the Martian Dichotomy Boundary, Tempe Terra/Mareotis Fossae Region, Mars [#4017]

Clark C. S.

Mars Crustal Dichotomy and World Maps with Constant Scale Natural Boundaries (CSNB) — “A Creative Approach to Visualizing Subtle Points of Geodesy” [#4020]

Fassett C. I. Head J. W. III

Magnetic Anomalies North of the Dichotomy Boundary: Possible Evidence for Dichotomy Retreat? [#4013]

Kochemasov G. G.

Mars and Earth: Two Dichotomies — One Cause [#4004]

Makarenko G. F.

The Martian Relief's Dichotomy and Planetary Axial Structural Symmetry [#4008]

Nussbaumer J.

Glacial Modification of the Martian Crust in Aeolis Region, Mars [#4018]

Roberts J. H. Zhong S.

Degree-1 Mantle Convection as a Process for Generating the Martian Hemispheric Dichotomy [#4028]

Rodriguez J. A. P. Sasaki S. Dohm J. M. Tanaka K. L. Miyamoto H. Baker V. Skinner J. A. Jr.
Komatsu G. Fairén A. G. Ferris J. C.

Outflow Channel Sources, Reactivation and Chaos Formation, Xanthe Terra, Mars [#4016]

Spagnuolo M. G. Dohm J.

Triggering the End of Plate Tectonics by Forced Climate Changes [#4001]

Spexarth G. R.

Mars Impact Energy Analysis in Support of the Origin of the Crustal Dichotomy and Other Anomalies [#4002]

Friday, October 1, 2004

NUMERICAL MODELING

9:00 a.m. Lecture Hall

Chairs: J. W. Head III

H. V. Frey

- 9:00 a.m. McGill G. E. * Smrekar S. E. Dimitriou A. M. Raymond C. A.
Crustal Evolution of the Protonilus Mensae Area, Mars [#4003]
- 9:15 a.m. Smrekar S. E. * Raymond C. A. McGill G. E.
Subsurface Structure of the Ismenius Area and Implications for Evolution of the Martian Dichotomy and Magnetic Field [#4021]
- 9:30 a.m. Guest A. * Smrekar S. E.
Constraints on Early Mars Evolution and Dichotomy Origin from Relaxation Modeling of Dichotomy Boundary in the Ismenius Region [#4036]
- 9:45 a.m. Nimmo F. *
Tectonic Consequences of Dichotomy Modification by Lower Crustal Flow and Erosion [#4006]
- 10:00 a.m. McGovern P. J. * Watters T. R.
Loading-induced Stresses and Topography Near the Martian Hemispheric Dichotomy Boundary [#4034]
- 10:15 a.m. Watters T. R. * McGovern P. J. Irwin R. P. III
Long Wavelength Topography of the Dichotomy Boundary in Northern Terra Cimmeria: Evidence for Flexure of the Southern Highlands [#4032]
- 10:30 a.m. Kiefer W. S. *
Gravity Modeling of the Isidis/Syrtis Major Region of Mars: Implications for Lithospheric Properties and for the Origin and Evolution of the Dichotomy Boundary [#4029]
- 10:45 a.m. Neumann G. A. *
Topographic Change of the Dichotomy Boundary Suggested by Crustal Inversion [#4033]
- 11:00 – 11:15 a.m. Break**
- 11:15 p.m. Nimmo F.
Discussion

PANEL DISCUSSION

11:30 – 12:45 p.m. Lecture Hall

Panelists: Lenardic A. Sleep N. H. Tanaka K. L. Watters T. R.

12:45 p.m. Meeting Adjourns

GEOMORPHIC ANALYSES OF DEBRIS APRONS ALONG THE MARTIAN DICHOTOMY BOUNDARY, TEMPE TERRA/MAREOTIS FOSSAE REGION, MARS. F. C. Chuang and D. A. Crown, Planetary Science Institute, 1700 E. Fort Lowell Rd., Suite 106, Tucson, AZ 85719-2395 (e-mail: chuang@psi.edu).

Introduction. Geomorphic indicators of sub-surface ice on Mars are currently the subject of intense study in the planetary community [1,2,3,4,5]. Lobate debris aprons, thick accumulations of mass-wasted material with lobate fronts, along with lineated valley fill and concentric crater fill, were first identified in regions of Martian fretted terrain along the highland-lowland boundary [6,7]. Squyres and others [6-8] postulated that features of this suite were saturated with ice and moved downslope by creep. Globally, debris aprons are found poleward of 30° N and 30° S latitude with several regions having high concentrations of these features [8]. The abundance of debris aprons along portions of the dichotomy boundary provide important clues about the types of geologic materials present in the region and the role that volatiles play in the modification of the boundary over time.

In this study, we use the abundance of new Mars orbital data to assess the geomorphic and geologic characteristics of debris aprons in the Tempe Terra/Mareotis Fossae region of Mars (43-55°N, 274-294°E). Comparison of apron populations from different parts of Mars will allow us to evaluate regional geologic controls and potential climatic differences on apron development.

Data and Methods. Viking, Mars Global Surveyor, and Mars Odyssey mission data were used in our analysis of debris aprons including Viking Orbiter mosaics (256 pxl/deg), gridded MOLA topography (128 pxl/deg), individual MOLA PEDR profiles, MOC narrow-angle images (2-7 m/pxl), THEMIS daytime and nighttime IR images (~100 m/pxl), THEMIS daytime VIS images (~19 m/pxl), THEMIS Brightness Temperature Record images (~100 m/pxl), and gridded TES thermal inertia data (~3 km/pxl). The individual datasets have been imported into ESRI ArcView 8.2 Geographic Information Systems (GIS) software for geo-registration, analysis, and generation of map products.

Regional Geology, Debris Aprons, and the Tempe/Mareotis Population. The Tempe/Mareotis study area lies along the dichotomy boundary with features typical of Martian fretted terrain [9]. Relief along the Tempe/Mareotis boundary reaches 4 km in places, particularly along escarpments to the north and northwest. The region is geologically diverse with abundant volcanic and tectonic features [10,11]. This activity, along with the possible existence of an ancient

northern ocean [12,13], has resulted in the deposition of many different types of material along the dichotomy boundary. A synopsis of the Tempe/Mareotis geologic history is provided in [11].

Recent studies of lobate debris aprons have focused on two large populations, eastern Hellas and Deuteronilus Mensae [14,15,16]. Aprons at these two locations have a few similar surface textures, but are different in terms of overall size and distance from their source regions. In contrast, the aprons along the dichotomy boundary at Tempe/Mareotis and Deuteronilus have more common planimetric morphologies, morphometries, and surface textures, suggesting that these two apron populations may have similar emplacement and degradational styles compared to those elsewhere on Mars.

We have identified 65 debris aprons in the Tempe/Mareotis region using MOC, THEMIS, and Viking Orbiter images. They are typically observed as single lobes or a coalesced mass of lobes that have converged below a common source area. These aprons, like those elsewhere on Mars, are commonly found at the base of features with moderate-to-high relief such as isolated or clustered massifs, escarpments, grabens, and the interior walls of craters. The movement of debris away from the source region is generally unconfined with the exception of those within grabens. The aprons do not appear to form below any preferentially pole-facing or equator-facing slopes and are generally tens of meters thick, with a maximum of 250 m.

We have compiled statistics for all of the debris aprons in the Tempe/Mareotis population including planimetric area, maximum volume, slope, relief, and elevation range. When the population was divided into two groups, massif-related and escarpment-related, massif-related aprons were smaller in nearly every statistical category (Table 1). This difference is probably due to the fact that the higher-relief escarpments have greater surface areas from which to contribute material to debris aprons. Massifs are isolated outliers of high-standing material away from the main boundary, but have significantly less relief than escarpments. If massifs are eroded portions of highland material, one would expect these aprons to be of similar size to escarpment-related aprons. However, this is not the case and it suggests that differences in the materials along the boundary may be present.

Apron Surface Textures and Features from MOC. Four distinctive textures are observed on Tempe/Mareotis apron surfaces in narrow-angle MOC images: a) smooth, b) pitted, c) ridge and valley, and d) knobby. The textures are commonly observed along mid-to- lower apron slopes and represent different stages of preservation of the top surface.

Smooth texture. This texture represents the uppermost unmodified apron surface. The smooth surface is generally featureless with a lack of craters and erosional features. Nearly all Tempe/Mareotis aprons contain some exposure of smooth material and in some cases, the entire imaged surface of an apron has this texture.

Pitted texture. This texture is defined by individual semi-circular to elliptically-shaped pits. Smaller pits measure a few meters across, whereas larger pits have dimensions up to 135x70 m. Most pits appear to form in rows across an apron surface and multiple pits may coalesce to form one or more pit chains that can reach up to a few hundred meters in length.

Ridge and valley texture. Adjacent rows of pit chains develop an undulating topographic pattern where the linear to curvilinear depressions are valleys and the remnant materials form ridges. Ridges are generally continuous along their length, but are sometimes segmented in places. From shadow length measurements, ridges have heights of 5-35 m. The spacing between sets of ridges is often 30-90 m.

Knobby texture. The knobby texture is defined by individual or clusters of knobs that are located between low-lying degraded areas. Individual knobs typically have widths from a few tens of meters across to 100 m across. From shadow length measurements, knobs have heights up to 20 m.

Surface features. Geomorphic features observed within low-lying smooth areas include longitudinal cracks, individual and multiple broad ridges circumferential to the bases of scarps and massifs, and circular-to-sub-circular depressions.

Apron Surface Degradation Sequence. The four textures observed on apron surfaces represent different stages of progressive surface degradation. The sequence begins with an unmodified uppermost smooth surface which then develops pits. The pits coalesce to form chains and any remnant high-standing material between the depressions forms ridges. Continued degradation causes the ridges to pinch-off, forming isolated knobs that indicate a textural transition from ridge and valley to knobby. There are also cases in which a direct transition from pitted to knobby is evident. In addition, we do not find a complete degradational sequence on every apron or every part of an apron surface.

The preserved textures in this degradational sequence likely occur on an upper dust+ice mantle that overlies a lower rock+ice mixture (the main apron mass). The overlying dust+ice mantle may be the same material that has been found globally throughout the mid-to- high latitudes (30-70 N) of Mars [17]. The dissected appearance of this global 1-10 m thick mantling layer is morphologically similar to our pitted and ridge and valley textures.

We attribute the surfaces of Tempe/Mareotis debris aprons to degradation by a combination of ice sublimation, melting of ice, and eolian activity. Ice contained within the mantle is most likely lost by sublimation, which forms an irregular surface exposing more of the internal ice to the atmosphere. Warming from seasonal changes could melt pockets of subsurface ice, forming voids that causes surface collapse and the eventual formation of pits. This process is analogous to the formation of thermokarst in periglacial regions on Earth, but on Mars thermokarst might be "dry" given the instability of liquid water under current atmospheric conditions [16,18].

Following the initial step of pit formation by surface collapse, ice sublimation could cause widening of the pits and the development of low-lying valleys or large depressions. As sublimation continues, remnant fine-grained material that collects on the walls and floors of pits may build-up to form a lag deposit. If sufficiently thick, the lag could arrest the sublimation process. However, if eolian activity in the area is sufficiently strong to lift and transport particles away, sublimation could then continue to further degrade the apron.

Table 1. Statistics of the Tempe/Mareotis apron population

	Total	Massif-related	Escarpment-related
Area ¹	12-2303	12-716	90-2303
Volume ²	0.5-1327	0.5-180	28-1327
Relief ³	0.01-1.8	0.01-1.45	0.33-1.8

¹ sq. kilometers ² cu. kilometers ³ kilometers

References. [1] Malin M.C. and Edgett K.S. (2001) *JGR*, 106, 23429-23570. [2] Costard et al. (2002) *Science*, 295, 100-113. [3] Christensen P.R. (2003) *Nature*, 422, 45-48. [4] Milliken et al. (2003) *JGR*, 108, 11-1 to 11-13. [5] Head et al. (2003), *Nature* 426, 799-802. [6] Squyres S.W. (1979) *JGR*, 84, 8087-8096. [7] Squyres S.W. et al. (1992) *Mars, Univ. of AZ Press*, 523-554. [8] Squyres S.W. and Carr M.H. (1986) *Science*, 231, 249-252. [9] Sharp, R.P. (1973) *JGR*, 78, 4073-4083. [10] Hodges C.A. and Moore H.J. (1992) *USGS, Prof. Paper #1592*. [11] Moore H.J. (2001) *USGS, Misc. Invest. Series Map I-2727*. [12] Parker T.J. et al. (1989) *Icarus*, 82, 111-145. [13] Parker T.J. et al. (1993) *JGR*, 98, 11061-11078. [14] Pierce T.L. and Crown D.A. (2003) *Icarus*, 163, 46-65. [15] Mangold N. and Allemand P. (2001) *GRL*, 28, 407-410. [16] Mangold N.A. (2003) *JGR*, 108, 2-1 to 2-13. [17] Mustard J.F. et al. (2001) *Nature*, 412, 411-414. [18] Costard F.M. and Kargel J.S. (1995) *Icarus*, 114, 93-112.

MARS CRUSTAL DICHOTOMY AND WORLD MAPS WITH CONSTANT SCALE NATURAL BOUNDARIES (CSNB)

"A creative approach to visualizing subtle points of geodesy." [8]

C. S. Clark, architect, 1100 Alta Avenue, Atlanta, Georgia 30307; rightbasicbuilding@yahoo.com

Introduction: It has long been known that world maps with natural boundaries have an advantage-in-principle over world maps without [3], because the mind is clouded by meaningless interruptions.

World maps with constant scale natural boundaries (CSNB) improves things because in it [6] [7], peripheries are not grossly distorted in shape, and map edges become recognizable places--a comprehensible overall view boosting scientific intuition [5] [9].

Context is clear in a CSNB map and, if boundaries well-chosen, clearer still, even on complex planets as Earth (see Fig. 6) and, Figures 1 and 4, Mars.

Other contexts for viewing Mars crustal dichotomy in CSNB are identified.

Mapping Précis: Begin at Valles Marineris and proceed downstream where, if Mars as Earth had "switched on" tectonically, we might find to map a linear system of basaltic magmatism [2]. Instead, we find a multi-legged dry-bed, the bottom of a "hill" [4], nether regions of Mars crustal dichotomy. See Fig. 1.

Other Mapping Précis: A "dales"-centered CSNB map (Fig. 4 inside out) would show lowlands as a single, watershed-edged basin, with Mars' continental divide as its perimeter boundary [4]. {POSTER}

And, a lowlands ridge-edged map, uplands still map midst like Fig. 4, would preserve on the map as sensible districts, at the expense of lowland peninsulas, the much-studied outflow channels [1]. {POSTER}

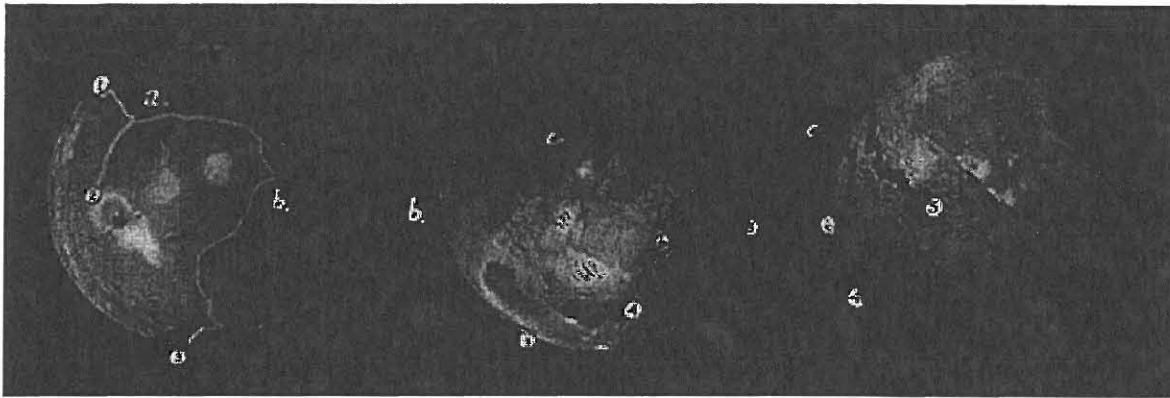


FIGURE 1: False color topo Mars globe marking dry-beds, the extremities of a single "hill" [4]. Commonly mapped Figure 2, this pattern may also be plotted as a CSNB map, Figures 3 and 4.

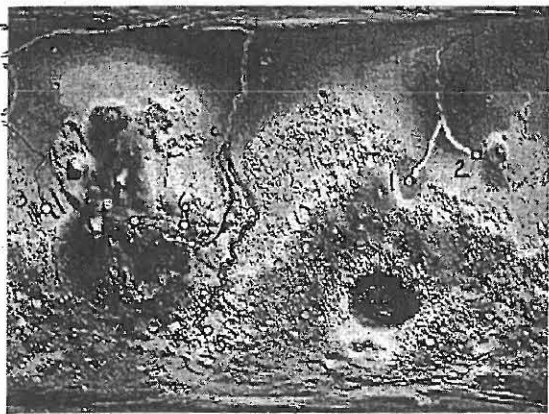


FIGURE 2: Dry-beds on a conventional Mars map. Note polar contortions and longitudinal interruption.

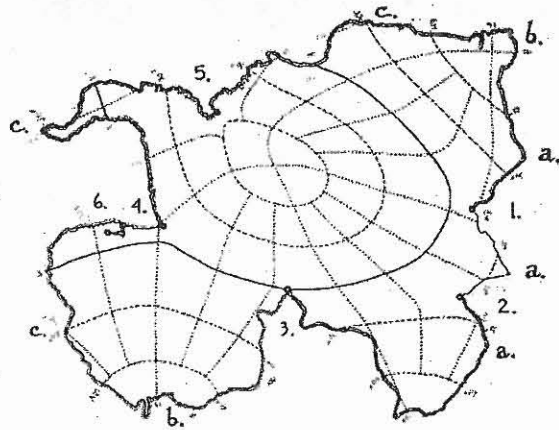


FIGURE 3: Mars dry-beds edging a CSNB map; a coarse calculus preserves their shapes [6]. See Fig. 4.

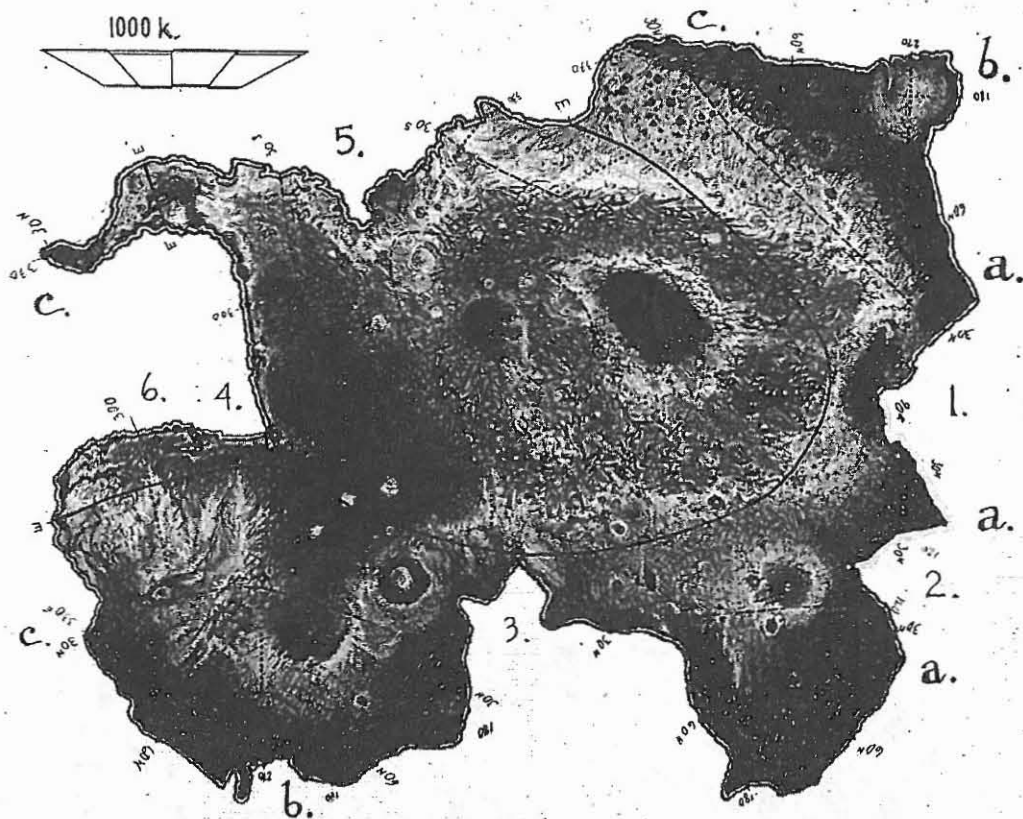


FIGURE 4: A world map of Mars edged by lowlands, its youngest crust. Compare Figure 2. It may surprise planetary scientists that a map's borders may be fruitfully entertained; compare also Figure 6.



FIGURE 5: CSNB map folds to a condensed-sphere model; a unique solid, unobtainable without CSNB and, happily, a check on mapmaker's accuracy.

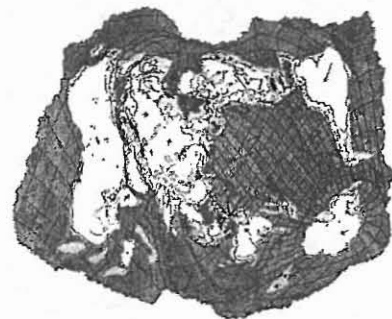
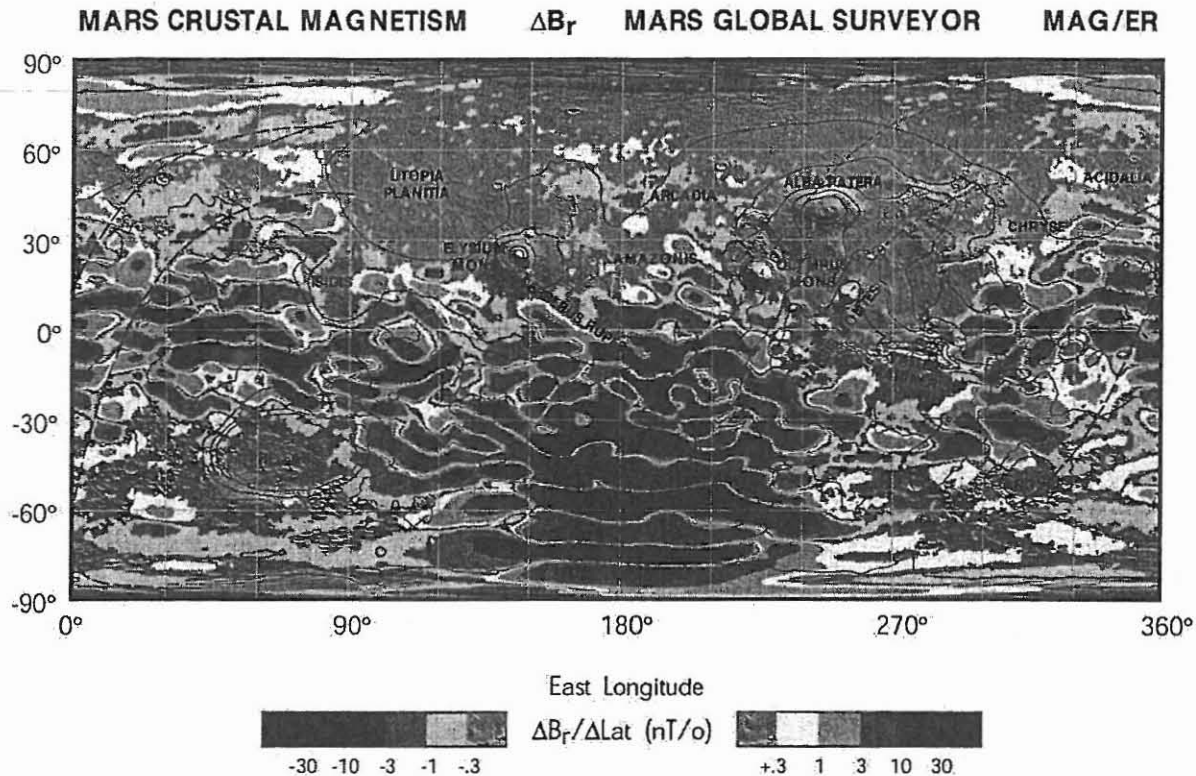


FIGURE 6: Earth, in a CSNB map edged by a portion (slowest moving) of its youngest crust.

References: [1] Carr M. H. (2000) *SPC The Surface of Mars* 11, 12. [2] Lowman P. D. (2002) *CUP Exploring Space, Exploring Earth* 254, 265. [3] Spilhaus A. F. and Snyder J. P. (1991) *CGIS-ACSM* 18 4 World Maps with Natural Boundaries. [4] Maxwell J. C. (1870) *Phil. Mag.* 40 269 On Hills and Dales. [5] Clark C. S. (2004) *NCGT News*. Illustrating Concepts in Global Tectonics with 'CSNB.' [6] Clark C. S. (2003) *ISPRS WG-IV/9 Visual Calculus or Perceptual Fribble? 'CSNB' A Novel Projection*

Method, Well-Suited to Our Era. [7] Clark C. S. (2002) *LPS XXXIII* #1794 'CSNB' and the Asteroid Eros. [8] Krantz S. K. (2003) *comment*--Krantz is former chair. of math. at Wash. U. St. L. [9] Morse, H. C. M. (1950) *manu. Kenyon Coll.* The Poet and Reality: a conf. in honor of Robert Frost/Some Reflections on Evaluations in Mathematics and the Arts, also (1959) *Bull. Atom. Sci.* XV 2 and (2004) *MAA Musings of the Masters Mathematics and the Arts*.

A MAGNETIC PERSPECTIVE ON THE MARTIAN CRUSTAL DICHOTOMY. J. E. P. Connerney¹, M. H. Acuna¹, N. F. Ness², D. L. Mitchell³, R. P. Lin³, and H. Reme⁴, ¹NASA Goddard Space Flight Center, Code 695, Greenbelt, MD 20771; Connerney@gsfc.nasa.gov, ²University of Delaware, Newark, DE 19716, ³Space Science Laboratory and Physics Department, University of California, Berkeley, CA, 94720.



R1599_1pub

Introduction: The Mars Global Surveyor spacecraft has completed two Mars years in nearly circular polar orbit at a nominal altitude of 400 km. The Mars crust is at least an order of magnitude more intensely magnetized than that of the Earth [1], and intriguing in both its global distribution and geometric properties [2,3]. Measurements of the vector magnetic field have been used to map the magnetic field of crustal origin to high accuracy [4,5]. This most recent map is assembled from > 2 full years of MGS night-side observations, and uses along-track filtering to greatly reduce noise due to external field variations.

The map: The radial field component was averaged along-track and decimated to 1 sample per degree latitude traversed by MGS in its polar orbit. A simple 3-point non-recursive digital filter (differentiating Lanczos filter) is then applied to the time series to attenuate constant offsets and variations of larger spatial scale than those associated with variations of crustal

magnetization. We then take the median value of all points falling in each 1 by 1 degree bin in latitude and longitude to create a global image of the field. The resulting map has about an order of magnitude greater sensitivity to crustal magnetic fields. This map of the *change* in radial field with latitude ($dB_r/d\theta$) is closely related to a map of the theta component of the field, with the added advantage of superior removal of external fields.

Overview: The crustal demagnetization previously associated [2] with the large impact basins (Hellas, Argyre, Utopia, Isidis) is even more obvious in this new map, as is the crustal demagnetization associated with the large volcanic structures (Tharsis, Olympus Mons, Elysium). A number of geologic features previously identified in imagery and topography (Cerberus Rupes, Valles Marineris) now can be seen to have magnetic signatures as well. Lack of magnetization seems to be associated with emplacement of lavas.

Crustal magnetization extends well beyond the older Noachian southern highlands terrain. We suggest that the smooth, flat northern lowlands are underlain by much older crust, an extension of the southern highlands crust. This is consistent with the inferred Noachian age of the underlying crust based on the detection of "Quasi-circular depressions", thought to be buried craters [6]. Much of the crustal magnetization originally imprinted in the underlying crust may have been erased by thermal remagnetization in a weak field (after the demise of the dynamo) following the catastrophic widespread emplacement of a ~1 km thick volcanic layer throughout the northern lowlands [7]. If so, a low temperature magnetic mineralogy (titano-magnetite, magnetite) is implicated and the magnetic layer must be relatively thin, e.g., few km in thickness. **Plate tectonics:** Another kind of fault, not previously recognized in imagery or topography, can be identified in the Meridiani region by inspection of the magnetic contours. Two long dashed lines are superposed on the map to identify the location of the proposed faults, along which the magnetic field pattern appears to shift. These lines are drawn by rotation of a vector about a common axis of rotation identified by a pole (marked with a cross) located at 23° S and 80.5° E, just north of Hellas. The magnetic imprint is best preserved near 0° latitude and 0° longitude, where the map shows a series of east-west trending features of alternating polarity extending from ~15° N to ~30° S. A similar pattern can be found on either side of the proposed fault lines. The magnetic imprint has been altered where the crust has been reworked by impacts (e.g., the multi-ring crater Ladon near 18° S, 331° E) and perhaps other events. The two proposed parallel great faults are separated by ~1400 km and a similar pattern in the magnetic field is found on both sides of the easternmost fault along ~2700 km of its length.

The magnetic imprint in Meridiani is consistent with crust formed by plate tectonics in the presence of a reversing dynamo. Essential characteristics: (1) a magnetic imprint aligned with the ridge axis or spreading center, (2) a comparable magnetic imprint observed at widely separated locations, and (3) the presence of transform faults, or great faults, along which relative plate motion has occurred. The relative motion of two rigid plates on the surface of a sphere may be described as a rotation about an axis. If two plates have as common boundaries a number of great faults, they must lie on small circles about the rotation pole. The great faults in Meridiani define an axis of rotation (23° S and 80.5° E) describing the relative motion of two ancient plates, north and south of the equator. The ~240 km offset of the putative ridge axis in Meridiani is comparable to that observed along ocean ridges on Earth.

The origin of the great Valles Marineris fault system is controversial, but it has been attributed to

planetary rifting [8] and compared to terrestrial plate tectonic rifts, e.g., the east African rift zone. A rift structure of parallel grabens and troughs forms, often along an arc, where the crust is being pulled apart by tensile forces. The west-northwest trend of Valles Marineris is oriented nearly perpendicular to the direction of plate motion implied by the great faults in Meridiani (relative plate motion occurs along the strike of transform faults). The direction of tensile forces required to form Valles Marineris, if it is a rift structure, is consistent with the motions implied by the proposed transform faults in Meridiani.

The great volcanic edifices of the Tharsis Montes (Arsia Mons, Pavonis Mons, Ascraeus Mons, extended to include Ceraunius Tholus/Uranus Patera and volcanic cones in Tempe Terra) and the pair Olympus Mons, Alba Patera lie nearly on two small circles (short dashed lines) about a common axis (through 35.5° N and 152° E). The motion of a single plate over a pair of mantle hotspots in a direction parallel to the dashed lines could form a chain of volcanoes if the magma source periodically breached the crust (e.g., the Hawaiian island chain of volcanoes in the Pacific). The relative ages assigned to these volcanoes is consistent with plate motion northward over a pair of putative mantle hotspots, with Alba Patera and Uranus Patera forming early, Olympus Mons and Arsia Mons later.

Dichotomy boundary: The dichotomy boundary is a reflection of crustal evolution, following (from Isidis to Tharsis south of Elysium and Lucas Planum) a series of relic transform faults and spreading centers [9], elsewhere defined by catastrophic lava flows encroaching upon highlands terrain. The Mars crust reflects the end of an era of plate tectonics, a relic of crustal spreading, rifting, plate motions, and widespread volcanism following the demise of the dynamo.

References:

- [1] Acuna, M. H., et al., 1998, *Science*, 279, 1676 – 1680.
- [2] Acuna, M. H., et al., 1999, *Science*, 284, 790 – 793.
- [3] Connerney, J. E. P., et al., 1999, *Science*, 284, 794 – 798.
- [4] Connerney, J. E. P., et al., 2001, *Geophys. Res. Lett.*, 28, 4015 – 4018.
- [5] Connerney, J. E. P., et al., 2004, *Science*, submitted.
- [6] Frey, H. V., et al., 2002, *Geophys. Res. Lett.*, 29, 10.1029/2001GL013832.
- [7] Head, J. W., III et al., 2002, *J. Geophys. Res.*, 107, 10.1029/2000JE001445.
- [8] Hartmann, W. K., 1973, *Icarus* 19, 550-575; Blasius, K. R., et al., 1977, *J. Geophys. Res.* 82, 4067-4091; Frey, H. V., 1979, *Icarus* 37, 142-155.
- [9] Sleep, N. H., 1994, *J. Geophys. Res.*, 99, 5639-5655.

ANCIENT GIANT BASIN/AQUIFER SYSTEM IN THE ARABIA REGION, MARS, AND ITS INFLUENCE ON THE EVOLUTION OF THE HIGHLAND-LOWLAND BOUNDARY

J.M. Dohm¹, N.G. Barlow², Jean-Pierre Williams³, J.C. Ferris⁴, H. Miyamoto^{5,6}, V.R. Baker^{1,5}, W.V. Boynton⁵, R.G. Strom⁵, Alexis Rodríguez⁷, Alberto G. Fairén⁸, Trent M. Hare⁹, R.C. Anderson¹⁰, J. Keller⁵, K. Kerry⁵, ¹Department of Hydrology and Water Resources, University of Arizona, Tucson, AZ, 85721, jmd@hwr.arizona.edu, ²Dept. Physics and Astronomy, Northern Arizona University, Flagstaff, AZ, 86011, ³Dept. of Earth and Space Sciences, Univ. of California, CA 90095, ⁴U.S. Geological Survey, Denver, CO, 80225, ⁵Lunar and Planetary Laboratory, University of Arizona, Tucson, AZ, ⁶Department of Geosystem Engineering, University of Tokyo, ⁷Department of Earth and Planetary Science, University of Tokyo, 7-3-1 Hongo, Bunkyo-ku Tokyo 113-0033, Japan, ⁸Centro de Biología Molecular, Universidad Autónoma de Madrid, 28049 Cantoblanco, Madrid, Spain, ⁹U.S. Geological Survey, Flagstaff, AZ, 86001, ¹⁰Jet Propulsion Laboratory, Pasadena, CA.

Introduction: Ancient geologic and hydrologic phenomena on Mars observed through the magnetic data [1,2] provide windows to the ancient past through the younger Argyre and Hellas impacts [e.g., 3,4], the northern plains basement and the rock materials that mantle the basement [e.g., 5,6], and the Tharsis and Elysium magmatic complexes (recently referred to as superplumes [7,8]). These signatures, coupled with highly degraded macrostructures (tectonic features that are tens to thousands of kilometers long [9]), reflect an energetic planet during its embryonic development (0.5 Ga or so of activity) with an active dynamo and magnetosphere [1,2,6]. One such window into the ancient past occurs northwest of the Hellas impact basin in Arabia Terra. Arabia Terra is one of the few water-rich equatorial regions of Mars, as indicated through impact crater [10] and elemental [11,12] information. This region records many unique characteristics, including predominately Noachian materials, a highland-lowland boundary region that is distinct from other boundary regions, the presence of very few macrostructures when compared to the rest of the cratered highlands, the largest region of fretted terrain on Mars, outflow channels such as Märs Valles that do not have obvious origins, and distinct albedo, thermal inertia, gravity, magnetic, and elemental signatures [13]. We interpret these to collectively indicate a possible ancient giant impact basin that later became an important aquifer, as it (1) provides yet another source of water for the formation of putative water bodies that occupied the northern plains [14,15], (2) helps explain possible water-related characteristics that may be observed at the Opportunity landing site, (3) identifies a potential contributor to the development of the long-lived Tharsis superplume [7,8], and (4) provides a viable explanation for the unique character of the highland-lowland boundary when compared to other boundary regions of Mars. This primary basin is approximately antipodal to Tharsis and estimated to be at least 3,000 km in diameter (see Fig. 1a,b of [13]).

Discussion: Collectively, the distinct characteristics of Arabia Terra add credence to the following proposed hypothesized sequence of events (from oldest to youngest): (1) an enormous ancient impact basin at least 1.5 times the size of Hellas forms during extremely ancient Mars when the dynamo is active and the lithosphere is relatively thin, (2) sediments and other materials infill the basin during high erosion rates and a productive Noachian aquifer system is established, (3) the basin isostatically adjusts, (4) uplift of basin materials related to the growth of antipodal Tharsis results in differential erosion, exposing ancient stratigraphic sequences, and (5) parts of the ancient basin/aquifer system remain water-enriched [13].

The putative Arabia impact basin should not be unexpected on Mars. During the earliest period of solar system history some 4.2 billion years ago, there were very large impacts on the Moon and terrestrial planets. Impact basins comparable in size and age occur on the Moon. The largest impact basin ever identified is the Procellarum basin, first discovered by Whitaker [16] and confirmed from Lunar Prospector chemical data by Feldman et al. [17]. Based on structural and elemental information, the manifestation of the extremely large impact event recorded on the lunar surface extends for an estimated radius of about 60° or a diameter of about 3600 km. Feldman, et al [17] present evidence, which includes elemental information, of yet another giant impact basin on the lunar far side with a radius of 50° or about 3000 km diameter. Both of these basins have also been heavily cratered by the period of late heavy bombardment as the Arabia basin. The South Pole-Aitken basin (2500 km diameter) is another example of a heavily cratered large basin on the Moon. On Mercury, there is also an old giant impact basin (Borealis Basin) with an estimated diameter of 1500 km, but only 25% of that planet has been observed at sun angles sufficient to detect old basins. Even larger basins may occur on the unexplored side. The surface of Venus is too young to record such extremely large impact basins, and on

Earth the earliest part of solar system history is not preserved.

An old impact basin the size of the putative Arabia should, in fact, be present on Mars. The primary impact basin proposed for the Arabia Terra region is estimated to be at least 3,000 km in diameter, or at least 1.5 the size of Hellas. However, its total deformational extent may approximate or even exceed the estimated total extent of the Procellarum impact event. Whether the proposed Arabia Terra impact basin included multi-ring structures and associated basins is difficult to ascertain due to the observed high degree of erosion and deformation of the region.

Although we do not know how much water the Arabia impact basin/aquifer held, we can get some idea by estimating the water content for a 5 kilometer-thick layer coincident with an approximated 3000 km diameter. The volume of such a layer is about $1.43 \times 10^7 \text{ km}^3$. If the porosity was about 10% then the total volume of water would have been about $1.4 \times 10^6 \text{ km}^3$. This is comparable to about 10% of the volume of the smallest ocean in the Northern Plains based on the interior shoreline dimensions of [15,18]. However, this estimated volume may be much higher if the basin had a greater depth and total extent.

Implications: Implications of the basin hypothesis include: (1) explaining the unique characteristics of the region, (2) providing another source of water for the putative water bodies that occupied the northern plains [15,19-20], (3) providing additional information to assess the water-related characteristics observed at the Opportunity landing site, (4) identifying a potential contributor to the development of the long-lived Tharsis superplume [7-8], and (5) providing a viable explanation for the unique character of the highland-lowland boundary when compared to other boundary regions of Mars. Furthermore, the existence of an ancient, gigantic basin in the Arabia terra region, especially when taken in conjunction with the smaller yet massive Tharsis basin [21], suggests that rapid obscuration of basins (be they tectonic or impact in origin) and infill with volatile-rich materials was a relatively common phenomena early in martian history. This has profound implications for rates of deposition in the earliest of martian times, and alludes to an environment with vigorous geomorphic processes being driven by a dynamic hydrosphere. The Arabia terra basin also brings into focus the timing of formation for the northern lowlands. Although this manuscript suggests that the formation of the highland-lowland boundary postdates the formation and infilling of the Arabia terra basin, several investigators have suggested that the dichotomy was shaped by geophysical phenomena present as the planet cooled and first formed a crust, such as mantle convection

associated with core formation [22]. If so, why were the northern lowlands not also infilled by materials and therefore obscured to the present day? Were rates of deposition somehow different for the polar regions, or was the mechanism that formed the northern plains and global dichotomy longer-lasting, perhaps related to incipient plate tectonism [6-7,9,23]? Although many questions are still left to be answered, the emerging picture is that the topography of extremely ancient Mars was drastically different from what is observed today. In addition, such geologic information should provide the constraints on theoretical models relating to the time-space relations of the formation of the highland-lowland boundary, including geophysical modeling of the planet's interior.

References: [1] Acuna M. H. et al. (2001) *JGR*, 106, 23,403-23,417. [2] Arkani-Hamed, Jafar (2003) *JGR*, 108, 10.1029/2003JE002049. [3] Scott, D.H. and Tanaka, K.L. (1986) *USGS I-Map 1802A*. [4] Greeley, Ronald, and Guest, J.E. (1987) *USGS I-Map 1802B*. [5] Frey, H.V. et al. (2002) *Geophys. Res. Lett.* 29, 10.1029/2001GL013832. [6] Fairén, A.G. and Dohm, J.M. (2004) *Icarus*, 168, 277-284. [7] Baker, V.R. et al. (2002) A theory of early plate tectonics and subsequent long-term superplume activity on Mars. *Electronic Geosciences* 7, (<http://lin.springer.de/service/journals/10069/free/conferen/superplu/>), 2002. [8] Dohm, J.M., et al. (2002a) *Superplume International Workshop*, Abstracts with Programs, Tokyo, 406-410, 2002. [9] Dohm, J.M., et al. (2002b) *Lunar Planet. Sci. Conf.*, XXXIII, #1639. [10] Barlow N.G. and Perez, C.B. (2003) *JGR*, 108, 10.1029/2002JE002036. [11] Boynton W.V. et al. (2002) *Science*, 297, 81-85 [12] Feldman W.C. et al. (2002) *Science*, 297, 75-78. [13] Dohm, J.M., et al. (2004) *Lunar Planet. Sci. Conf.*, XXXV, #1209. [14] Baker, V. R. (2001) *Nature*, 412, 228-236. [15] Fairén, A.G., et al. (2003) *Icarus*, 165, 53-67. [16] Whitaker, E.A. (1981) *Proc. Lunar Planet. Sci.* 12A, 105-111. [17] Feldman, W.C., et al. (2002) *J. Geophys. Res.*, 107, E3, 10.1029/2001JE001506, 2002. [18] Ormo, Jens, et al. (2004) *Meteoritics & Planetary Science*, 39, 333-346. [19] Parker, T.J., et al. (1987) in *Symposium on Mars: Evolution of its Climate and Atmosphere*, *LPI Tech. Rept.* 87-01, 96-98. [20] Baker, V.R., et al. (1991) *Nature*, 352, 589-594. [21] Dohm, J.M., et al. (2001) *J. Geophys. Res.* 106, 32,943-32,958, 2001. [22] Wise, D.U., et al. (1979) *Icarus*, 38, 456-472. [23] Fairén, A.G., et al. (2002). *Icarus* 160, 220-223.

MARTIAN EARLY MAGNETIC FIELD AS A RESULT OF MAGMA OCEAN CUMULATE

OVERTURN. L.T. Elkins-Tanton, S. Zarnek, and E.M. Parmentier, Department of Geological Sciences, Brown University, Providence, RI 02912 (Linda_Elkins_Tanton@brown.edu, Sarah_Zarnek@brown.edu, EM_Parmentier@brown.edu).

Introduction: Dynamical models of Martian differentiation and early evolution need to be consistent with several major attributes of Mars that are believed to have developed before 4.0 Ga: differentiation of mantle source regions into isotopically distinct reservoirs; development of an early, brief, strong magnetic field; and the formation of an early crust to record that field. Significant and perhaps complete melting of the large terrestrial planets is expected due to the conversion of kinetic energy to heat during accretion of planetesimals, and to the potential energy release of core formation [e.g., 1-5]. Previous results of Martian magma ocean investigations indicated that magma ocean crystallization and subsequent overturn on Mars could be fast and complete [6], and is consistent with magma source region differentiation and the development of an alumina-poor Martian mantle [7]. The further results presented here demonstrate that magma ocean crystallization and overturn can produce a magnetic field of between 10 and 50 million years duration.

Magma ocean model: The fundamental, relevant processes of cooling to the liquidus of the magma ocean, crystallizing between the liquidus and solidus, crystal setting, and convection are well summarized in Solomatov [8]. Vigorous convection in the low viscosity liquid magma ocean is assumed to result in an adiabatic variation of temperature with depth. As the liquid magma ocean cools by the loss of heat convected to the surface of the planet, the adiabat first intersects the liquidus at the bottom of the mantle. As the ocean continues to cool a partially solid region develops at the bottom of the mantle.

The simplified Martian mantle mineralogy used here follows from the bulk mantle composition of Bertka and Fei [9] and the phase relations of Longhi *et al* [10]. All phases are fractionally crystallized in increments of one-half percent from the evolving liquids of the magma ocean. One percent of interstitial liquid is retained in the solids throughout the magma ocean, acting as a reservoir for radiogenic incompatible elements, which are partitioned from the solid phases using coefficients from [11-13]. Major and trace element liquid and solid compositions are tracked throughout the crystallization process.

As crystallization progresses the solids remain at their solidus temperatures, but the temperature of the solidus decreases as liquid composition evolves. The final cumulate stratigraphy, lying at its solidus, ranges in temperature from 2,100°C at the core-mantle boundary to about 700°C near the surface.

The resulting cumulate stratigraphy is unstable to gravitational overturn mainly due to the effects of iron enrichment as fractional solidification proceeds. Because the

time scale for Rayleigh-Taylor overturn is inversely dependent upon the thickness of the layer, overturn is not likely to initiate until the magma ocean is largely crystalline, whereupon the cumulates flow as solids into an equilibrium density profile [7]. A more detailed description of this model is available in the companion abstract in this volume and in Elkins-Tanton *et al.* [7].

Core heat flux model: Because cumulate overturn is expected to occur on a time scale significantly less than that of heat conduction, the core-mantle boundary will effectively remain at its pre-overturn temperature during and immediately after overturn. The density profile of the solidified magma ocean predicts the stratigraphy of the overturned cumulates, from which the temperature profile directly follows since the solids move adiabatically during the rapid reshuffling. Moving cold cumulates from near the surface to the core-mantle boundary during overturn can produce a brief and intense heat flow out of the hot core and into the cold cumulates.

A finite difference computer program in spherical coordinates has been written to predict heat flux from the core by solving the conductive heat equation while incorporating conductive cooling at the top of the mantle, cumulate heating from incompatible radiogenic elements (whose distribution is produced by the initial fractional crystallization of the magma ocean), and the initial temperature distribution in the overturned cumulates. No convection is allowed in this model; the stable density profile created by cumulate overturn should prevent initiation of convection on these time scales.

Stevenson [14] estimates that a superadiabatic core cooling rate on the order of 80K per Ga (corresponding to about 0.022 J/m²sec) is required to initiate a Martian core dynamo. Our calculations indicate that a minimum superadiabatic heat flux from the core required to initiate a dynamo may be as high as 0.11 J/m²sec, but is likely between 0.05 and 0.02 J/m²sec, using equation 3 from [14].

Results for core heat flow following cumulate overturn: Assuming that the Martian silicate mantle begins with a chondritic trace element composition, the final one percent of liquid contains a trace element concentration of about 65 times chondritic, similar to bulk Earth crust (fig. 1). An evolved liquid fraction is spread over a radius of about 250 km by a critical crystal network and possible stagnant crust at the surface of the planet. Some portion of this ~700°C material falls during overturn to the core-mantle boundary, which remains at the silicate solidus temperature of about 2,100°C, carrying with it U, Th, and K concentrations that will produce significant heating. The falling layer is sufficiently thick that even a stagnant lid on

the planet will not prevent some quantity of cold radiogenic material from foundering. Core heat flux is therefore driven by the initial steep temperature gradient between the core and the cold fallen cumulates, but increasingly limited both by core cooling and by radiogenic heating in the lowermost cumulates.

All the models in this suite produced a final cumulate overturn stratigraphy where the coolest, shallowest cumulates fell to the core-mantle boundary. (Results from [7] showed the garnet layer falling to the core-mantle boundary, but the more evolved liquid compositions allowed in these more sophisticated models prevent complete fall of the garnet layer in every case.) The preferred initial temperature difference across the core-mantle boundary is therefore $2,100-700^{\circ}\text{C} = 1,400^{\circ}\text{C}$ (fig. 2).

If the temperature difference is $1,400^{\circ}\text{C}$, heat flux from the core begins at about $0.6 \text{ J/m}^2\text{sec}$, dropping off exponentially and falling below $0.05 \text{ J/m}^2\text{sec}$ about 50 million years later (fig. 3). In this model the Martian core therefore has sufficient superadiabatic heat flux to initiate a core dynamo for about 50 million years after magma ocean crystallization, as shown in figure 2. Over this period the core cools by about 80 degrees.

If the temperature difference across the core-mantle boundary is only $1,000^{\circ}\text{C}$, heat flux remains above the necessary $0.05 \text{ J/m}^2\text{sec}$ for about 30 Ma. To prevent core heat flux from ever exceeding the $0.05 \text{ J/m}^2\text{sec}$ value the temperature difference across the core-mantle boundary must be 150°C or less.

Discussion and Conclusions: All the models run in this suite produced superadiabatic core heat flux thought to be sufficient to produce a core dynamo magnetic field for at least 30 to 50 million years after magma ocean cumulate overturn. Overturning cumulates moves cold cumulates to the core-mantle boundary, producing core heat flux, and also moves hot cumulates nearer the surface, where they can melt adiabatically and produce an early crust. These models predict the formation of tens of kilometers of new crust during the time the magnetic field is active. This new crust is at the surface at temperatures cooling to and then below the Curie temperature of approximately 600°C , available to record the magnetic field.

References: [1] Safronov (1978) *Icarus* 33, 3. [2] Kaula (1979) *JGR* 84, 999. [3] Stevenson (1987) *Ann. Rev. EPS* 15, 271. [4] Halliday (2001) *Space Sci. Rev* 96, 197. [5] Hess (2001) *32nd LPSC*, 1319. [6] Zaranek (2004) *35th LPSC*. [7] Elkins-Tanton (2003) *MAPS* 38, 1753. [8] Solomatov (2000) in *Origin of the Earth and Moon*. [9] Bertka (1997) *JGR* 102, 5251. [10] Longhi (1992) In *Mars*. [11] Draper (2003) *PEPI* 139, 149. [12] Green (2000) *Lithos* 53, 165. [13] Skulski (1994) *Chem. Geo.* 117, 127. [14] Stevenson (2003) *EPSL* 208, 1.

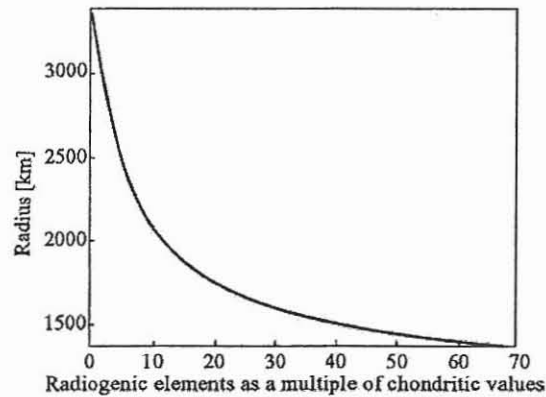


Figure 1. Profile of radiogenic trace elements immediately following cumulate overturn, as a multiple of chondritic values.

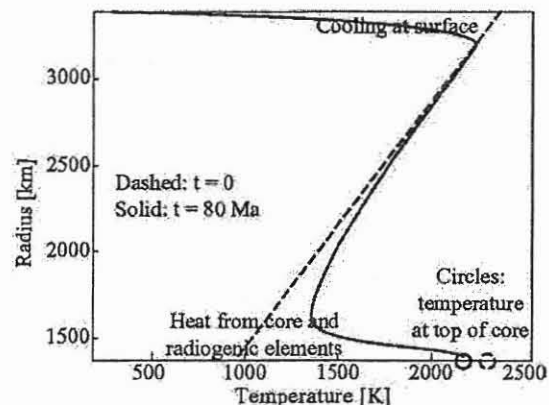


Figure 2. Temperature profiles through the Martian mantle immediately following overturn, and at 80 Ma, approximately 30 Ma after cessation of the Martian magnetic field in these models.

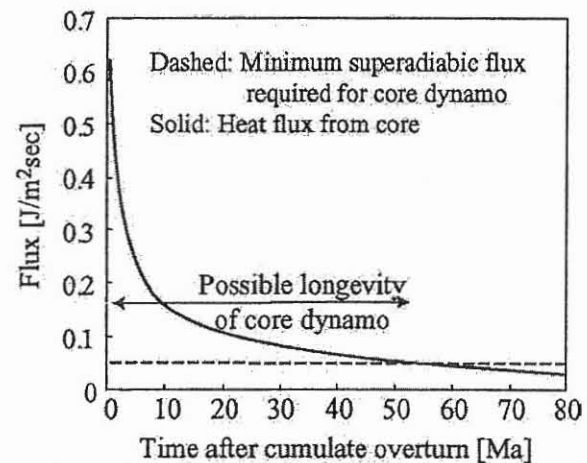


Figure 3. Heat flux from the Martian core following magma ocean cumulate overturn. Heat flux values above about $0.05 \text{ J/m}^2\text{sec}$ (horizontal dashed line) should be sufficient to produce a core dynamo.

MAGNETIC ANOMALIES NORTH OF THE DICHOTOMY BOUNDARY: POSSIBLE EVIDENCE FOR DICHOTOMY RETREAT? C. I. Fassett¹ and J. W. Head III¹, ¹Dept. of Geological Sciences, Brown University (Caleb_Fassett@brown.edu & James_Head@Brown.edu).

Introduction: The Mars Global Surveyor magnetometer experiment revealed strong crustal magnetic anomalies, predominately in the southern highlands [1]. It is generally believed that these anomalies were emplaced quite early in Mars' history given the apparent demagnetization of the major impact basins [1]. Besides the correspondence of the major basins with regions of low magnetism and the broad difference between hemispheres, there are relatively few correlations between the crustal magnetic signature and other geological features.

A particular region of interest where remanent magnetism is poorly correlated with geology is observed near the dichotomy boundary, especially in the region from 60° to 160° E (Fig. 1, modified from [2]). A magnetic signature appears to extend at least 500 km north from the present dichotomy. At present, we are attempting to understand the implications that this observation may have for helping to unravel the complicated history of the dichotomy boundary, as well as for understanding of the magnetic anomalies and their modification history. In what follows, we briefly outline several possible models.

Erosion and Retreat of the Dichotomy Boundary: One possible interpretation of this observation is that the magnetic signature observed north of the dichotomy may be a sign of widespread and substantial retreat of the dichotomy itself. In this model, the magnetic anomalies north of the dichotomy boundary act as a tracer for old highlands crust that was subsequently eroded and perhaps partially buried by younger volcanism. Widespread backward erosion (on the order of hundreds of kilometers) of the dichotomy boundary has been suggested before based upon geological evidence [3]. Moreover, the location of these anomalies (and their formation by erosion of highland crust) appears to be somewhat consistent with the Hbl (Hesperian boundary plains 1) unit mapped by Tanaka et al. [4].

The simplest model for erosional retreat of several hundred kilometers is water-associated erosion; groundwater sapping, fluvial erosion, ice-related mass-wasting, or glaciation may all have played a role. This widespread removal of material is consistent with the formation of the knobby terrain spottily distributed north of and adjacent to the dichotomy boundary (HNk in [4]). Erosion would presumably have predominantly occurred in the

Noachian and early Hesperian, when the dichotomy boundary may have intersected with the ancient groundwater table [5] and when erosion rates on Mars were higher [6].

Northern Lowlands Demagnetization and Formation: Another possible explanation for the magnetic anomalies that lie north of the present dichotomy boundary is that they represent northern lowlands crust which has not lost its magnetization. A clear mechanism for demagnetizing the northern lowlands remains uncertain, although the emplacement of volcanic plains appears to be insufficient. More promising is demagnetization related to a large impact (or impacts) which may have formed the northern lowlands [7] or from hydrothermal activity postdating lowland formation [8]. If the northern plains formed via one or several large impacts, it is unclear why the margins of such an impact would not be demagnetized; however, our understanding of the nature of such a large impact (and its thermal and shock effects on remanent magnetization) are presently rather limited. Alternatively, if hydrothermal demagnetization was the dominant reason for the lack of magnetic anomalies in the northern lowlands, the degree of demagnetization might decrease around the edges, because as elevation increases it is possible that groundwater availability might be decreased.

Edge Effect: A final possibility is that the observed magnetic anomalies near the dichotomy boundary might simply represent an edge effect caused by the contrasting regions of magnetized highlands and demagnetized lowlands crust [e.g., 9]. Although we are attempting to model such an effect, and have not yet ruled such a possibility out completely, it seems somewhat unlikely that this effect would produce features of the wavelength and magnitude seen here; this is especially true given the limited edge effects seen on the boundaries of other demagnetized regions, such as Hellas.

Summary and Future Work: The crustal magnetic signature adjacent to and north of the dichotomy boundary provides a potential constraint on the boundary's geological evolution. Although we need to explore alternative hypotheses more fully, we believe that this magnetic signature plausibly supports the model that the ancient dichotomy boundary was substantially north of its present location [3].

References: [1] Acuña, M.H. et al. (1999) *Science*, 284, 790-793. [2] Connerney, J.E.P. et al. (2001), *GRL*, 28, 4015-4018. [3] Tanaka, K.L. & Scott, D.H. (1987), *U.S.G.S. Misc. Inv. Series Map I-1802-C*. [4] Tanaka, K.L. et al. (2003), *JGR*, 108, 8043. [5] Head, J.W. et al. (2004), *LPSC XXXV* abstract no.

1379. [6] Craddock, R.A. & Maxwell, T.A., (1993) *JGR*, 98, 3453-3468. [7] Wilhelms, D.E. & Squyres, S.W. (1984), *Nature*, 309, 138-140. [8] Solomon, S.C. et al. (2003), *LPSC XXXIV*, abstract no. 1382. [9] Smrekar, S.E. et al. (2002), *LPSC XXXIII*, abstract no. 2068.

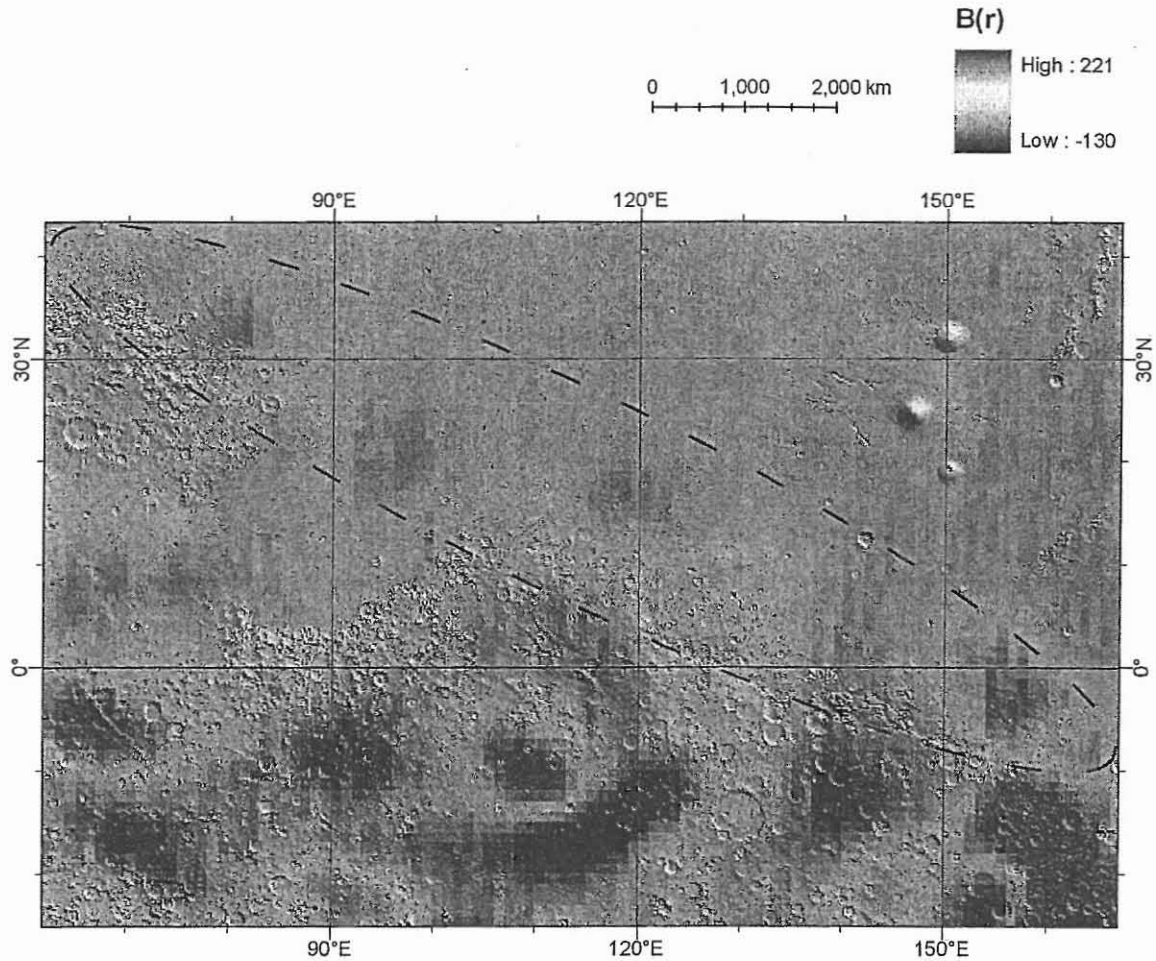


Figure 1. MGS radial magnetic measurement at 400 km modified from [2], superposed upon MOLA shaded relief. The data is stretched to bring out the weak features north of the dichotomy boundary. The relative weak signal is consistent with removal of magnetized crust during retreat of the dichotomy, though this is not a unique explanation. Magnetic anomalies extend ~500 km from the dichotomy boundary. In parts of this region, knobby terrain (HNk) appears to be correlated with the magnetic signature (e.g. 80°E, 32°N).

IMPACT CONSTRAINTS ON THE AGE AND ORIGIN OF THE CRUSTAL DICHOTOMY ON MARS.

H.V. Frey, Geodynamics Branch, Goddard Space Flight Center, Greenbelt, MD 20771; Herbert.V.Frey@nasa.gov.

Introduction: MOLA data have revealed a large population of "Quasi-Circular Depressions" (QCDs) with little or no visible expression in image data. These likely buried impact basins [1,2] have important implications for the age of the lowland crust, how that compares with original highland crust, and when and how the crustal dichotomy may have formed [3-6]. The buried lowlands are of Early Noachian age, likely slightly younger than the buried highlands but older than the exposed (visible) highland surface. A depopulation of large visible basins at diameters 800 to 1300 km suggests some global scale event early in martian history, maybe related to the formation of the lowlands and/or the development of Tharsis. A suggested early disappearance of the global magnetic field can be placed within a temporal sequence of formation of the very largest impact basins. The global field appears to have disappeared at about the time the lowlands formed. It seems likely the topographic crustal dichotomy was produced very early in martian history by processes which operated very quickly. This and the preservation of large relic impact basins in the northern hemisphere, which themselves can account for the lowland topography, suggest that large impacts played the major role in the origin Mars' fundamental crustal feature.

QCDs > 200 km Diameter: Figure 1 shows polar views of QCDs > 200 km diameter. Features of this size, which number >500, are difficult to bury completely (rim heights 1-1.5 km, depths ~4 km [7]) and therefore might be expected to survive over all of martian history. This is also a size appropriate for comparison with gravity and magnetic anomalies [8-11].

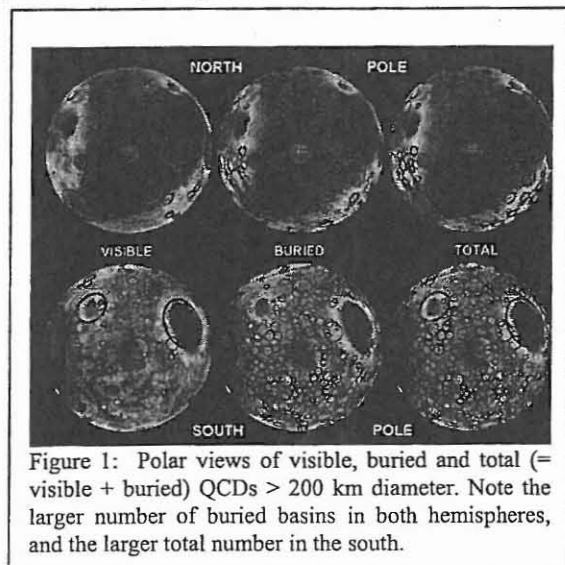


Figure 1: Polar views of visible, buried and total (= visible + buried) QCDs > 200 km diameter. Note the larger number of buried basins in both hemispheres, and the larger total number in the south.

In both highlands and lowlands the buried population is always much greater than the visible population. There is a significant number of very large basins ($D > 1000$ km), equally divided between the two hemispheres, including two Utopia-size buried highland features. One is near but not identical to an earlier proposed "Daedalia Basin" [12,13] and the other centered near 4N, 16W. This "Ares" basin may have influenced early fluvial drainage through the Uzboi-Ladon-Arden Valles and Margaritifer-Iani Chaos depressions.

Cumulative Frequency Curves and Crater Retention Ages: A small (~10) population of very large basins ($D = 1300-3000$ km) follow a -2 power law slope on the log-log cumulative frequency plots. At $D < \sim 500$ km the total populations in both highlands and lowlands again follow a -2 slope; for the planet-wide visible population this is the same slope as for the very large diameter basins. The relative positions of the lowland and highland curves indicate the buried lowland crust is slightly younger than the original (now buried) highland crust, consistent with our earlier result [2]. By direct comparison with the oldest exposed surface units on Mars (Nh_1 , SE of Hellas [3,4]), the buried lowland crust is Early Noachian in age [14].

At intermediate diameters (1300 to about 800 km) the global visible population falls off the -2 slope before recovering at smaller diameters. This depletion of intermediate size basins may be the signature of some global-scale event very early in martian history. Candidates include formation of the slightly younger lowland crust (i.e., the formation of the topographic crustal dichotomy), and the growth of Tharsis (or both), both of which could have removed pre-existing intermediate-size basins.

Implications for the Age and Origin of the Crustal Dichotomy: Unless there is some way to preserve the large population of Early Noachian (now buried) impact craters while lowering the crust in the northern third of Mars, it appears the lowland crust not only formed in the Early Noachian but also became low during that time [2,14]. The slight crater age difference (which could be a very short absolute time interval), does suggest the lowlands formed after the highlands were in place and preserving craters. It may be hard to form the lowlands by endogenic processes in the short time available. Most mechanisms suggested [15-17] have a relatively late formation of the lowlands. Even if degree one convection does occur, it appears to take hundreds of millions of years to become established, even with extreme viscosity gradients [17]. How much longer, and by what exact means,

the crust then becomes low, is generally discussed in only vague terms. In contrast, three large "lowland-making" QCDs (Utopia, Acidalia and Chryse) do account for most of the lowland topography and offer a simple impact mechanism for the early formation of a topographic dichotomy on Mars [18].

Comparison with Magnetic Anomalies: We compared the distribution of QCDs (both buried and visible) with the distribution of magnetic anomalies [9,10,19-21]. Only the two oldest very large basins, Daedalia and Ares, have prominent anomalies lying within their main rings. Daedalia and Ares likely pre-date the disappearance of the global magnetic field. The "lowland-making" basins Utopia, Acidalia and Chryse have only a few moderate amplitude anomalies within their main rings, and are of intermediate age between Ares and the younger Hellas, Argyre and Isidis basins (see below). The demise of the global magnetic field may have been at about the time of formation of these "lowland-making" basins.

A Chronology of Major Events in the Early History of Mars: We used the cumulative number of basins larger than 200 km diameter per million square km [N(200)] to place the large diameter basins in a relative chronology [6, 18, 22]. The N(200) relative crater retention ages can be converted into "absolute ages" [22,23] using the Hartmann-Neukum (H&N) model chronology [24]. This is uncertain by at least a factor 2 [25]. We use Tanaka's [26] crater counts at small diameters (2, 5, 16 km) to convert his N(16) ages for major epoch boundaries (Early Noachian/Middle Noachian [EN/MN], etc.) to N(200) ages assuming a -2 power law. Hartmann and Neukum [24] give a model absolute age for each of these epoch boundaries. We consider two cases for the H&N value for the earliest age we find, extrapolated from the large basin population ($D > 1300$ km diameter): a linear extrapolation from the EN/MN and MN/LN points and the unlikely case that the origin of Mars at 4.6 BYA is the upper limit.

Table 1 shows the resulting N(200) and "absolute ages" in billions of Hartmann-Neukum years for major events in martian history. With the factor of 2 and an additional pre-Noachian crater saturation caveat, the buried highlands are slightly younger (4.08-4.27) than the Ares Basin (4.09-4.28), and distinctly older than the buried lowlands at 4.01-4.11 BY. These buried lowlands are slightly younger than the "lowland-making" basins Utopia, Acidalia and Chryse at 4.04-4.20 BY, as they should be. We take this to be the age of the formation of the crustal dichotomy. This is also close to the time when the global magnetic field died, based on which basins do and do not have anomalies within their main rings. It may be that the two events, formation of the fundamental crustal dichotomy and the demise of the global magnetic field, are related.

Table 1. A Proposed N(200) Time-Line for the Early Crustal Evolution of Mars

N(200)	Feature	Event	Epoch	H/N Age
-0.1	Visible Lowlands		EH	3.65
0.16	EH / LN BOUNDARY		EH/LN	3.70
-0.6	Visible Highlands		LN/MN	3.79
0.64	LN / MN BOUNDARY		LN/MN	3.80
1.28	MN / EN BOUNDARY		MN/EN	3.92
-1.3	Isidis	Impact	EN	3.92
-2.2	Argyre	Impact	EN	4.00-4.07
-2.5	Buried Lowlands		EN	4.01-4.11
-2.7	Hellas	Impact	EN	4.02-4.14
3.0-3.2	Chryse, Utopia, Acidalia	Lowlands formed?		4.04-4.20
-3.57		Core Field Dies?		4.07-4.23
-3.8	Buried Highlands		pre-N	4.08-4.27
-4.0	Ares	Impact	pre-N	4.09-4.28
-4.5	Total Highlands		pre-N	4.10-4.33
-8.5	Large Basin Highlands (ext)	Impacts	pre-N	4.20-4.60

Conclusions: The (visible and buried) large diameter crater population suggest the buried lowlands are slightly younger than the buried highlands, but significantly older than the exposed highland surface. The buried lowland crust is Early Noachian in age and the lowlands likely formed by processes that operated relatively quickly. In a Hartmann-Neukum model chronology, a crustal dichotomy produced by large "lowland-making" impact basins formed by 4.12 +/- 0.08 BYA and the global magnetic field died at about or slightly before the same time (4.15 +/- 0.08 BYA).

References. [1] Frey, H. et al., GRL 26, 1657-1660, 1999. [2] Frey, H. et al., GRL 29, 10.1029 /2001 GL013832, 2002. [3] Frey, E.L. and H.V. Frey, AGU Paper P32A-01. [4] Frey, H. et al., LPSC 34 abstract #1848, 2003. [5] Frey, H., GSA Fall 2002 Meeting paper 26-3, 2002. [6] Frey, H. LPSC 34, abstract # 1838, 2003. [7] Garvin, J.B. et al. LPSC 33, abstract 1255, 2002. [8] Smith, D.E. et al., Science 286, 94-97, 1999. [9] Acuna, M.H., et al., Science 284, 790-793, 1999. [10] Connerney, J.E.P. et al., GRL 28, 4015-4018, 2001. [11] Frey, H. LPSC 35, abstract #1384, 2004. [12] Craddock, R.A. et al., JGR 95, 10729-10741, 1990. [13] Schultz, R. A. and H.V. Frey, JGR 95, 14,175-14,189,1990. [14] Frey, H. et al. LPSC abstract #1680, 2002. [15] Wise, D.U. et al., JGR 84, 7934-7939, 1979. [16] McGill, G.E. and A.M. Dimitriou, JGR 95, 12595-12605, 1990. [17] Zhong, S. and M.T. Zuber, Earth Planet. Sci. Lett. 189,75-84,2001. [18] Frey, H. 6th Intern. Coll. On Mars, abst #3104, 2003. [19] Purucker, M.E. et al., GRL 27, 2449-2452, 2000. [20] Cain, J. unpublished data, 2001. [21] Langlais, B. JGR 10.1029/2003JE002048, 2003. [22] Frey, H., GSA Fall 2003 Meeting, paper 67-5, 2003. [23] Frey, H., LPSC35, abstract #1382, 2004. [24] Hartmann, W.K. and G. Neukum, Space Sci. Rev., 96, 1-30, 2001. [25] Hartmann, W.K., personal communication, 2002. [26] Tanaka, K. L et al., Chap. 11 in *Mars*, Kieffer et al. (ed.), 1992.

CONSTRAINTS ON EARLY MARS EVOLUTION AND DICHOTOMY ORIGIN FROM RELAXATION MODELING OF DICHOTOMY BOUNDARY IN THE ISMENIUS REGION. A. Guest¹ and S. E. Smrekar¹,
¹Jet Propulsion Laboratory, California Institute of Technology, M.S. 183-501, 4800 Oak Grove Dr. Pasadena, CA 91109; alice.guest@jpl.nasa.gov.

Introduction: The Martian dichotomy is a global feature separating the northern and southern hemispheres. The 3.5-4 Gyr old feature [1,2] is manifested by a topographic difference of 2-6 km and crustal thickness difference of ~15-30 km between the two hemispheres [3,4,5]. In the Ismenius region, sections of the boundary are characterized by a single scarp with a slope of ~20°-23° and are believed to be among the most well preserved parts of the dichotomy boundary. The origin of the dichotomy is unknown. Endogenic hypotheses do not predict the steep slopes (scarps) of the dichotomy boundary. Exogenic models for forming the northern lowlands by impact cratering, associate the scarps along the dichotomy boundary with craters' rims [6], but are not globally consistent with the topography and gravity [5]. In order to better understand the origin of the Martian dichotomy, it is necessary to know if the steep scarps along the boundary represent the original shape of the dichotomy.

Smrekar et al. [7] presented evidence showing that the boundary scarp in Ismenius is a fault along which the highland crust was down faulted [8]. We test whether the relaxation process could produce faulting along the dichotomy boundary and examine the crustal and mantle conditions that would allow for faulting to occur within 1 Gyr and preserve the long wavelength topography over another 3 Gyr. We approach the problem by a combination of numerical and semi-analytical modeling. We test different viscosity profiles and crustal thicknesses by comparing our modeled magnitude, location and timing of plastic strain and displacements to detailed geologic observations in the Ismenius region.

Previous Works: Nimmo and Stevenson [9] modeled relaxation of the Martian dichotomy. They argue that the topographic boundary is not relaxed and that the boundary can be preserved for a crustal thickness of 80 km or less. Their model uses viscous rheology, assumes a dry diabase flow law [10], and compares the predicted topographic relaxation to 10 evenly spaced (excluding Tharsis) profiles across the dichotomy, averaged along track. The focus of their study was on constraining crustal thickness and the amount of crustal heat production.

Numerical Model: We construct a visco-elasto-plastic finite-element model to predict the relaxation of the topography over time. The model is 1500 km wide and 1000 km deep, and consists of two materials, the crust and the mantle. We test two

different crustal thicknesses (35, 80 km) and a plateau elevation 5 km. The width of the dichotomy boundary is 143 km and the average slope, smoothed using a cosine function is 2°. Assuming a crustal density of 2900 kg/m³, a mantle density of 3500 kg/m³, we include a 24.17 km thick crustal root below the plateau to produce an isostatic compensation [10]. In the equation, the total strain is defined as a sum of elastic, viscous and plastic strains [11]. We use wet diabase [10] and wet dunite [12] as a representative for the creep strain of the crust and mantle, respectively. We use a Mohr-Coulomb criterion for plasticity, with cohesion of 9 MPa and friction of 40°. The temperature in our model is represented by an error function connecting a surface temperature of 220 K, a temperature 1400 K (assumed to be the base of the lithosphere) at 60 km depth, which gives a thermal gradient of ~20 K/km, and a mantle temperature 1600 K or 2150 K.

Semi-analytical Model: Assuming an incompressible viscous fluid, the equilibrium and constitutive equations can be solved semi-analytically in the frequency domain [13]. The horizontal variations of the stress and velocity are transformed using a FFT allowing us to numerically integrate the equilibrium and constitutive equations only along the vertical axis. The vertical velocity at the surface is then converted to the change of topography over time. The numerical integration allows for variations of viscosity with depth. The viscosity variations are input in the model a priori and represent the effective viscosity in the given depth.

Results: First, we run the finite-element model till relaxation slows significantly, and then we continue the calculations by semi-analytical solution.

The evolution of the topographic relief for a model with 80-km thick crust and 1600 K mantle temperature is shown in Fig. 1. The relaxation is focused into a few hundred km thick belt along the dichotomy boundary. After 30 years the topography changes by 1 km. The plastic strain develops in four locations: 1) 200-300 km south of the dichotomy boundary (tension), 2) 200-300 km north of the boundary (compression), 3) along the bottom of the slope of the boundary (tension) and 4) along the top slope (compression). The model with 35-km thick crust and 1600 K mantle temperature behaves similarly, only relaxation occurs more slowly.

Our semi-analytical solutions match the finite-element solutions assuming a simple two-layered

constant-viscosity profile. Continuation of the finite-element calculations by semi-analytical modeling shows that 80-km thick crust relaxes too fast to preserve the long topographic wavelengths over 3 Gyr, even if cooling of the Martian interior is considered. If we assume plausible cooling rates, the 35-km thick crust will allow the preservation of long wavelengths while relaxing the 300-500 km wavelengths.

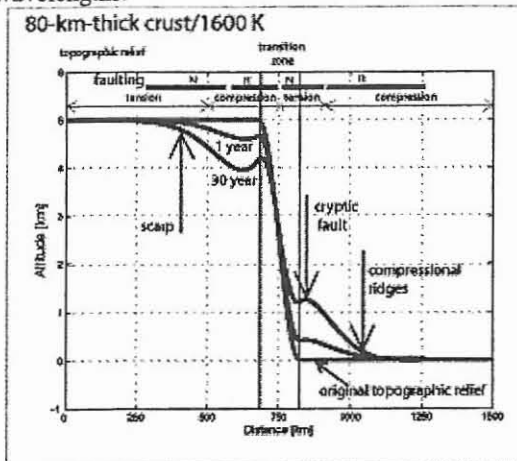


Fig. 1: Topographic relaxation, plastic strain (faulting), and stress distribution on surface of the finite-element model.

In order to preserve the long topographic features (10,000 km) over 3 Gyr and relax the 300-500 km wavelengths within 0.5 Gyr, the contrast of effective viscosity between the upper and lower crust must be 4-6 orders and a lower crustal channel of 10 km thickness must develop. The viscosity of the lower crust of 10^{19} Pa s for 35-km thick crust, or 10^{21} Pa s for 80-km thick crust, averaged over 30 Myr, (Fig. 2) provides a reasonable viscosity estimate that satisfies both criteria. The viscosity is one order higher if we average over 300 Myr time. If cooling rates are taken into account, lower viscosities will be allowed.

Conclusion: Our finite-element model predicts relaxation of the topography within several hundreds km along the dichotomy boundary. The relaxation, and the faulting associated with the relaxation, matches the geologic observations in the Ismenius region. The faulting, located 200-300 km south from top slope of the boundary, probably results in a steep scarp. Thus relaxation of a gently sloped boundary, as predicted by many formation models [14] can result in the steep slopes observed in many areas today. The deformation of the boundary is dependent on the lower crustal rheology, which is dependent on the crustal thickness and temperature. From our finite-element modeling, the temperature gradients of 20 K/km 4 Gyr ago provides the best fit to the

geologic observations. This gradient is consistent with those inferred from elastic thickness estimates [15].

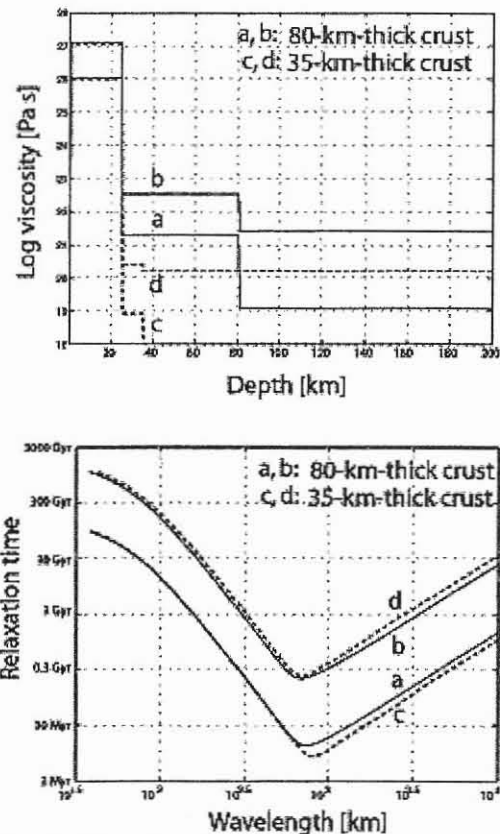


Fig. 2: The viscosity profiles (top) and relaxation curves (bottom) that will preserve 10,000 km features over 3 Gyr and relax 300-500 km features in 0.5 Gyr. Curves a and c average viscosity over time 30 Myr, curves b and d average viscosity over 300 Myr.

References: [1] McGill G. E. and Dimitriou A. M. (1991) JGR, 95, 12595-12605. [2] Frey H. V. (2004) LPSC XXXIV, #1382 [3] Frey H. A. et al. (1998) GRL, 25, 4409-4412. [4] Smith D. E. et al. (1999) Science, 284, 1495-1503. [5] Zuber M. T. et al. (2000) Science, 287, 1788-1793. [6] Frey and Schulz, (1988) GRL, 15, 229-232. [7] McGill et al., 2004, this volume [8] Smrekar S. E. et al. (2004) submitted to JGR. [9] Nimmo F. and Stevenson D. J. (2001) JGR, 106, 5085-5098. [10] Mackwell, S. J. et al. (1998) JGR, 103, 975-984. [11] Nunes D. and Phillips R. (2004) JGR, 109, E01006 [12] Chopra P. N. and Paterson M. S. (1984) JGR, 89, 7861-7876. [13] Cathles, L. M. (1975) The Viscosity of the Earth's Mantle, Princeton University Press, [14] Zhong S. and Zuber M. T. (2001) EPSL, 189, 75-84 [15] McGovern et al. (2003) JGR, 107, 5136.

APPLICATION OF RECENT MISSION RESULTS TO THE ORIGIN AND EVOLUTION OF THE DICHOTOMY BOUNDARY. J. W. Head, Dept. of Geol. Sci., Brown Univ., Providence, RI 02912 USA, james_head@brown.edu.

Introduction and Background: The origin of the dichotomy boundary and the processes that have been responsible for its modification since its formation have been a matter of debate and speculation ever since the distinctive contrast the northern lowlands and cratered southern uplands was first discovered. Part of the difficulty in making significant advances on these problems has been the lack of new data. The recent focus on the exploration of Mars has considerably changed this and the prospect of even more new data promises to bring major advances in the characterization of the crust of this region and new insight into its origin and evolution. The purpose of this contribution is to review some of these new data and to point out where new advances are likely to be made.

Geophysical data: The Mars Global Surveyor (MGS) mission acquired abundant new geophysical data, including improved gravity, topography, and magnetic field data (Fig. 1, radial magnetic measurements on MOLA shaded relief). These data have permitted new determinations of crustal thickness, and the relative types and intensity of magnetic anomalies in the northern lowlands and southern uplands and across the boundary (Fig. 1). Radar instruments such as MARSIS on Mars Express and SHARAD on MRO are designed to probe and to profile the subsurface to add to the three-dimensional view of the shallow crust and differences across the dichotomy boundary.

Crustal mineralogy and chemistry: Interpretations of crustal mineralogy and chemistry have been forthcoming from the thermal emission spectrometer (TES) on MGS and THEMIS and the GRS/NS complement of instruments on Mars Odyssey. Furthermore, surface exploration and rock and soil analyses by the Mars Exploration Rovers have provided ground truth for surface geological units. The Mars Express OMEGA spectrometer and the multispectral High Resolution Stereo Camera (HRSC) together provide high spatial and spectral resolution data at wavelengths complementing previous missions. Upcoming Mars Reconnaissance Orbiter mission experiments, such as CRISM, will also contribute both high spatial and high spectral resolution data.

Surface physical properties: TES and THEMIS data have opened up a whole new world of interpretation of the physical properties of surface units such as slopes and crater ejecta deposits. Quantitative thermal inertia data have been useful in understanding the distribution of rocks and soils on the surface and the relative ages of some units.

Geological data: The dichotomy boundary is known to have undergone significant modification since its formation and the nature of this modification provides information on the processes responsible for the destruction and lateral migration of the boundary, as well as clues to its original configuration. The acquisition with MGS of very high-resolution images (MOC) and global altimetry (MOLA), combined with the improved spatial resolution and spectral diversity of THEMIS images, has revolutionized the analysis of these processes.



FIGURE 4

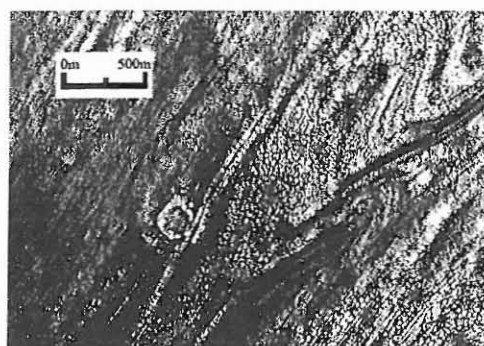


FIGURE 5C

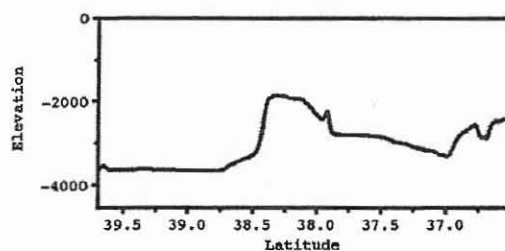


FIGURE 3

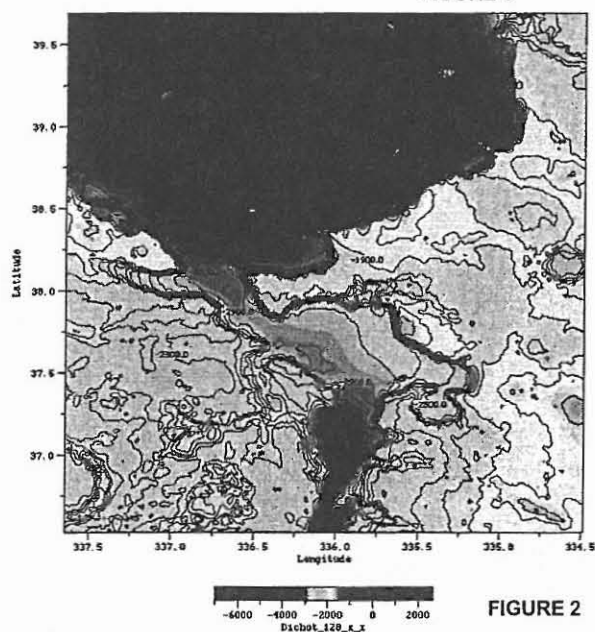


FIGURE 2

For example, it is now possible to compile detailed high-resolution topographic maps of Mars (Fig. 2) that can combine contours, color-coded topography and shaded relief. Altimetric profiles (both directly from individual data swaths and from the gridded data; Fig. 3) provide abundant information about landform morphometry and slopes. THEMIS images can be draped over the topography data to visualize geological relationships and assess unit characteristics (Figure 4). Very high-resolution MOC images reveal spectacular detail (Figure 5a, b, c) and provide new insight into the nature of processes modifying the dichotomy boundary. Data to be obtained by the HiRISE imaging experiment on the upcoming MRO mission will be of even higher resolution.

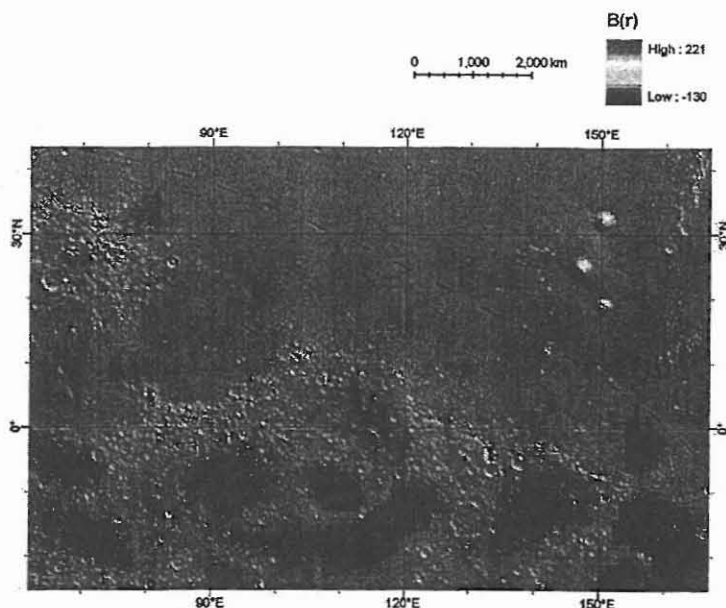


FIGURE 1



FIGURE 5A



FIGURE 5B

These new data, for example, have revealed evidence for the accumulation and flow of ice in glacial-like patterns in and near the dichotomy boundary (e.g., Figures 1-6).

MARS DICHOTOMY BOUNDARY DEGRADATIONAL PROCESSES: EVIDENCE FOR EXTENSIVE AMAZONIAN GLACIATION. J. W. Head¹, M. C. Agnew¹, C. I. Fassett¹, D. R. Marchant² and M. A. Kreslavsky¹

¹Dept. of Geol. Sci., Brown Univ., Prov., RI, 02912. ²Dept. of Earth Sciences, Boston Univ., Boston, MA 02215.

Among the hallmark morphologies of the dichotomy boundary, particularly at higher latitudes are 1) the debris aprons the surround many of the massifs and valley walls, and 2) the lineated valley fill that occurs in many of the valleys themselves (1-11). The ages of these deposits are typically much younger than the adjacent plateau terrain or its breakup and the formation of the valleys themselves (e.g., 8, 11). The margins of the debris aprons are rounded and convex upward topography, and the debris aprons and the valley fill can appear smooth and relatively homogeneous or, in contrast, can be characterized by closely spaced parallel ridges and grooves a few to several tens of meters high. These sets of parallel ridges have been interpreted to have formed both parallel and normal to valley and mesa walls. Some (1) argue that the lineations for mostly normal to flow due to converging flow from debris aprons on opposite sides of valleys or mesas, while others (3) argue that bending of ridges and grooves entering valleys from a side tributary supports flow in the direction parallel to the valley. All agree that the materials represent some sort of viscous flow processes, but opinions differ on the details of the mechanism; most authors call on processes of gravity-driven debris flow, assisted by ice or water in the interstices derived from either groundwater or the atmosphere (e.g., see 6, 9-11).

New THEMIS, MOLA and MOC data provide additional perspectives on the origin of the debris aprons and lineated valley fill, suggesting that at least in some areas, glaciation (accumulation of snow and ice to sufficient thickness to cause its local and regional flow) may have played a significant role. We have analyzed numerous areas along the dichotomy boundary north of 30 degrees north latitude and present the results from one area as an example. In this region (Fig. 1) just south of Deuteronilus Mensae, a T-shaped valley occurs just south of a large depression. The walls of the large depression are characterized by debris aprons and there is a break in the southern rim of the depression that leads to the top of the T-shaped valley (about 100 km across). A topographic profile (Fig. 2) from the floor of the large depression across the southern wall, across the top of the T and along the vertical part of the T shows 1) the flat floor of the large depression, 2) the classic convex upward slope of the debris apron, 3) the elevated floor of the top of the T, 4) the convex upward slope of the vertical part of the T. Note that the floor of the T-shaped valley along the top of the T lies at elevations as high as -2600 m, almost a kilometer above the large depression floor. Note too, that the bottom of the valley along the vertical part of the T is almost at the same level as the floor of the large depression. THEMIS data superposed on MOC altimetry and viewed perspectively shows strong evidence for flow lineations (Fig. 3), their characteristics and their directions; details of the lineations are shown in the MOC images (Figs. 4-6). Examination of Figs. 1 and 3 shows evidence of numerous lineations in the 20 km diameter crater south of the eastern arm of the T. The lineations on the floor of the crater converge and can be traced through the gap in the crater wall (Fig. 5, lower part)

joining lineations beginning at the eastern edge of T (Fig. 5, upper right). Similar lineated valley fill extends from the mouth of a north-trending valley in the lower western part of the T, is deformed by valley lineations from valley fill apparently moving from the higher terrain to the west, and then joins the general lineated valley fill just to the east (Fig. 5). Furthermore, additional lineated valley fill begins at the base of the broad amphitheater on the western part of the top of the T, and converges with at the T-junction with the lineated valley fill coming from the west (Fig. 4) and the east (Fig. 5). From here, these three major flow lineation directions converge and extend down the vertical part of the T, with many of the lineations contorted at the margins of the convergence (Fig. 6). At the end of the major lobe, the topography is broadly convex upward (Figs. 2, 3) and the perspective view (Fig. 3) shows the distinctive lobe like nature of the lobe as it extends into the adjacent low-lying terrain.

What processes are responsible for the valley fill? These lineations and their complex patterns resemble flow lines in glacial ice, particularly where glacial ice converges from different directions at different velocities and deforms (compare Figs. 4, 6 and 7). Detailed analysis of the MOC, THEMIS and MOLA data suggests that changing environments and local topographic conditions (such as the crater wall and the narrow valleys) favored accumulation and preservation of snow and ice, and its glacial-like flow down into surrounding areas for distances approaching 70 km. Such environments are typical of snow and ice accumulation and debris-covered glacial flow in the Antarctic Dry Valleys, a cold polar desert analogous to the environment on Mars. Alternative hypotheses focus predominantly on groundwater or ice from atmospheric water vapor lubrication of debris flows (e.g., see 6, 9-11). We believe that the thickness of the deposit, the great lateral extent and continuity of flow lineations, and their complex interactions consistent with glacial-like flow, are all evidence that supports glacial-like flow of debris rich ice, rather than ice-containing debris. The relationship between the lineated valley fill and the classic debris aprons is not yet firmly established; however, the contiguous nature of many examples of lineated valley fill and debris aprons (Fig. 1) suggests that if the glacial interpretation of the valley fill is supported by further observations, then glacial ice may play more of a role in the formation of debris aprons than previously suspected.

The age of the deposits in this region are Amazonian (~300 Ma, with some of the deposits as young as 10 Ma (11)), broadly similar in age to the tropical mountain glaciers of Tharsis Montes and Olympus Mons (14). This suggests that there may have been periods during the Amazonian when tropical and mid-latitude glaciation were extensive. Thus, glaciation may have played a significant role in evolution of the dichotomy boundary during the Amazonian; significant amounts of ice could remain today in these valleys beneath a protective cover of sublimation till.

References: [1] Squyres, S.W. (1978), *Icarus*, 34, 600. [2] Squyres, S.W. (1979), *JGR*, 84, 8087. [3] Luchitta, B.K. (1984), *LPSC XIV*, abs. no. B409. [4] Kochel, R.C. & Peake, R.T. (1984)

LPSC XV, abs. C336. [5] Carr, M.H. (1995), *JGR*, 100, 7479. [6] Carr, M.H. (1996), *Water on Mars*. [7] Colaprete, A. & Jakosky, B.M. (1998), *JGR*, 103, 5897. [8] McGill, G.E. (2000), *JGR*, 105, 6945 [9] Mangold, N. & Allemand, (2001), *GRL*, 28, 407. [10] Mangold, N. et al. (2002), *PSS*, 50, 385. [11] Mangold, N. (2003), *JGR*, 108, doi: 10.1029/2002JE001885. [12] Benn, D.I. & Evans,

D.J.A. (1998), *Glaciers and Glaciation*. [13] Marchant, D.R. & Head, J.W. (2004), *LPSC XXXV*, abs. no. 1405. [14] Head, J.W. & Marchant, D.R. (2003), *Geology*, 31, 641. [15] Head, J.W. et al. (2003), *Nature*, 426, 797. [16] Post, A. & Lachapelle, E.R. (2000), *Glacier Ice*.

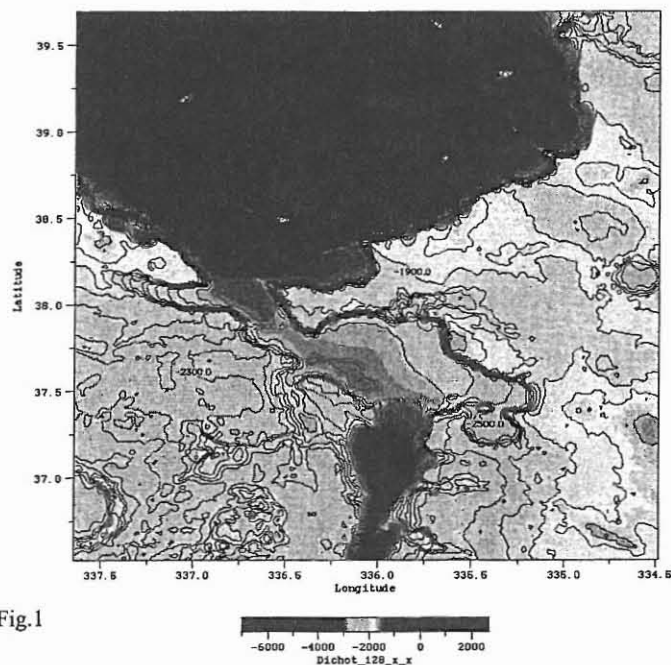


Fig.1

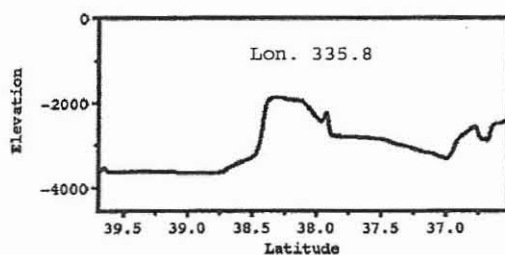
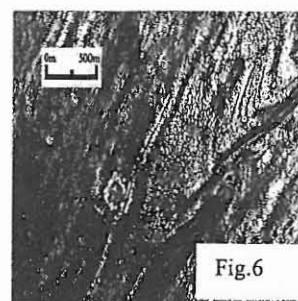
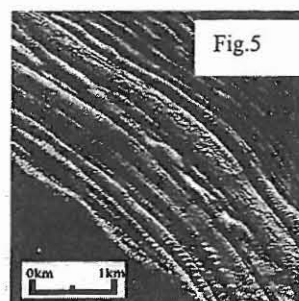
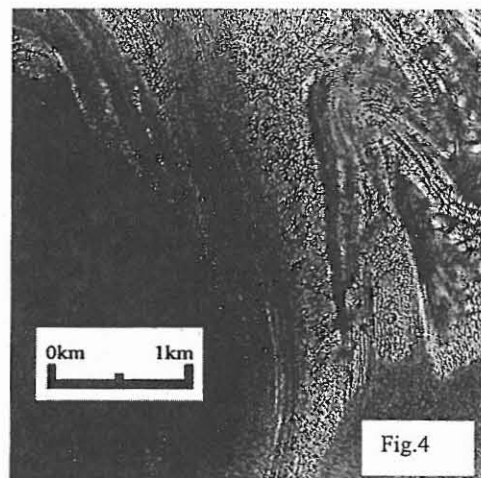


Fig.2



MARS DICHOTOMY BOUNDARY DEGRADATIONAL PROCESSES: MODEL OF THE NOACHIAN-HESPERIAN HYDROLOGICAL CYCLE. James W. Head¹, Michael H. Carr², Caleb I. Fassett¹, and Patrick S. Russell¹. ¹Department of Geological Sciences, Brown University, Providence, RI 02912, ²U. S. Geological Survey, 345 Middlefield Road, Menlo Park, CA 94025 (james_head@brown.edu)

Summary: The global climate of Mars is thought by many to have changed to its present cold and dry state from warmer and wetter conditions earlier in its history during the Noachian. Here we summarize evidence for a major transition in near-surface hydrogeologic conditions in the Late Noachian, and a fundamental change in the martian hydrological cycle. Hydrogeologic conditions then were characterized by five main domains: 1) an accumulation zone at higher altitudes, where atmospheric water entered the system through pluvial/nival activity and was transported laterally by valley networks for tens to hundreds of kilometers before evaporating, sublimating, or completely reentering the vadose zone, 2) an upper mid-altitude region dominated by the vadose zone where pluvial/nival activity was less important, and valley networks were much less common, 3) a lower mid-altitude region where the groundwater table occasionally reached the surface and theater-headed valleys and large fretted channels formed by groundwater sapping and headward retreat, 4) a lower altitude region, where the groundwater table normally (the dichotomy boundary) and where fretted and knobby terrain formed by large-scale groundwater sapping, and 5) a very low altitude region (the northern lowlands), largely below the groundwater table, where groundwater discharge accumulated. Variations in the exact altitude distribution of these zones and the often transitional boundaries between them, strongly suggest that the groundwater system was irregularly recharged during this period and that the groundwater table oscillated vertically with time. Changing atmospheric and near-surface conditions at the end of this period resulted in the freezing of the outer layers of the crust to form a global cryosphere. At the end of this period, the hydrological cycle changed from one which was vertically interconnected from the atmosphere through the surface and subsurface to the groundwater system, to a horizontally layered one in which the groundwater reservoir is separated from the surface reservoir by a global cryosphere, a condition that still characterizes Mars today, ~3.5 billion years later.

Introduction and Background: Controversy surrounds that nature of early climatic conditions on Mars [1, 2]. In our approach, rather than trying to uniquely determine the nature of the Noachian climate from the geological record (e.g., valley networks [3]) or from global climate models [4], we have adopted the strategy of using the present environmental conditions (cold dry polar desert [5]) as a baseline, and working back in geological time until the geological evidence forces us to the conclusion that the climate must have been different. When and if such evidence emerged, this information might provide insight into the manner in which the environment changed and thus provide independent insight into Noachian climatic conditions. We outline elsewhere [6] the detailed evidence that leads us to the conclusion that cold, dry polar desert conditions and a globally continuous cryosphere [7] characterized the martian climate and near-surface conditions as far back as into the Early Hesperian. Local breaching of the cryosphere and outflow of sequestered groundwater characterized major hydrogeological activity during this 3+ billion year period, and although short-term climate variations may have occurred at these times [8], any changes appear to have been insufficient to alter the globally continuous cryosphere. Three

major types of features common in the Late Noachian signal a fundamental change in these conditions: 1) **Fretted and knobby terrain**, which we interpret to represent the presence of a groundwater table intersecting the surface, and the consequent sapping and erosion of the globe-encircling highland-northern lowland boundary [9]. 2) **Theater-headed valleys/Fretted channels/Large valley networks**, which we interpret to represent groundwater sapping occurring commonly near the dichotomy boundary, and focused sufficiently to cause significant erosion and headward retreat to form large sapping valleys [10]. 3) **Valley networks**, [e.g., 3, 11] which occur primarily at higher elevations [1] are interpreted to represent overland flow and seepage of water and channelization; we interpret these to represent the result of pluvial/nival activity and to produce recharge through the vadose zone into the groundwater system [12]. Previously, we have outlined the basic hydrologic principles that govern the hydrological cycle and related processes in environments like those on Mars [13,14]. Here we outline a synthesis of these findings that describe a model of Late Noachian hydrogeology and the transition to a radically different hydrologic cycle than that in existence today [e.g., 7, 15].

The Late Noachian Hydrologic System: We believe that the Late Noachian hydrologic system shares many of the basic characteristics of the present terrestrial hydrologic cycle [13,14], modulated by some of the conditions described above. On the basis of our interpretation of the major terrain types listed above, we envision the hydrogeologic elements and hydrologic cycle at this time as follows.

The most critical element for recognizing the nature of the hydrological cycle is the location of the top of the groundwater system, the water table. This most commonly occurs in the subsurface in land areas on Earth, or at the edge of large standing bodies of water, such as lakes, seas and oceans, where the margins of the water body and the water body equipotential surface itself delineate the water table. On Mars, any Late Noachian standing body of water [e.g., 15] is no longer present, and thus indirect evidence must be sought as to its location.

We interpret the fretted and knobby terrain occurring at the dichotomy boundary and encircling the majority of the boundary between the northern lowlands and the southern uplands at elevations between -1 and -4 km to represent the approximate location of the water table during the Late Noachian [9]. The fretted and knobby terrain is clearly derived from the collapse and degradation into knobs and mesas of adjacent upland cratered terrain. On the basis of 1) its very widespread distribution around almost the entire edge of the exposed upland terrain at the northern lowland boundary, 2) its apparent Late Noachian age (although degradation processes continued to modify it), and 3) its consistent distribution in terms of altitude range [9], we interpret this unit as marking the location of the water table and having originated in the following manner. Above this general level, the surface of Mars was a zone of infiltration, where water falling on the surface ultimately percolated vertically through the vadose zone into the saturated zone and then flowed laterally. In the vicinity of the north-south dichotomy boundary scarp, the water table intersected the surface [7]. In this region, ground-

water flows through the porous rock and soil layers discharged to the surface by seepage, and by localized flow as springs. This eroded and undercut the surface topography causing channelization and backwasting of the scarp and upland cratered terrain. Discharged water and sediment flowed down-slope into the northern lowlands. If this fretted and knobby zone is correctly interpreted as the location of the water table, then its presence means that groundwater readily exchanged with the surface on a global scale and that the global cryosphere had not yet developed. Furthermore, the fact that this terrain is not seen in any abundance in younger terrain elsewhere on Mars suggests that this extensive distribution is revealing geological processes that are not common later in Mars' history.

What were the processes responsible for charging and recharging the global aquifer under these conditions? The valley networks provide evidence for the presence of liquid water, surface runoff, and stream activity at higher elevations in the southern uplands. Their presence strongly suggests that water was falling onto the surface due to pluvial or nival activity, leading to subsequent overland flow and stream channel formation. Valley networks are more common at higher elevations [16,17] in the southern uplands and occur on the flanks of craters at the highest elevations there. If the valley networks were to represent *effluent streams* drawing groundwater from the surrounding regions and were also undergoing significant related groundwater sapping, as envisioned by some [e.g., 16], then the implication is that the water table is just below the surface at elevations of ~3 km, for example in the circum-Hellas highlands. This implies that the global water inventory involves virtually all crustal pore space and thus provides a global water volume well in excess of 1 km global equivalent layer [1,7]. Instead, we believe that the upper part of the regolith in the highlands represents the vadose zone and that the water table occurs at a much deeper level below the surface. We interpret valley networks to be *influent streams*, not *effluent streams*. As *influent streams*, valley network channels form from collection of overland flow from pluvial or nival water deposition on the surface, lateral transport in the channels, and ultimate drainage down into the vadose zone over the course of their flow. In this manner, they feed the groundwater system largely from above and maintain the level of the water table, which varies depending on the amount of water entering the groundwater system by precipitation and infiltration and the amount leaving the system, for example by evaporation or sublimation back into the atmosphere. Although the depth to the water table is not necessarily constant across the surface, the location of the intersection of the water table and the surface in the fretted and knobby terrain suggests that there may be as much as 3-4 km between the highest surface in the southern uplands and the water table there. This strongly suggests that there is a vadose zone in the southern uplands that may be up to several kilometers thick, depending on rates of infiltration and recharge.

Evidence supporting the presence of a vadose zone comes from the mid-altitude region of the southern uplands where valley networks are much less common. We interpret these to represent areas where pluvial/nival activity was much less important than in the highlands, and where valley networks had largely lost their transported water by influent processes and seepage and infiltration into the vadose zone. In this model, the lower abundance of valley networks at lower elevations are a natural consequence of their formation in the vadose zone and their influent behavior. Indeed, the unusual

nature of many aspects of valley networks [17] can be readily explained by influent streams. If this interpretation is correct, convolved in their characteristics is important information about soil porosity and permeability, and water flux [12].

Located in a zone between the fretted/knobby terrain and the valley networks is a series of very large valley network-like features known as fretted channels and theater-headed valleys [17]. These are broad, flat-floored, steep-walled valleys up to 20 km wide that extend from the margins of the northern lowlands deep into the uplands. The presence of headward linear closed depressions and collapsed margins strongly suggest that the channels and valleys formed by subsurface groundwater movement and sapping [17]. They are primarily located between elevations of -3 km and +1 km, overlapping with the elevation range and area in which there are fewer valley networks. The range in the elevation distribution of the sapping channels may be due to their headward erosion, or could signal differences in the level of the water table. More discharge into the regolith would raise the water table and enhance sapping at higher levels. Alternatively, as the northern lowlands freeze and the cryosphere migrates southward, perhaps the water table rises and the groundwater builds up hydrostatic head [10].

Summary: These data and correlations, and the similarities to terrestrial hydrogeologic features and the hydrologic cycle, suggests that this model (Fig. 1) may reasonably approximate the nature of the Late Noachian hydrologic cycle. This scenario predicts that the northern lowlands were largely below the level of the water table and thus may have been flooded, although the high latitudes indicate that much of the region might have been frozen. This scenario and hydrologic system configuration optimizes the erosion and modification by significant seepages, fluvial activity, and sapping, all leading to erosion and retreat of the dichotomy boundary during the Noachian and Hesperian.

- References:** [1] Carr, M. H., *Water on Mars*, Oxford, 1996. [2] Pollack, J. et al., *Icarus*, 71, 203-224, 1987. [3] Craddock, R. and A. Howard, *JGR*, doi:10.1029/2001JE0011505, 2002. [4] Haberle, R. *JGR*, 103, 28467-28490, 1998. [5] Hecht, M., *Icarus*, 156, 373-386, 2002. [6] Head, J. and L. Wilson, *LPSC* 32, #1218, 2001. [7] Clifford, S., *JGR*, 98, 10973-11016, 1993. [8] Baker, V., *Nature*, 412, 228-236, 2001. [9] Head, J. et al., *Vernadsky-Brown Microsymposium* 38, ms30,31, 2003. [10] Head, J., et al., *Vernadsky-Brown Microsymposium* 38, ms28, 29, 2003. [11] Hynek, B. and R. Phillips, *Geology*, 29, 407-410, 2001. [12] Fassett, C. and J. Head, *Vernadsky-Brown Microsymposium* 38, ms16, 17, 2003. [13] Head, J. et al., *Vernadsky-Brown Microsymposium* 38, ms26, 2003. [14] Head, J. et al., *Vernadsky-Brown Microsymposium* 38, ms27, 2003. [15] Clifford, S. and T. Parker, *Icarus*, 154, 40-79, 2001. [16] Grant, J., *Geology*, 28, 223-226, 2000. [17] Carr, M. *JGR*, 100, 7479-7507, 1995.

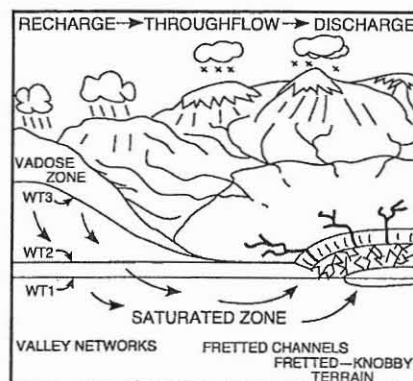


Figure 1. The Late Noachian hydrological cycle.

MARS DICHOTOMY BOUNDARY DEGRADATIONAL PROCESSES IN SPACE AND TIME: CLUES TO GLOBAL CLIMATE EVOLUTION. James W. Head and Caleb I. Fassett. Department of Geological Sciences, Brown University, Providence, RI 02912, (james_head@brown.edu)

Introduction

It has long been known that the boundary between the northern lowlands and the southern uplands (the dichotomy boundary) is characterized by both a generally distinctive topographic change, as well as characteristic geological units that appear to represent processes of weathering, topographic degradation and scarp retreat southward from the dichotomy boundary. We first examine the nature and distribution of the units that characterize this boundary and then discuss how modification processes have varied over time and space.

General description and distribution. A variety of terrains characterize the dichotomy boundary (Figures 1-4). At the largest scale (1:15M; [1-3]), the southern uplands are characterized by a variety of Noachian-aged units, most prominently the Plateau and high plains assemblage [1,2] of units, of which the Plateau sequence is the most important. Members of the Plateau sequence form "rough, hilly, heavily cratered to relatively flat and smooth terrain, covering most of the highlands". The most widespread of the units there are of Noachian age and include the heavily cratered units (Npl1 and Npl2), the heavily cratered unit dissected by a higher density of valley networks (Npld), an etched terrain "similar to the cratered unit but deeply furrowed by sinuous, intersecting, curved to flat-bottomed grooves producing an etched or sculptured surface" (Nple), and smoother intercrater ridged plains of possible volcanic origin (Nplr). The surface of the northern lowlands, on the other hand, is largely covered by the younger Hesperian-aged Vastitas Borealis Formation, and older units are virtually absent at the surface [1-3].

The intervening area between the southern uplands and the northern lowlands, commonly referred to as the dichotomy boundary, is a broad region hundreds of km wide that extends along the border and has a variety of units with a range of ages. Previous mappers at the 1:15M scale have put a symbol on the map described as the "Highland-Lowland boundary scarp" which was defined as a "Diffuse zone of transition between highland and lowland physiographic provinces" [1-3] (Figs. 1-4). One of the most prominent units in association with this zone is mapped as HNu, Noachian-Hesperian, undivided [1,2]. This unit forms "closely spaced conical hills a few kilometers across whose distribution indicates that they are remnants of numerous craters." The unit also "forms rugged terrain on margins of cratered plateaus, and isolated remnants..." The unit is gradational with the Apk, the Amazonian-aged knobby plains material, where the two units adjoin, but hills in the HNu unit "are more closely spaced, larger, and occupy more than about 30 percent of the area." The HNu unit is interpreted as "eroded remnants of ancient cratered terrain produced by mass-wasting processes, possibly as result of removal of ground ice..." Etched plains material (AHpe) is composed of irregular mesas and pits, and ranges from mid-Hesperian to to mid-Amazonian in age [1-3]. Also characteristic of the boundary at this scale are outflow channels of Hesperian age and younger channels of Amazonian age, both of which strike generally normal to the slope of the dichotomy boundary and modify it.

Later regional units obscure and heavily modify large portions of the dichotomy boundary (the Tharsis volcanic complex, the Chryse basin and outflow channel complex, and the thick mantling deposits of the Medusae Fossae Formation). We now proceed to characterize the broad dichotomy boundary zone where it is not obscured by later events (Fig. 1).

Detailed Areal Distribution. One of the most prominent and aerially significant developments of this terrain occurs in the Deuteronilus Mensae region, extending ~1500 km from about 320 to 355 W, and occupying a band of terrain up to ~800 km wide along the northern lowland-southern upland dichotomy boundary. In this region, the terrain spans an eleva-

tion range from ~4 km to ~2 km. It is largely made up of fragmented and isolated islands of Hesperian ridge plains (Hr) and Noachian plains, where the fragments are large enough to map as specific outcrops, rather than components of a separate specific unit, as with HNu. Also mapped are large swaths of Apk, in the lows between the large islands, and preferentially toward the eastern edge of the region.

A second major area of development is adjacent to Deuteronilus, extending eastward along the dichotomy boundary for about 2400 km from ~275 to 320 W to the Isidis Basin. Here the terrain is more knobby and occupies a 500-700 km wide belt that spans an elevation range from ~3 km to ~0 km. The major map unit in this area is HNu, with minor amounts of Apk.

East of the break in the dichotomy boundary formed by the Isidis Basin, the knobby terrain reappears in a swath at, and parallel to, the dichotomy boundary extending from the eastern rim of Isidis (~260 W) for about 4700 km to the vicinity of 180 W, before it becomes largely mantled by the younger Medusae Fossae Formation. In this region, the elevation range is about ~2 km to 0 km. The major unit mapped in the eastern part of this area is HNu, with minor amounts of Apk. At the crater Gale (~222 W) the proportion changes so that to the east of Gale, Apk dominates.

Description of the dichotomy boundary using MOLA detrended topography: MOLA detrended topography (Fig. 4) where the regional slope has been removed and local slope variations are enhanced, is ideally suited to demonstrate the nature of the progressive disintegration of the southern uplands at the dichotomy boundary. Figure 4 shows a significant portion of this boundary between longitude 288W and 298W, and latitude 30 to 39N. At the base of the image, heavily cratered Noachian aged etched plains (Nple) [1,2] are exposed over the lower 200 km of the area. At the northern edge of this area, a series of complex generally east-west trending faults cut the Nple in to a series of polygonal blocks. Theater-headed valleys and channels form in and adjacent to these faults, and enlarge and often interconnect them. Northward of this, approximately in the middle of the image, is a broad, 150-200 km wide zone in which the polygonal terrain is further broken up and degraded into smaller polygons. This area is mapped as part of the Hesperian-Noachian undivided (HNu) terrain [1,2] and is clearly transitional to the larger blocks of polygons toward the southern uplands. In the upper right-hand part of the image, the terrain is mapped as Amazonian-Hesperian etched plains (AHpe) [1,2], characterized by irregular mesas and pits. This terrain is characterized by even smaller and more rounded knobs that appear to be transitional to the mesas and polygons of HNu. Thus, the case has been historically made that the units and facies that are mapped across the dichotomy boundary here represent the progressive degradation and mass wasting of the original margin of the dichotomy boundary (see summary in [3, 4]). The distance over which this terrain occurs suggests that the retreat in this area (Fig. 4) could have been 200-400 km.

Facies and terrains: In the broader context of this and related areas (Fig. 1-4) we observe a series of features and facies that characterize the dichotomy boundary across the zone. These features are not always all present in the same locations, and they also overlap with each other to some degree. They are as follows: 1) **Unmodified plains/uplands terrain:** 2) **Polygonized Craters (PCs):** These have polygons developed in crater interiors and often have exit channels, which are usually fretted valleys. 3) **Theater-headed valleys (THVs):** These develop from PCs as well as the fracture zones and polygonal plateaus. 4) **Fracture zones (FZs):** Linear fractures ranging from graben to valleys, that are narrow to wide and oriented usually parallel but sometimes normal to the

dichotomy boundary. **5) Polygonal plateaus (PPs):** These are highly polygonized plains units that have been cut by the fractures seen in the FZ, but along which erosion and removal of material has occurred. **6) Hummocky terrain (HT):** Transitional to polygonal plateaus; smaller and less distinct, more rounded, but has polygons interspersed throughout, with generally fewer toward the knobby terrain. **7) Knobby terrain (KT):** Abundant small knobs, smaller and lower elevation than the hummocks in the HT, occasional hummocks. **8) Etched terrain:** Appears to have undergone some combination of thermokarst and eolian reworking.

Summary and interpretation: On the basis of the successive degradation of the terrain as represented by the faulting, polygonization, polygon degradation to mesas, and their further degradation to knobs, and on the features mapped within the zone (theater headed valleys, sapping features, channels, etc.), we favor the interpretation that a significant amount of groundwater was involved in the initial degradation and subsequent retreat of the dichotomy boundary. We further hypothesize that this boundary represents the altitude region at which the water table intersected the surface in the late Noachian and into the early Hesperian. This boundary may thus be the focal point for the top of the groundwater system at this time. Above this existed the vadose zone in the southern uplands, and the water table sloped upward toward the southern uplands at an angle that was related to the level of recharge in the system at any given time.

Following this early period, geological evidence suggests that the cryosphere continued to thicken and to become regionally stable and then globally extensive and thick [e.g. 4]. During this transition period, groundwater leakage at the base of scarps may have continued and freezing water may have assisted the downslope movement of material to cause debris aprons and lineated valley fill [5; Fig. 4-16]. Additional evidence suggests that the lineated valley fill and perhaps many debris aprons were characterized by a significant percentage of ice, placing them beyond the realm of simple ground water or ground ice-assisted creep, and into the range of glacial and rock covered glacial activity. New MOC, MOLA and THEMIS data strongly suggest that many examples of lineated valley fill are the result of glaciation [e.g. 6]. We have mapped numerous examples of apparent glaciation and ice-assisted creep along the dichotomy boundary from Deuteronilus Mensae to near the Isidis Basin (about 30-50 degrees N). Between just NW of Isidis and Gale Crater (30N-10S), the dichotomy boundary is narrower and less complex, in part reflecting the lack of prominent debris aprons and lineated valley fill related to ground ice and glaciation in the mid-latitudes.

In summary, erosional processes operating on the dichotomy boundary have varied in time and space. Valley networks, groundwater flow and seepage, sapping, and channel formation all operated to modify the boundary in the Noachian and Hesperian. By the Amazonian, the presence of a global cryosphere had minimized the role of groundwater and the general cooling climate had enhanced the role of surface ice-assisted creep and possible glaciation. At this point, variation in orbital parameters cause insolation changes that from time to time made water ice stable in the 30-50 latitude region [e.g., 7] and 'ice ages' occurred. When these were of long duration, sufficient ice and snow could accumulate to make ice-assisted creep and glaciation a major process in the modification of the dichotomy boundary in the mid-latitudes [6].

Reference: [1] D. Scott and K. Tanaka, USGS Map I-1802A, 1986. [2] R. Greeley and J. Guest, USGS Map I-1802B, 1987. [3] K. Tanaka et al., JGR, 108, 8043, 2003. [4] S. Clifford, JGR, 98, 10973, 1993; S. Clifford and T. Parker, Icarus, 154, 40, 2001. [5] M. Carr, Water on Mars, Oxford, 229p., 1996. [6] J. Head et al, this volume. [7] J. Head et al., Nature, 426, 797, 2003.

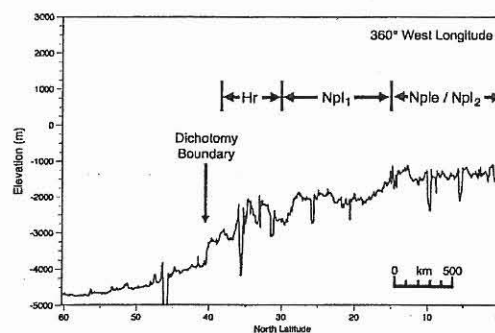


Figure 1.

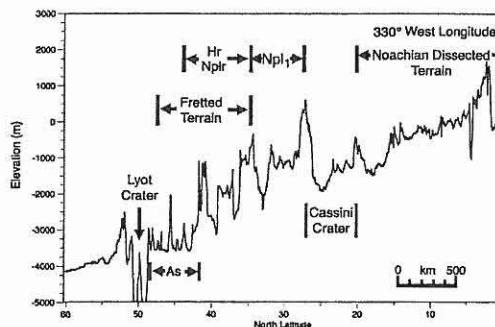


Figure 2.

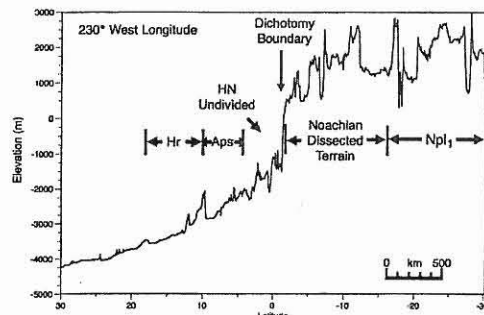


Figure 3.

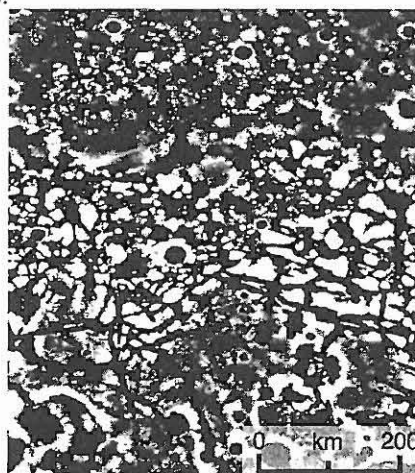


Figure 4.

CRUSTAL DICHOTOMY BOUNDARY AND FRETTED TERRAIN DEVELOPMENT AT AEOLIS

MENSAE, MARS. R. P. Irwin III^{1,2} and T. R. Watters¹, ¹Center for Earth and Planetary Studies, National Air and Space Museum, Smithsonian Institution, 4th St. and Independence Ave. SW, Washington DC 20013-7012, Irwinr@nasm.si.edu, twatters@nasm.si.edu. ²Department of Environmental Sciences, University of Virginia, Charlottesville VA 22904.

Introduction: The origin of Martian fretted and knobby terrain has remained uncertain since the landforms were first described by Sharp in 1973 [1]. As a control on modeling efforts, it is important to establish the relationship of these landforms, if any, to the origin of the crustal dichotomy. Most studies have focused on fretted terrain in northern Arabia Terra, where investigators generally agree that ground ice has been important in modifying precursor knobs and fretted valleys [2–5]. The initial processes that isolated mesas from the high-standing terrain are less certain. Characteristics of some fretted valleys suggest an origin by fluvial erosion, despite their poorly developed drainage networks [5]. Other proposed mechanisms include crustal extension and structural control of sapping [6].

Situated near the martian equator at the crustal dichotomy boundary, Aeolis Mensae (Fig. 1) provides a pristine example of fretted terrain development without the younger landforms attributed to ground ice. We examined an area bounded by 15°S, 15°N, 120°E, and 150°E, adjacent to the cratered and dissected area described by Irwin and Howard [7]. Our observations indicate that Aeolis Mensae fretted terrain developed in a thick aeolian sedimentary deposit of late Noachian/early Hesperian age, which was emplaced along an older dichotomy boundary. Sediments were emplaced and eroded as fluvial activity declined, with minimal influence from highland valley networks.

Distinguishing highland bedrock from sedimentary deposits: The extensive degradation of Aeolis Mensae relative to the adjacent cratered highlands, where 20–50 m deep valley networks are preserved [7], suggests either that the mensae are composed of different materials than the highland crust, or that geomorphic processes were concentrated along the dichotomy boundary [1]. Malin and Edgett [8] describe criteria for distinguishing sedimentary deposits on Mars from highland bedrock. Mesas in this area have boulder-free talus at MOC resolution, small-scale spur and gully morphology (suggestive of poorly cohesive materials, Fig. 2), massive and layered stratigraphic units, pedestal craters, knobs and yardangs, a near absence of fluvial valleys, and they overlie the termini of some valley networks in the area. The fretted materials supported high erosion rates on the order of 10^{-2} mm/year within fretted valleys, which formed only in materials with these morphologic characteristics. Fretted valleys breached crater rims in the plateau materi-

als, but the rims are resistant to erosion when developed in the adjacent highland rocks. The fretted plateau deposits have thermal properties and rock abundances that suggest a well-sorted deposit of fine sand and smaller grains, which overlie coarser materials that are exposed at deflation pits and in ejecta [9].

Elevation (m)

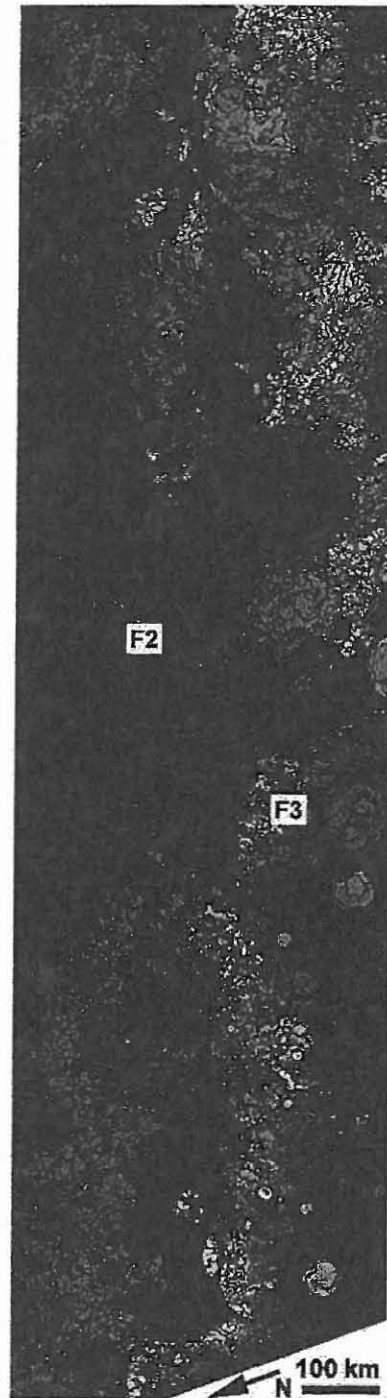
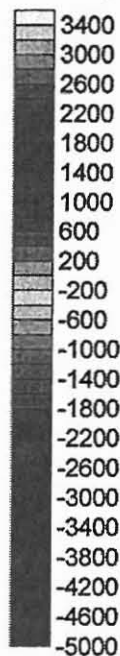


Fig. 1. Mars Orbiter Laser Altimeter topography of the study area in Aeolis Mensae, 1830 km across.

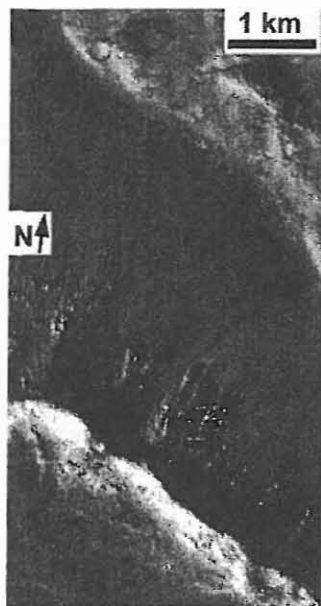


Fig. 2. Fluted valley crests and boulder-free talus on the an outlying isolated mesa in the fretted terrain. All observed outcrops in the fretted plateau materials have these characteristics, which suggest mass wasting of poorly cohesive materials without fluvial erosion. The strong albedo contrast at the base and crest of valley walls is an effect of high-pass filtering. MOC M10-03605.

Age relationships: Aeolis Mensae mesas and knobs are not dissected by valley networks as are adjacent highland slopes (Fig. 2). Most valley networks crossing the boundary have a hanging relationship with fretted valleys [7] (Fig. 3), consistent with a base-level reduction or southward advancement of the boundary scarp [7,10]. Fretted terrain likely formed between late Noachian/early Hesperian episodes of fluvial activity. These valley networks do not appear to continue into the lowland fretted/knobby terrains.

As a cratered slope underlies the fretted terrain, the dichotomy very likely predates the early Hesperian fretting processes [11,12]. Degraded crater morphology suggests that middle and late Noachian craters formed and were eroded on a precursor slope. Noachian craters are not modified by extensional faulting along the boundary in this area, as would be expected for a middle Noachian or later origin of the dichotomy. It is possible that a precursor dichotomy boundary slope dates to the early Noachian epoch (~3.95–4.5 Ga) and is coeval with the formation of the lowlands.

Possible emplacement and erosional processes: Observed aeolian deflation sites and pedestal craters require that the sediments were very well sorted, with no major lag-forming component of granules (2–4 mm) or larger particles. Whereas wind is a capable mechanism for sorting these particles, valley networks would probably deliver some coarse materials that would form a lag during deflation. Given few examples of fluvial valleys interacting with the fretted plateau deposit, it appears to have been emplaced mainly by wind. The confinement of the well-sorted deposit as a discrete sedimentary wedge along the older dichot-

omy boundary suggests emplacement primarily by aeolian processes from lowland sediment sources.

Erosion of these knobs may have been limited by the backwasting or disaggregation of the capping unit. Yardangs, etched terrain, absence of continuous flow paths, and the temporal relationships with valley networks favor wind as the main erosional medium [13].

Fig. 3. Valley networks crossing the dichotomy boundary scarp. (a) A valley developed a wide floor with a –900 m base level, which is presently armored by relatively coarse materials (thermally dark in daytime IR, white arrows). Development of knobby terrain to the north caused a base-level decline to –2300 m and development of a knickpoint in the longitudinal profile (black arrow). Mosaic of THEMIS I02367004, I02005008, and I01306006. (b) Longitudinal profile of the valley in (a).



- References:** [1] Sharp R. P. (1973) *JGR*, 78, 4073–4083. [2] Squyres S. W. (1978) *Icarus*, 34, 600–613. [3] Lucchita B. K. (1984) *JGR*, 89, B409–B418. [4] McGill G. E. (2000) *JGR*, 105, 6945–6959. [5] Carr M. H. (2001) *JGR*, 106, 23,751–23,593. [6] McGill G. E. and Dimitriou A. M. (1990) *JGR*, 95,12,595–12,605, 1990. [7] Irwin R. P. and Howard A. D. (2002) *JGR*, 10.1029/2001JE001818. [8] Malin M. C. and Edgett K. S. (2000) *Science*, 290, 1927–1937. [9] Irwin R. P. et al., *JGR*, in press. [10] Kochel R. C. and Peake R. T. (1984) *JGR*, 89, C336–C350. [11] Frey, H. V. et al. (1988) *Proc. LPSC 18*, 679–699. [12] Maxwell T. A. and McGill G. E. (1988) *Proc. LPSC 18*, 701–711.

Gravity Modeling of the Isidis/Syrtis Major Region of Mars: Implications for Lithospheric Properties and for the Origin and Evolution of the Dichotomy Boundary

Walter S. Kiefer (Lunar and Planetary Institute, 3600 Bay Area Blvd., Houston TX 77058, kiefer@lpi.usra.edu, (281) 486-2110 (Office), (281) 486-2162 (Fax))

Introduction

Analysis of the gravity [1,2] and topography [3] of Mars provides our best view of the internal structure of Mars [4-9]. In this work, I model the gravity of the martian hemispheric dichotomy boundary in the region near the Isidis impact basin and Syrtis Major. I focus on two tasks. First, I estimate how the lithosphere's elastic thickness varies with location in this region of the dichotomy boundary. This constrains the thermal structure at the time the bulk of the topography was emplaced, roughly the first few hundred million years of martian history. Second, I develop models for the mascon beneath Isidis. The long-term preservation of this mascon constrains the thermal structure at the time of basin formation. Taken together, these results constrain the early thermal history of this portion of the dichotomy boundary. I use gravity model JGM95I-01, obtained from the Planetary Data System [10]. Results presented here are for spherical harmonic degrees 2 to 60, because the amplitude of terms above degree 60 are restricted by imposition of a power-law constraint in the gravity inversion.

Flexure Model

The thickness of the elastic lithosphere is an important parameter because it helps to constraint the thermal structure of the lithosphere at the time a topographic load was emplaced. The usual practice in planetary geophysics is to constrain the lithospheric thickness using a

spectral admittance model [5-7]. However, this approach does not work well when substantial, uncorrelated surface and subsurface loads are both present in a region. In the Isidis/Syrtis region, there is 5.5 km of surface relief, and both the Syrtis Major cumulate chamber [8] and the Isidis mascon [1,2] are large subsurface loads, which limits the utility of the admittance approach.

As an alternative, I have assessed the lithospheric thickness by calculating the RMS misfit in the spatial domain between the observed gravity and a suite of models calculated assuming that the gravity anomalies are due solely to flexurally-supported topography [11]. The parameters that are varied in these models are the lithospheric thickness and the density of the crust. The mean crustal thickness is 50 km [9] and the mantle density is 3400 kg m^{-3} [12]. The elastic constants are appropriate for basalt.

The results in Figure 1 are for the region between 15° South and 0° North latitude and between 75° and 105° East longitude. For a crustal density of 2800 kg m^{-3} (intact, non-vesicular basalt), the best fit for the elastic lithosphere thickness is 10-15 km. The density of the crust could be reduced due either to vesicles in the basalt or by impact brecciation. Reducing the density to 2600 kg m^{-3} increases the required lithosphere thickness to 20-25 km. The minimum RMS misfit is virtually the same for the two density models and provides no means for distinguishing among them.

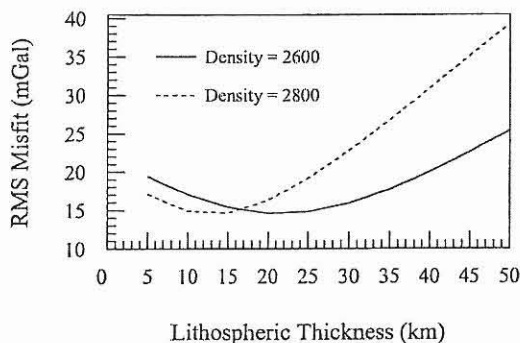


Figure 1: RMS gravity misfit as a function of elastic lithosphere thickness for the region south of Isidis. The solid line is for a crustal density of 2600 kg m^{-3} . The dashed line is for a crustal density of 2800 kg m^{-3} .

Other recent studies of the dichotomy boundary have favored relatively small crustal densities and a wide range of elastic thicknesses. Nimmo examined the dichotomy east of Isidis [7] and found a preferred elastic thickness of 61 km and a crustal density of 2500 kg m^{-3} . Kiefer [8] examined Syrtis Major, slightly northwest of the region studied here, and favored an elastic thickness of 5-15 km and a crustal density of 2600 kg m^{-3} . Preliminary modeling of the northwest part of the Isidis rim (20° - 40° North, 50° - 80° East) suggests that the lithosphere may exceed 30 km, but further modeling is required to assess the trade-off among model parameters and the possible role of bottom loading in that region.

Mascon Model

Isidis is one of the most prominent mascon basins on Mars. The peak gravity anomaly exceeds that expected from the surface topography by 440 mGal, requiring a substantial superisostatic uplift of the crust-mantle interface. Previous models have suggested that the mantle may reach within 3 km of the surface [4], assuming that the crust is relatively dense (2900 kg m^{-3}). If

the crust is less dense due to impact brecciation or vesicularity, less mantle uplift is required. I am assessing these tradeoffs using a buried cylinder modeling method [8].

Regardless of the precise crustal density, it is clear that significant mantle uplift is required by the gravity data. Assuming that Isidis is similar in age to large lunar impact basins, this mantle uplift has been preserved against viscous relaxation for roughly 3.8 billion years. As a simple, first order approximation, this probably requires that the base of the elastic lithosphere was below the depth of the isostatic crustal thickness, roughly 50 km in this region, at the time of the Isidis impact. This result, combined with the elastic thickness results in Figure 1, indicates that the lithosphere in this region of Mars cooled and thickened rapidly in the first 700 Ma of martian history.

References

- [1] Lemoine et al., *J. Geophys. Res.* 106, 23,359-23,376, 2001. [2] Yuan et al., *J. Geophys. Res.* 106, 23,377-23,401, 2001. [3] Smith et al., *J. Geophys. Res.* 106, 23,689-23,722, 2001. [4] Zuber et al., *Science* 287, 1788-1793, 2000. [5] McGovern et al., *J. Geophys. Res.* 107 (E12), doi:10.1029/2002JE001854, 2002. [6] McKenzie et al., *Earth Planet. Sci. Lett.* 195, 1-16, 2002. [7] Nimmo, *J. Geophys. Res.* 107 (E11), doi:10.1029/2000JE001488, 2002. [8] Kiefer, *Earth Planet. Sci. Lett.* 222, 349-361, 2004. [9] Wieczorek and Zuber, *J. Geophys. Res.* 109 (E01009), doi:10.1029/2003JE002153, 2004. [10] Mars Global Surveyor Radio Science archive volume mors_1024, Planetary Data System Geosciences node, <http://pds-geosciences.wustl.edu>, 2004. [11] Turcotte et al., *J. Geophys. Res.* 86, 3951-3959, 1981. [12] Bertka and Fei, *Earth Planet. Sci. Lett.* 157, 79-88, 1997.

The Crustal Dichotomy as a Trigger for Edge Driven Convection: A Possible Mechanism for Tharsis Rise Volcanism? S. D. King¹ and H. L. Redmond^{2, 1&2} Department of Earth and Atmospheric Sciences, 550 Stadium Mall Drive, Purdue University, West Lafayette, IN 47907-2051, ¹sking@purdue.edu, ²redmondh@purdue.edu

Introduction: A vertical constant temperature boundary is convectively unstable and drives convective motion. This is the essence of the Edge Driven Convection (EDC) hypothesis [1]. On Earth, cratonic keels [1] and continent-ocean boundaries [2] are locations where small-scale convection could be triggered from the vertical step in the thermochemical boundary layer at the surface. Because Earth has global, plate-scale motion, it isn't clear whether EDC instabilities can form at all (or any?) passive margins or cratonic keels; although seismic evidence supporting EDC has been observed under the African cratons [3].

While a mantle plume has been argued as the source of the volcanism that formed Tharsis rise, there are concerns that the plume model may not be consistent with other observations (e.g., thermal history calculations [5], the fact that there is a single large volcanic swell on the planet [6], and the ability to explain present day topography and gravity with crustal variations alone [7]). While none of these observations are strong enough to completely rule out a plume origin for the formation of Tharsis, the spatial correlation of the crustal dichotomy boundary and Tharsis rise is intriguing and a relationship between these has been suggested by a number of investigators.

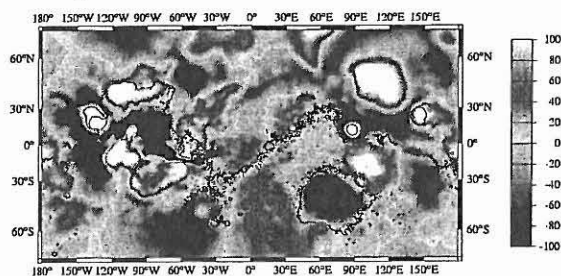


Figure 1. Spherical harmonic degrees 5-60 of the areoid. The black line is the zero contour of the topography, a proxy for the crustal dichotomy. There is no obvious correlation between the areoid and the elevation difference.

Mars is in a stagnant-lid mode of convection and inhibiting EDC by a plate-scale flow may not be a concern for Mars. Because of the lack of correlation between the areoid and the dichotomy boundary (Figure 1), it is almost certain that the crustal dichotomy has a vertical step much like passive margins or cratonic keels on Earth [4]. The question

is whether this step is large enough to initiate a small-scale instability and whether this small-scale instability will survive long enough to produce the extended period of volcanism needed to create Tharsis rise.

Boundary Instability Questions: 1) *Could the dichotomy boundary support a small-scale convective instability?* The answer to this depends on the differential crustal thickness and the gradient of the transition in crustal thickness between the northern and southern hemispheres. If we assume a crustal density of 2900-3000 kg/m³, a mantle density of 3300-3500 kg/m³, and an average dichotomy height of 4 km, an isostatic balance predicts a differential crustal thickness of 20-40 km. This alone seems to be insufficient to nucleate a small-scale instability. If the process that formed the southern hemisphere led to the development of a deep depleted layer beneath the southern hemisphere, much like cratonic keels on Earth, then the difference in 'crustal' thickness between the northern and southern hemispheres could be much larger than indicated by the simple isostatic balance and it might be reasonable to expect small-scale instabilities to form.

One additional complication is that maintaining stable continental keels on Earth requires not only that the keel be buoyant relative to normal sublithospheric mantle but a relatively high viscosity [10]. Thus, keel material is expected to be cold, depleted, and dehydrated. There is yet no evidence for a depleted, dehydrated region of the Martian mantle. Without seismology, our best hope for additional constraints on Martian crustal structure are thermobarometric studies of xenolith inclusions in lavas and/or discovery of kimberlites.

Since gravity on Mars is roughly one third of that on Earth, the growth time for EDC instabilities will be approximately three times as long on Mars as on Earth. This implies that the velocities of EDC flow on Mars will be smaller than on Earth, hence the total amount of mantle cycled through the melt zone will be less than on Earth for the same given period of time. This works against viability of the small-scale instability idea.

2) *Would this boundary have been likely to exist at the time of the formation of the dichotomy boundary?* Cratering studies demonstrate that northern plains are similar in age to the southern hemisphere [8,9]. Thus, the dichotomy boundary is

an old feature. Numerical small-scale convection experiments show that an EDC instability can last for at least 50-100 million years, limited mostly by the erosion of the step in the boundary [1]. (This is highly dependent on the mechanical properties of the step boundary.) The EDC instability continuously draws new (unmelted) mantle material through the melting zone, and melting occurs dominantly by pressure release. This time period is reasonably consistent with the time period for the major phase of Tharsis volcanism. It is possible that a series of EDC type instabilities along the dichotomy boundary through time together form Tharsis rise. King and Anderson [1] estimated that an EDC instability could produce the volume of volcanic material observed at flood basalt provinces such as the Parana basalts of South America. Tharsis rise is 10-30 times the volume of volcanic material of typical flood basalt provinces on Earth. The very-short duration of flood basalt volcanic activity is problematic for the EDC mechanism; however, this does not appear to be the case for Tharsis rise. Given the age of the major phase of Tharsis volcanism, it seems highly improbable that if a small-scale instability was responsible for the formation of Tharsis, the instability remains active today.

Summary: The most intriguing aspect of a Tharsis-dichotomy connection is the spatial relationship. Not only does the Tharsis rise straddle the dichotomy boundary, it is located in the interior of a concave arc of the boundary. Thus small-scale instabilities from 5,000 km of arc-length along the boundary could potentially feed Tharsis volcanism. If an EDC existed and formed the volcanism comprising Tharsis rise in the Late-Noachian to Early-Hesperian period, it is unlikely that the same instability remains active today. If an EDC mechanism is responsible for the small, late-stages of volcanic activity, it is possible that it could be observable in the present areoid and topography. Figure 2 shows the residual areoid from degrees 5-60 after the best fitting isostatic areoid, in a least-squares sense, has been removed. The best fitting isostatic model has a crustal thickness of 110 km and a crustal density of 2800 kg/m^3 . The result is relatively insensitive to whether we use degrees 5-8 as the low-end cut off. The zero km elevation line of the topography is plotted as a proxy for the crustal dichotomy. The linear relative areoid highs in the residual that parallel the dichotomy could represent mantle structures paralleling the crustal feature.

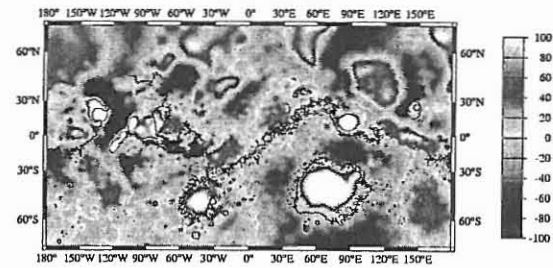


Figure 2. Spherical harmonic degrees 5-60 of the areoid where the best fitting isostatic areoid (crustal density 2800 kg/m^3 , crustal thickness 100 km) has been removed. The black line is the zero contour of the topography, a proxy for the crustal dichotomy.

A number of factors appear to work against an EDC instability as the major source of Tharsis volcanism; however, given our limited knowledge of the thermo-chemical state of the Martian lithosphere it is not possible to rule out an EDC mechanism. More importantly, an EDC mechanism could easily explain the minor, late-stage volcanic activity associated with Tharsis and present day small-scale convection could have a signature in the Areoid.

Another interesting possibility is that the major phase of Tharsis volcanism could be related to a lower-crustal Rayleigh-Taylor type instability [11]. A similar mechanism has been proposed as the source of the Yellowstone-Newbury volcanism in the western US [12]. The most striking question that these mechanisms do not address is the same one that plagues the plume mechanism; why is there a single, long-lived volcanic feature on Mars?

References: [1] King S. D. and Anderson D. L. (1998) *Earth Planet. Sci. Lett.*, 160, 289-296. [2] Vogt P. R. (1991) *Geology*, 19, 41-44. [3] King S. D. and Ritsema J. (2000) *Science*, 290, 1137-1140. [4] Kaula W. M. (1967) *Rev. Geophys.*, 5, 83-107. [5] Hauck II S. A. and Phillips R. J. (2002) *JGR*, 107, 10.1029/2011JE001801. [6] Harder H. and Christensen U. R. (1996) *Nature*, 380, 507-509. [7] Lowry A. R. and Zhong S. (2003) *JGR*, 108, 10.1029/2003JE002111. [8] Frey et al. (2002) *GRL*, 29, 10.1029/2001GL013832. [9] Solomon S. C. (2002) *Nature*, 418, 27-29. [10] Lenardic A. et al. (2003) *JGR*, 108, 10.1029/2002JB0001859. [11] Jull M. and Kelemen P. B. (2001) *JGR*, 106, 6423-6446. [12] Humphreys et al. (2000) *GSA Today*, 10(12), 1-7.

MARS AND EARTH: TWO DICHOTOMIES – ONE CAUSE. G. G. Kochemasov. IGM Russian Academy of Sciences, 35 Staromonetny, 119017 Moscow, Russia, kochem@igem.ru.

The wave planetology [1, 2, 3 and others] is based on this fundamental thesis: orbits make structures. It means that inertia-gravity forces arising in planetary bodies due to their movements in non-round (elliptical, parabolic) keplerian orbits with periodically changing curvatures and accelerations produce in planetary spheres oscillations. Having standing character and four directions (ortho- and diagonal) these oscillations (waves) interfere forming uplifting (+), subsiding (-) and neutral compensated (0) tectonic blocks. These blocks, naturally, are regularly disposed and their sizes depend on wavelengths. The longest fundamental wave 1 (long $2\pi R$, where R is a body radius) inevitably produces tectonic dichotomy (Fig. 1) with one hemisphere rising (+) and another falling (-). The rising (continental) hemisphere increases its planetary radius thus occupying larger space (surface) and tending to extend itself. That is why it is normally profoundly and intensively cracked (rifted) giving way up to deep-seated (mantle) melts; volcanoes, plateau flood basalts appear, intrusions fill weakness zones. The falling (oceanic) hemisphere diminishes its planetary radius thus occupying smaller space (surface) and tending to contract itself. That is why it is normally folded and extra material is pushed up (squeezed out), finds its way to the surface forming volcanoes and ridges. As all planetary bodies rotate, tectonically and hypsometrically different levels blocks (hemispheres) must regulate (equilibrate) their angular momenta: otherwise a globe will tend to fall to pieces (destroy itself). As the angular velocity of rotation of all blocks in one body is the same, the equilibration must be done by play between radii and densities. The subsiding blocks thus must be denser than the uplifting blocks. Our observations confirm this: at Earth oceans are basaltic and continents are on average andesitic. Mars also obeys this law: the northern lowlands are Fe-basaltic and the southern highlands are andesitic at least at the dichotomy boundary ("Pathfinder") and must be else less dense further south (we proposed albitites, syenites and granites as candidates to these low density rocks [3, 4, 5, 6 and others]).

The density contrast between highlands and lowlands at Earth is about 0.25 g/cm^3 , at Mars this contrast must be even higher because the martian wave tectonics is sharper (coarser) and produces relatively larger blocks with higher relief range [4]. The martian lowlands, indeed, are denser than the terrestrial ones (Fe-basalts against tholeiites). The recent martian lander's data published in Internet show that highlands layered rocks (by the way, such thin layering is typical of terrestrial nepheline syenites, for an example, Lovozero massif at Kola peninsula [7, 8]) covered by crusts of sulphates, chlorides, bromides are Si, Al, alkali – rich. High Cl and sulphur oxides are typical for syenites [7, 8]. Mg/Fe and Al/Ca in martian analyses are high and there is a sharp increase of them from lowlands to highlands indicating a pronounced global chemical fractionation (no more dull entirely basaltic Mars!). Global Si and Fe distribution according to the Odyssey gamma-spectrometry means that the southern highlands are Si-rich and the northern lowlands Fe-rich. The global gravity [9] also shows that the southern buckling hemisphere is built of relatively light (not dense) lithologies (albedo supports this conclusion).

So, the E-W and S-N dichotomies of Earth and Mars, where are opposed uplifting deeply rifted highlands and subsiding markedly ridged (folded) lowlands, are identical wave features of the first order. In both cases the lowlands (the primary oceans) occupy $\sim 1/3$ of the whole global surface, that is an another indication of waves involved (Fig. 1).

According to the wave theory the first harmonic – wave 1 typically is adorned by overtones. The first overtone – wave 2 is the most pronounced and shows itself by separate block-sectors – continents and separating them secondary oceans. At Earth the eastern continental hemisphere (segment) is composed of continents and oceans (sectors), the western oceanic hemisphere (segment) of oceanic plateaus and depressions (sectors). The sectoral features of two hemispheres are antipodean (i. g., Africa and East-Pacific depression). The martian segments also are composed of different level sectors. The most pronounced on the southern highland segment are two depressions – Hellas planitia and Argyre planitia. They have their anti-counterparts on the northern lowland segment – antipodean but uplifted features. Hellas is antipodean to appearing at high oceanic latitudes "continental" block of Alba patera and Tempe terra. Argyre is nearly antipodean to lonely protruding oceanic floors Elysium planum (together with its northern extension – Phlegra montes) (Fig. 2). Isidis planitia is antipodean to the complex of three plana: Solis, Syria, Sinai. And so on...

Structural similarities of two planets completely differing in size, mass and average density could be continued and found also in other planetary bodies including small ones – asteroids and the boss – Sun (aster), more precisely, its photosphere [10, 11]. These structural regularities allowed us to generalize them in four theorems of planetary tectonics [12]: 1. Celestial bodies are dichotomic; 2. Celestial bodies are sectoral; 3. Celestial bodies are granular; 4. Angular momenta of different level blocks tend to be equal.

Two more remarks. 1) Why dichotomies of Mars and Earth are differently oriented (S-N & E-W)? Because in the interference process take place waves of 4 directions; they have several possibilities to combine, to superimpose on each other forming "+" and "-" at different sides. 2) Why the dichotomy boundary is so sharp? Because waves we deal with are quantum-mechanical ones that means they do not have smooth sinusoidal

transitions between phases: there is discrete sharp transition between "+" and "-" (remember sharp boundaries between continents and oceans on Earth).

References: [1] Kochemasov G. G. (1994) 20th Russian-American microsposium on planetology. Abstr., Moscow, Vernadsky Inst., 46-47; [2] Kochemasov G. G. (1998) Proceedings of international symposium on new concepts in global tectonics ('98 TSUKUBA), Tsukuba, Japan, Nov. 1998, 144-147; [3] Kochemasov G. G. (1999) The Fifth International Conference on Mars, July 18-23, 1999, Pasadena, California. Abstr. # 6034. LPI contribution # 972. LPI, Houston, (CD-ROM); [4] Kochemasov G. G. (1995) Golombek M.P., Edgett K.S., Rice J.W. Jr. (Eds). Mars Pathfinder Landing Site Workshop II: Characteristics of the Ares Vallis Region and Field trips to the Channeled Scabland, Washington. LPI Tech. Rpt. 95-01. Pt.1.LPI, Houston, 1995, 63 pp.; [5] Kochemasov G. G. (1997) Annales Geophysicae, Suppl. III to Vol. 15, Pt. III, 767; [6] Kochemasov G. G. (1998) Annales Geophysicae, Suppl. III to vol. 16, Pt. III, 1027; [7] Kochemasov G. G. (2001) Eleventh Annual V. M. Goldschmidt Conference. Hot Springs, Virginia, USA. Abstr. # 3070. LPI, Houston, 2001, (CD-ROM); [8] Kochemasov G. G. (2001) Field Trip and Workshop on the Martian Highlands and Mojave Desert Analogs, Las Vegas, Nevada, and Barstow, California, Oct. 20-27, 2001. LPI contribution # 1101, LPI, Houston, 35-36; [9] Smith D. E., Sjogren W. L., Tyler G. L. et al. (1999) Science, v. 286, 94-97; [10] Kochemasov G. G. (2003) 38th microsposium on comparative planetology, Abstr., Moscow, Vernadsky Inst., (CD-ROM); [11] Kochemasov G. G. (2004) Lunar and Planetary Science XXXV, 35th LPSC, Houston, March 15-19, 2004, Abstr. # 1041, (CD-ROM); [12] Kochemasov G. G. (1999) Geophys. Res. Abstr., v. 1, # 3, 700; [13] Zuber M. T., Solomon S. C., Phillips R. J., Smith D. E. et al. (2000) Science, v. 287, # 5459, 1788-1793.

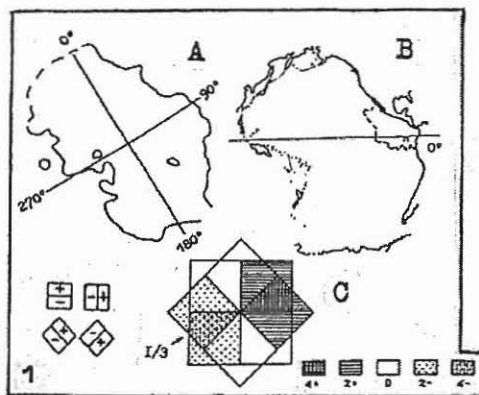


Fig. 1. Identical formation of Mars' and Earth's tectonic dichotomy: a model of wave interference. A-Vastitas Borealis of Mars. Crustal thickness inside the contour is less than 50 km [13] (as viewed from inside the globe what makes the contour mirrored). B- Pacific basin. C- Flat geometric model of wave interference (4 wave directions). One needs mentally to wrap up it around the globe.

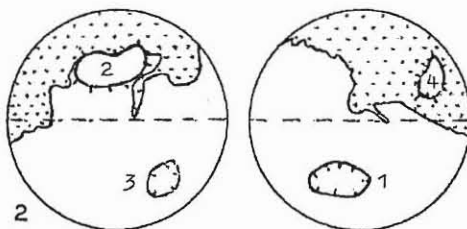


Fig. 2. Martian hemispheres with dichotomy boundary. Antipodality of Hellas (1) to Alba patera and Tempe terra (2) and Argyre (3) to Elysium planum with Phlegra montes (4).

DEPTH-DEPENDENT RHEOLOGY AND THE WAVELENGTH OF MANTLE CONVECTION WITH APPLICATION TO MARS. A. Lenardic, *Department of Earth Science, Rice University, Houston, Texas, (adrian@esci.rice.edu)*, M.A. Richards, *Department of Earth and Planetary Science, University of California, Berkeley, California*, F.H. Busse, *Institute of Physics, University of Bayreuth, Bayreuth, Germany*, S.J.S. Morris, *Department of Mechanical Engineering, University of California, Berkeley, California*.

Abstract: Numerical simulations have shown that depth-dependent viscosity can increase the wavelength of mantle convection. The physical mechanism behind this observation and, by association, its robustness remain to be fully elucidated. Towards this end, we develop theoretical heat flow scalings for a convecting fluid layer with depth-dependent viscosity. Bottom and internally heated end-members are considered. For the former, the viscosity structure consists of a high viscosity central region bounded from above and below by horizontal low viscosity channels. For internally heated cases, only a surface low viscosity channel is present. The theoretical scalings show how depth-dependent rheology lowers the lateral dissipation associated with convective cells. This allows longer aspect ratio cells to form as the viscosity contrast between the channels and the central region is increased. The maximum cell extent is determined by the condition that the pressure gradients that drive lateral flow in the channels do not become so large as to inhibit vertical flow into the channels. Scaling predictions compare favorably to results of numerical simulations at low to moderate Rayleigh numbers. As the Rayleigh number driving convection is increased, time-dependence sets in in the form of small scale boundary layer instabilities. This increases lateral dissipation within the channels and the maximum cell extent decreases as a result. Internally heated simulations show that a near surface high viscosity layer, a lithosphere analog, can suppress these small scale instabilities. This allows a low viscosity channel to maintain large aspect ratio cells at high Rayleigh numbers.

Introduction: Several models for the formation of the Martian Hemispheric Dichotomy invoke long wavelength mantle convection [1,2,3]. Understanding the physical mechanisms by which long wavelength flow can be generated and maintained is crucial to evaluating the physical plausibility of such models under parameter conditions pertinent to Mars. Numerical simulations have been used to argue that depth-dependent viscosity can generate long wavelength flow within a convecting mantle [2,4]. However, numerical simulations have also been used to argue that depth-dependent viscosity will not be effective at generating long wavelength flow at the high degrees of convective vigor that characterize the Earth's present day mantle and the Martian mantle at the time the dichotomy formed [5]. Clearly the simulations are mapping different dynamic regimes within the full parameter space of the system. To augment and extend the numerical work done to date, we have developed a scaling theory that explores the heat transfer properties of a convecting layer with depth-dependent rheology. The theory provides an efficient way to map regime transitions. It also provides physical insight into the observation that numerical simulations with depth-dependent rheology can generate long wavelength flow, i.e., it can isolate the

physical reason why this is so and also determine the specific conditions required.

Analysis: Although the criteria that determines the selection of convective planforms within a thermally convecting fluid is not generally understood [6], it is agreed that it is lateral dissipation that principally limits the formation of large aspect ratio cells [7]. We develop a boundary layer theory based on the key assumption that the presence of horizontal regions of low viscosity (e.g. the Earth's asthenosphere, a low viscosity upper Martian mantle) within a convecting layer allow lateral flow to become channelized within the low viscosity regions [8]. The analysis shows that channelization lowers the lateral dissipation in fully developed, large amplitude convective flow systems heated from below or from within. This shifts the limit on the maximum cell extent that is energetically favorable. That is, with depth-dependent viscosity, the cell wavelength that is most effective at transporting heat is longer than for the isoviscous case. Although this does not guarantee that long cells will form preferentially to shorter cells, it does show how depth-dependent viscosity can make this more likely. Theory predictions for maximum cell wavelength as a function of viscosity variations, channel thicknesses, and convective vigor compare favorably to the results of numerical simulations. The theory explains why increased Rayleigh numbers can cause the wavelength to shift back to shorter length scales and suggests that the presence of a high viscosity, active lithosphere can offset this shift. The theory also predicts the counterintuitive results that long wavelength cells can increase the cooling rate of a planet and that thinner low viscosity channels can also increase the cooling rate. Both predictions are confirmed via full numerical simulations.

Discussion: For application to Mars, our theory suggests that: 1) Horizontal regions of low viscosity can lead to long wavelength mantle flow by lowering the lateral dissipation within the mantle; 2) The viscosity contrast between low viscosity regions and the bulk mantle must approach 1000 to generate wavelengths at the scale of a degree 1 mantle convection pattern; 3) Internal heating can favor long wavelength flow by decreasing the lateral dissipation associated with a hot lower thermal boundary layer; 4) For long wavelength flow to have occurred at the high degrees of convective vigor during Dichotomy formation, the Martian lithosphere needed to be active as opposed to stagnant; 5) If long wavelength flow did occur it could have helped to cool Mars at a faster rate than it would have in the absence of long wavelength flow; 5) Very thin low viscosity regions can have a significant effect on mantle cooling rate, i.e., potentially thinner than can be detected via geoid and topography analysis [9].

[1] McGill and Dimitriou, *Geology*, 28, 391-394, 1990. [2] Zhong and Zuber, *Earth Planet. Sci. Lett.*, 189, 75-84, 2001.

- [3] Lenardic et al., *J. Geophys. Res.*, 109, 10.1029/2003JE002172, 2004. [4] Bunge et al., *Nature*, 379, 436-438, 1996. [5] Tackley, *Geophys. Res. Lett.*, 23, 1985-1988, 1996. [6] Ahlers, *25 Years of Nonequilibrium Statistical Mechanics*, 91-124, Springer-Verlag, Berlin, 1995. [7] Busse, *Hydrodynamic Instabilities and the Transition to Turbulence*, 97-137, Springer-Verlag, Berlin, 1985. [8] Lenardic et al., *Geophys. J. Int.*, Submitted. [9] Thorval and Richards *Geophysical J. Int.*, 131, 1-8, 1997.

THE MARTIAN RELIEF'S DICHOTOMY AND PLANETARY AXIAL STRUCTURAL SYMMETRY.

Makarenko G. F., General Physics Institute of RAS, 119991 Moscow, Vavilov str. 38

mkrm@kapella.gpi.ru

www.gpi.ru/~mkrm/lpsr

The basic property of the Earth is axial structural symmetry of its outer shell [1,2]. This indisputable phenomenon is not visible from the space (oceans). Rejecting the displacement of earthen shell (plate drifting) **only** allows to compare Earthen tectonic tracteries with the seams on other planets. Similarity of large dislocated zones position on the Earth and Mars are reflected in relief, in faults picture and in Earthen structures without relief.

Confront the 60 martian meridian with the 0 Earthen meridian [3]. We see (upper Fig., Earth – lines, Mars – points, dotted lines and small rings - martian volcanoes) the coincidence of huge arcs on the planets in their south hemispheres, arcs bend near 0 and 180 meridians of the Earth. Here we have ocean ridges curves. The form of the south arc on the Mars is accented by the margin of Argir depression and on the other globe side – by Eridania stair, eastwards of crater Kepler. Alike near latitude planet fault systems are placed around the equator. On the Mars their images are fault seams (Mariner canyon; on another planet side – Amentes set-off and Eolyda rise). They have branches to NE also around 60 and 260-240 meridians accordingly.

Olimp is a huge martian volcano, with ambient rings with lavas. Let us “relax” the volcanic “disk” (altitude to basis ratio 1 : 20), i.e. embed it to the martian entrails. Their images on the Earth are the rears of hercinides of Apallachians and Uoashito with their coats of ocean and Mexican Bay's lavas. On the other Earthen side there are basalt lavas of Eymeshan Plato at the Sikkan-Yunnan fold zone rear. Southwards we see young lavas among the young island arcs. Patera Alba is an appreciable volcanic place. Its reflection on the Earth are basalts of Atlantic arc Corner-Miln and lavas in the Japan Isles rear.

On the scheme (Fig. below) from Martian

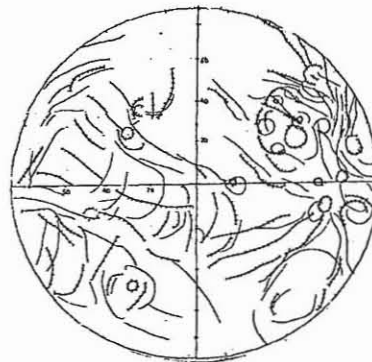
map [4] the structural lines and volcanoes of “Olimp's” side (lines with trites) and of the other side (lines) are shown.



0-Earth (60W Mars)

Six volcanoes- now rings only- fix the Olimp's place on this planet side: near the center Flammarion, Antoniadi (N 25), Schroeter (0), Tichonravov (N 13), Cassini (N 24), Quenisset (N 35) and Rudaux (N 38).

This volcanic field looks alike trapp Earthen field with long living deep channels.



The Earth and the Mars are twins (both without the “plate tectonics” and without the grand impacts).

The relief's Martian dichotomy (N-S) is clear; the relief's Earthen dichotomy (W-N hemispheres) is evidential too.

References: [1] Makarenko G.F. (1998) Japan islands... Proc. Int. Simp. NCGT, Tsukuba, Japan, p.244-249 (Engl), [2] Makarenko G.F. (1997) Periodicity of basalts, biocrisises... Mosc. Geoinformmark, 95p. (Rus). [3] Merrill R. (1999) Science. Vol 284, 28 May 1495-1502. [4] Mars map 1:25 mln., Dresden Un. Of Techn. Ed. M. Buchroither, Cons. MIIGAIG., 2001.

CRUSTAL EVOLUTION OF THE PROTONILUS MENSAE AREA, MARS. G. E. McGill¹, S.E. Smrekar², A.M. Dimitriou^{1,3}, and C.A. Raymond², ¹ Dept. of Geosciences, Univ. of Massachusetts, Amherst, MA (gmccgill@geo.umass.edu). ² Jet Propulsion Lab., MS 183-501, 4800 Oak Grove Dr., Pasadena, CA, ³ SLR Alaska, 2525 Blueberry Rd., Suite 206, Anchorage, AK.

Despite research by numerous geologists and geophysicists, the age and origin of the martian crustal dichotomy remain uncertain. Models for the origin of this dichotomy involve single or multiple impact, mantle megaplumes, primordial crustal asymmetry, and plate tectonics [1 - 10]. Most of these models imply a Noachian age for the dichotomy. A major problem common to all genetic models is the difficulty separating the features resulting from the primary cause for the dichotomy from features due to younger faulting, impact cratering, volcanism, deposition, and erosion.

The boundary between northern lowlands and southern highlands (the dichotomy boundary) approximates a small circle that ranges in latitude from about -10° in Elysium Planitia to about $+45^{\circ}$ north of Arabia Terra. For much of its length the boundary is characterized by relatively steep scarps separating highland plateau to the south from lowland plains to the north, generally with a complex transition zone on the lowland side of these scarps [11]. These scarps are almost certainly due to normal faulting. The type fretted terrain [12], which defines the boundary in north-central Arabia Terra, also is characterized by scarps but has undergone a more complex history of faulting and dissection [13]. In some places, notably in the Acidalia Planitia region, the dichotomy boundary is gradational. In the Tharsis region the boundary is obscured by younger volcanics.

The present study concerns the segment of dichotomy boundary between about 50°E and 90°E (310° - 270°W), within the Ismenius Lacus and Cassius quadrangles. This site was chosen because: 1) within part of the site the boundary is a single well defined scarp ~ 2.5 km high, 2) parallel to this scarp are several grabens, which support an extensional origin for the boundary scarp, and which also provide a means to estimate strain, 3) erosion appears not to be extreme, 4) the geology and structural history allow constraining the age of the boundary scarp, and 5) there are areal correlations among topography, geology, remanent magnetism, and gravity anomalies. The combination of tractable geology with magnetic and gravity data provides a rare opportunity to infer the evolution of the crust and mantle along the highland/lowland boundary.

Terrains within the study site may be divided into three structural blocks based on surface morphology and elevation. From southwest to northeast these are: 1) highland plateau, 2) lowland bench, and 3) lowland plains [14]. The highland plateau block is within the large region Arabia Terra, which is somewhat anomalous because it is topographically lower than most highland areas despite its highland crater population. The highland plateau has been resurfaced following accumulation of most of its large craters. The crater age of the highland plateau is Early Noachian; the age for craters younger than the resurfacing event is Middle Noachian. High resolution THEMIS and MOC images indicate that resurfacing was accomplished at least in part by deposition of a layer of material that is thin enough to permit the rims of older craters larger than a few km in diameter to show

through as inliers. Thus the post-resurfacing crater age is interpreted to be the age of the material deposited on the highland basement.

The boundary between the highland plateau and the lowland bench is a fault or zone of faults. The lowland bench is 2-3 km lower than the highland plateau, and is characterized by an abundance of knobby inliers projecting through a younger layer of smooth plains material. Some of these knobs clearly define circles that are inferred to be structurally disrupted crater rims ("knob ghosts"). A count of all craters and knob ghosts yields a Late Noachian age. However, the presence of the knob ghosts indicates that the basement surface under the lowland bench has experienced greater structural disruption than the basement of the highland plateau where rims of large, ancient craters, although degraded, have not been dissected into rings of knobs. The basement of the lowland bench also is partially covered by plains material that is similar to the material underlying the lowland plains block. Thus it is very likely that the age of the basement beneath the lowland bench is similar to the age of the basement beneath the highland plateau; that is, Early Noachian. This is consistent with the basement age determined for the entire lowland using all craters visible in images plus "Quasi-Circular Depressions" (QCD's) visible only in MOLA digital terrain models [15].

Is it possible that the scarp separating highland plateau from lowland bench is erosional rather than structural? The highland plateau and lowland bench have similar basement ages. It is not possible for the scarp to be older than these basement ages because it could not have survived formation of the craters yielding these basement ages. If the scarp formed by erosion after the cratering of the highland plateau and lowland bench basement, then on the order of the scarp height (2.5 km) of material must have been removed over what is now the lowland bench. This depth of erosion would have completely destroyed the rims of all of the craters used to date the lowland bench basement. It thus appears to be impossible to create the current topography within the Protonilus Mensae area by extensive erosion alone.

The boundary between the lowland bench and the lowland plains is characterized by the abrupt loss of the knobs that are so abundant on the lowland bench. This boundary is parallel to and about 400 km NE of the scarp that separates highland plateau and lowland bench. The loss of the knobby topography along this boundary is most likely due to an increase in thickness of smooth plains material, resulting in complete burial of the knobs in the lowland plains block. The abruptness of this loss of knobby topography suggests that the lowland bench/lowland plains boundary is a fault, down on the NE [14]. There is no topographic signature of this fault other than the loss of knobby topography, indicating that its fault scarp has been completely destroyed or buried. The minimum vertical displacement needed to completely bury the knobs of the lowland bench block is about one kilometer; the actual displacement is probably greater

but is not constrained. Poorly defined ridges that are similar to wrinkle ridges occur in the lowland plains block. These ridges are locally parallel to the dichotomy boundary. The age of the smooth surface material in the lowland plains block is Late Hesperian [11,14]. The smooth plains material surrounding the knobs on the lowland bench is continuous with the plains material in the lowland plains block, and thus also is inferred to be Late Hesperian.

Both the dichotomy boundary scarp separating highland plateau from lowland bench, and the buried fault separating lowland bench from lowland plains cut basement rocks of Early Noachian age. The boundary scarp also cuts the Middle Noachian resurfacing material of the highland plateau. Thus the old age limit for faulting in this area is Middle Noachian. The smooth plains material underlying the lowland plains is also present as a thin veneer on the lowland bench. This plains material embays the boundary scarp in places, and it buries the buried fault, indicating that the young age limit for faulting in this area is Late Hesperian. The relative age range Middle Noachian-Late Hesperian is interpreted to correspond to an age range in years of 3.9-3.1 Ga [16]. The old limit is only 140 Ma younger than the young age limit for lowland basement as determined using QCD's [17].

The dichotomy boundary scarp and the scarps bordering the grabens that are present SW of the boundary scarp have slopes in the range 13-21°; thus, as we would expect, these scarps are degraded from the presumed ~60° slope of a pristine normal fault scarp. Using MOLA altimetry profiles and assuming 60° fault dips, the extensional strain in the immediate vicinity of the dichotomy boundary scarp is determined to be ~3.5%.

The lowland bench block is part of an extensive transitional zone between highland and lowland. Lowland bench crater ages determined in this study are completely consistent with crater ages determined for this entire transitional zone [11]. Furthermore, the old age limit on dichotomy boundary faulting in the Amenthes area [18] is similar to or perhaps slightly younger than the old limit in this study area. Thus the present morphology of the dichotomy boundary for segments characterized by scarps is due to faulting between Middle Noachian and Late Hesperian. The remanent magnetic field and gravity anomalies correlate with the morphology and structure of the dichotomy boundary zone in the Protonilus Mensae area, providing an excellent opportunity to model the crust and upper mantle where there are relatively robust geological constraints. The geology and topography of the study site are consistent with either the creation of the dichotomy by faulting between Middle Noachian and Late Hesperian, or with an earlier creation followed by crustal-scale processes that were responsible for the faulting. We currently are exploring the latter possibility.

- [1] Wilhelms, D.E., and S.W. Squyres (1984) *Nature*, 309, 138-140. [2] Frey, H., and R.A. Schultz (1988) *Geophys. Res. Lett.*, 15, 229-232. [3] Mutch, T.A., R.E. Arvidson, J.W. Head, III, K.L. Jones, and R.S. Saunders (1976) *The geology of Mars*, Princeton Univ. Press. [4] Wise, D.U., M.P. Golombek, and G.E. McGill (1979a) *Icarus*, 38, 456-472. [5] Wise, D.U., M.P. Golombek, and G.E. McGill (1979b) *J. Geophys. Res.*, 84, 7934-7939. [6] Breuer, D., D.A. Yuen, and T. Spohn (1997) *Earth Planet. Sci. Lett.* 148, 457-469. [7] Breuer, D., D.A. Yuen, T. Spohn, and S. Zhang (1998) *Geophys. Res. Lett.* 25, 229-232. [8] Zhong, S., E. and M.T. Zuber (2001) *Earth Planet. Sci. Lett.*, 189, 75-84. [9] Sleep, N.H. (1994) *J. Geophys. Res.*, 99, 5639-5655. [10] Lenardic, A., F. Nimmo, and L. Moresi (2004) *J. Geophys. Res.*, 109, doi: 10.1029/2003JE002172. [11] Frey, H., A.M. Semeniuk, J.A. Semeniuk, and S. Tokarcik (1988) *Proc. 18th Lunar Planet. Sci. Conf.*, 679-699. [12] Sharp, R.P. (1973) *J. Geophys. Res.*, 78, 4073-4083. [13] McGill, G.E. (2000) *J. Geophys. Res.* 105, 6945-6959. [14] Dimitriou, A.M. (1990) M.S. Thesis, Univ. Massachusetts, Amherst. [15] Frey, H.V., J.H. Roark, K.M. Shockey, E.L. Frey, and S.E.H. Sakimoto (2002) *Geophys. Res. Lett.*, 29, 10.1029/2001 GL013832. [16] Hartmann, W.K., and G. Neukum (2001) in Kallenback, R., J. Geiss, and W.K. Hartmann, eds., *Chronology and evolution of Mars*, Kluwer Academic Publishers, 165-194. [17] Frey, H.V. (2004) *Lunar Planet. Sci. XXXIV*, Abstract #1382. [18] Maxwell, T.A., and G.E. McGill (1988) *Proc. 18th Lunar Planet. Sci. Conf.*, 701-711

Loading-induced Stresses and Topography Near the Martian Hemispheric Dichotomy Boundary. P. J. McGovern¹ and T. R. Watters², ¹Lunar and Planetary Institute, 3600 Bay Area Blvd., Houston TX 77058, (mcgovern@lpi.usra.edu), ²Center for Earth and Planetary Studies, National Air and Space Museum, Smithsonian Institution, Washington D.C. 20560 (twatters@nasm.si.edu).

Introduction: The dichotomy between the northern and southern hemispheres of Mars is one of the fundamental physiographic features of the planet. The dichotomy is manifested in the topography, geology, tectonics, cratering record, magnetic field, and crustal structure. The origin of the crustal dichotomy between northern (relatively thin, constant thickness) and southern (relatively thick and thickening southward) crustal provinces [1] appears to date to the earliest Noachian [2], a period with scant remaining traces in the geologic record. However, subsequent geologic and tectonic events may contain clues as to the nature of the hemispheric dichotomy.

The Eastern Hemisphere Dichotomy Boundary (or "EHDB") of Mars between 40°E (western Arabia Terra) and 160°E (Terra Cimmeria) is characterized by a prominent topographic scarp (several km in height), compressional features on the highlands side and extensional features on the boundary ramp [3, 4]. Loading of the lithosphere due to emplacement of volcanic or sedimentary material on the lowlands side, erosion on the highlands side, and an episode of global compression in the Hesperian may be responsible for the observed topography and tectonics. A broken-plate flexural model with elastic lithosphere thickness $T_e = 31\text{--}36$ km provided a good fit to Mars Orbiter Laser Altimeter (MOLA) topography data across the EHDB [3].

Method: We use the finite element code Tekton [5] to model the response of the Martian crust and mantle to surface loads emplaced near the hemispheric dichotomy boundary. The model grid accounts for crustal and mantle structure in the vicinity of EHDB, as constrained by studies of gravity and topography [e.g., 1, 6–8]. The grid exhibits plane strain geometry and extends 2720 km horizontally and 1720 km vertically. In the left-hand section of the model, a crust of 40 km thickness (representing the northern lowlands of Mars) lies at the surface. In the right-hand section (representing the southern uplands), the crust is ~55 km thick, yielding isostatic compensation for a 3 km difference in topography between "North" and "South" sections [e.g., 3] corresponding to densities $\rho_{\text{crust}} = 2900 \text{ kg/m}^3$ and $\rho_{\text{mantle}} = 3500 \text{ kg/m}^3$. A section of elements 160 km wide, cosine tapered, accommodates the corresponding transition in crustal thickness. These dimensions simulate the change in elevation and width

of the dichotomy boundary in the Eastern Hemisphere of Mars.

The finite element grid starts in an isostatic configuration to reflect likely conditions at the time the crustal thickness variations were established. Rheological parameters are determined by flow laws for diabase [9] and olivine [10], as functions of temperature governed by pre-set thermal gradients. Models termed "uniform" assign material properties in horizontal rows of elements based on the thermal gradient the northern highlands. We also explore the effects of lateral variations in thermal gradients by assigning independent values to the lowlands, transition region, and highlands. Three types of loading were modeled. For depositional loading, density was increased in a line of elements "northward" (to the left) of the boundary ramp to represent the emplacement of sediments or volcanic material in the northern lowlands. Conversely, erosional loading southward of the dichotomy was modeled by decreasing element densities. An episode of large-scale compression (i.e., the event that caused widespread compressional ridged plains formation in the early Hesperian [e.g., 11, 12]) was modeled by moving the lateral boundaries of the model inward by an amount corresponding to 0.2% horizontal strain.

Results: Topographic profiles resulting from several types of dichotomy boundary loading are shown in Figure 1. Models with purely surface depositional loads in the northern lowlands do not generate appreciable flexural topography on the highlands side. For the thermal gradients (10 and 15 K/km) used here, lower crustal elements exhibit low viscosities that allow relaxation of surface topography [e.g., 13–16], such as flexurally induced arching [13]. The depositional loads induce horizontal extension in the highlands proximal to the boundary, consistent with the observed presence of normal faulting at the dichotomy boundary [e.g., 3], but the Mohr-Coulomb failure criterion is not exceeded. Erosional unloading of the highlands results in flexural uplift of the margin (Figure 1), but the plotted curve substantially overestimates the actual topography if the eroded material is removed from the surface. The curve in Figure 1 could represent the actual topography only for an erosive mechanism that removed subsurface material while leaving the surface relatively undisturbed, such as hydrothermal circulation or karst formation. Erosional unloading produces horizontal extension in the unloaded area,

and the failure criterion is satisfied over most of this area.

Models with large-scale compression yield predictions of ubiquitous thrust faulting at the surface of the model. The “uniform” models and models with higher thermal gradients in the lowlands than in the highlands produce more pervasive thrust faulting in the lowlands than in the highlands, a consequence of weaker lithosphere in the former. This finding is consistent with the presence of numerous ridges in the northern plains [11–12], although such ridges are not prevalent near the dichotomy boundary. In contrast, models with higher thermal gradients in the highlands than in the lowlands result in more pervasive thrusting in the highlands. This result is in accord with presence of compressional faults in the highlands near the EHDB [3, 4]. Intriguingly, large-scale compression can also produce a topographic arch on the highland side of the dichotomy boundary. For models with enhanced thermal gradients in the highlands, such relief resembles the observed topography (Figure 1). This feature is essentially a buckling instability, localized by the contrast in rheological structure at the dichotomy boundary.

How was the characteristic topographic profile of the EHDB derived? Our results suggest that simple depositional surface loading of continuous lithospheric plate is not a likely explanation [see 17]. An erosive mechanism that removes subsurface material while preserving topography can qualitatively reproduce an arched profile (Figure 1), but such a scenario is unlikely given the evidence for removal of surface deposits at the EHDB. Analytic flexure modeling suggests that broken lithospheric plates provide the best fits to EHDB topography [17], although it is unclear how the lithosphere beneath the boundary becomes discontinuous. The compression-induced scenario presented above for generating arched boundary relief relies on lateral lithospheric heterogeneity (rather than sharp discontinuities), generated by variations in thermal gradient. The most successful such model (Figure 1) invokes elevated thermal gradients in the highlands. Such gradients could result from a higher concentration of radiogenic heat-producing elements in the thicker southern highlands crust, or from a mantle upwelling beneath the highlands [18].

Future Directions. This reconnaissance of parameter space has only considered viscoelastic behavior in plane-strain geometry. Further modeling will include the effects of plastic yielding, in order to better constrain the interaction of the various loading processes and the spatial and temporal distributions of faulting. We will also use Tekton’s spherical axisymmetric geometry capabilities to explore the effects of planetary curvature.

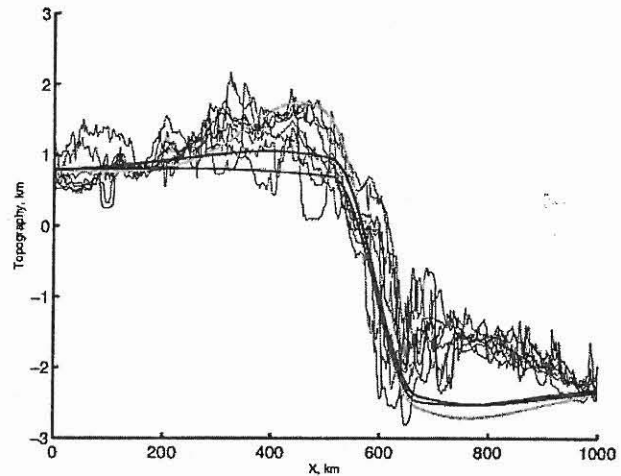


Figure 1. Topography of the Eastern Hemisphere Dichotomy Boundary (EHDB) for nine profiles (black lines, from [3]), and surface topography for three models of lithospheric loading and deformation. South is to the left. Red line: “uniform” model subject to surface depositional loading in the lowlands. Blue line: same as red line but after erosive unloading in the highlands. Green line: model with enhanced thermal gradient in the highlands, after 0.2% horizontal compressive strain.

References: [1] Zuber, M. T., et al. (2000) *Science*, 287, 1788. [2] Frey, H. (2002) *GRL*, 29, doi 10.1029/2001GL013882. [3] Watters, T. R. (2003) *Geology*, 31, 271. [4] Watters, T. R. (2003) *JGR*, 108, 8-1, 8-12. [5] Melosh, H. J., and Raefsky, A. (1983), *JGR*, 88, 515. [6] McGovern, P. J., et al. (2002) *JGR*, 107, doi 10.1029/2002JE001854. [7] McKenzie, D. (2002) *EPSL*, 195, 1. [8] Neumann, G. A., et al. (2004) *JGR*, 109, in press. [9] Caristan, Y. (1982), *JGR*, 87, 6781. [10] Karato, S.-I., et al. (1986), *JGR*, 91, 8151. [11] Withers, P., and Neumann, G. A. (2001) *Nature*, 410, 610. [12] Head, J. W., et al. (2002), *JGR*, 107, doi 10.1029/2000JE001445. [13] McGovern, P. J., and Watters, T. R. (2004), *LPS XXXV*, abstract 2148. [14] Guest, A., and Smrekar, S. E. (2004), *LPS XXXV*, abstract 1362. [15] Nunes, D. C., et al. (2004), *JGR*, 109, doi10.1029/2003JE002119, 2004. [16] Nimmo, F. and Stevenson, D. J. (2001) *JGR*, 106, 5085. [17] Watters, T. R., et al. (2004), this volume. [18] Wüllner, U., and Harder, H. (1998), *PEPI*, 109, 129.

TOPOGRAPHIC CHANGE OF THE DICHOTOMY BOUNDARY SUGGESTED BY CRUSTAL INVERSION. G. A. Neumann^{1,2}, ¹ *Department of Earth, Atmospheric and Planetary Sciences, Massachusetts Institute of Technology, Building 54, 77 Massachusetts Avenue, Cambridge, MA 02139-4307, (neumann@tharsis.gsfc.nasa.gov),* ² *Laboratory for Terrestrial Physics, Code 926, NASA/Goddard Space Flight Center, Greenbelt, MD 20771.*

Linear negative gravity anomalies in Acidalia Planitia along the eastern edge of Tempe Terra and along the northern edge of Arabia Terra have been noted in Mars Global Surveyor gravity fields [1, 2, 3]. Once proposed to represent buried fluvial channels [4, 5], it is now believed that these gravity troughs mainly arise from partial compensation of the hemispheric dichotomy topographic scarp [6]. A recent inversion for crustal structure [7] finds that mantle compensation of the scarp is offset from the present-day topographic expression of the dichotomy boundary. The offset suggests that erosion or other forms of mass wasting occurred after lithosphere thickened and no longer accommodated topographic change through viscous relaxation.

Introduction Using MOLA topography and the most recent gravity field from MGS and Mars Odyssey tracking, jgm95h01, we invert for the crustal structure required to plausibly match gravity, crustal topography and density variations to degree and order 90, allowing for the effects of power-law constraints applied at degrees 60 and higher to reduce noise primarily in the gravity solution. The effective resolution (minimum resolved pixel size) of this inversion is approximately 125 km (4 degrees of longitude). The inversion does not assume any particular compensation model. If all of the mantle relief were locally compensated by surface topography, a 14.5-km thicker crust in the highlands would have topography elevated by 3 km, while a 14.5-km thinner crust (on average) in the northern lowlands would have 3 km lower topography. This crustal model predicts the known center-of-figure to center-of-mass offset of Mars. Not all of the crustal thickness variation is compensated. The difference between the actual topography (filtered to degree and order 90) and that predicted by the crustal model is shown in Figure 1. This isostatic topography represents the excess (or deficit) relative to locally compensated terrain, much as an isostatic anomaly represents the difference between observed gravity and that of locally compensated terrain.

Results The areas shaded in reddish hues have excess topographic loads, such as Tharsis Montes and Alba Patera. Bluish hues represent uncompensated topographic deficits. We find that the linear gravity troughs coincide with up to 2 km of uncompensated topographic relief (green to blue). Such topography also coincides with the steepest portions of the dichotomy boundary (contour). If these regions were buried channels, they would likely be found north and east of the boundary scarps.

Discussion The model we propose is that such features were formed in early Martian history during a time of elevated mantle temperature, when the lithosphere was too thin to support uncompensated loads. Erosional modification of

the surface expression of the dichotomy occurred after the crust had cooled significantly and was able to support elastic stresses. There are similar but less pronounced gravity troughs along the edges of Hellas and Isidis, as well as the inferred rim of Utopia. Topographic edge effects of partially compensated relief may be responsible for some of these troughs [6]. Edge effects do not explain the isostatic deficit along steep slopes, and are not the primary reason for the linear gravity troughs.

References

- [1] D. E. Smith, W. L. Sjogren, G. L. Tyler, G. Balmino, F. G. Lemoine, A. S. Konopliv, The gravity field of Mars: Results from Mars Global Surveyor, *Science* 286 (1999) 94-96.
- [2] F. G. Lemoine, D. E. Smith, D. D. Rowlands, M. T. Zuber, G. A. Neumann, D. S. Chinn, D. E. Pavlis, An improved solution of the gravity field of Mars (GMM-2B) from Mars Global Surveyor, *J. Geophys. Res.* 106 (2001) 23,359-23,376.
- [3] D. N. Yuan, W. L. Sjogren, A. S. Konopliv, A. B. Kucinskis, Gravity field of Mars: A 75th degree and order model, *J. Geophys. Res.* 106(E10) (2001) 23,377-23,401.
- [4] M. T. Zuber, S. Solomon, R. J. Phillips, D. E. Smith, G. L. Tyler, O. Aharonson, G. Balmino, W. B. Banerdt, J. W. Head, F. G. Lemoine, P. J. McGovern, G. A. Neumann, D. D. Rowlands, S. Zhong, Internal structure and early thermal evolution of Mars from Mars Global Surveyor topography and gravity, *Science* 287 (2000) 1788-1793.
- [5] R. J. Phillips, M. T. Zuber, S. C. Solomon, M. P. Golombek, B. M. Jakosky, W. B. Banerdt, R. M. E. Williams, B. M. Hynek, O. Aharonson, S. A. H. II, Ancient geodynamics and global-scale hydrology on Mars, *Science* 291 (2001) 2587-2591.
- [6] A. J. Dombard, M. L. Searls, R. J. Phillips, An alternative explanation for the "buried channels" on Mars: The gravity signal from a sharp boundary on partially compensated, long-wavelength topography, *Geophys. Res. Lett.* 31(5) (2004) L05106, doi:10.1029/2003GL019162.
- [7] G. A. Neumann, M. T. Zuber, M. A. Wieczorek, P. J. P. J. McGovern, F. G. Lemoine, D. E. Smith, The crustal structure of Mars from gravity and topography, *J. Geophys. Res.* in press (2004) 2004JE002262.

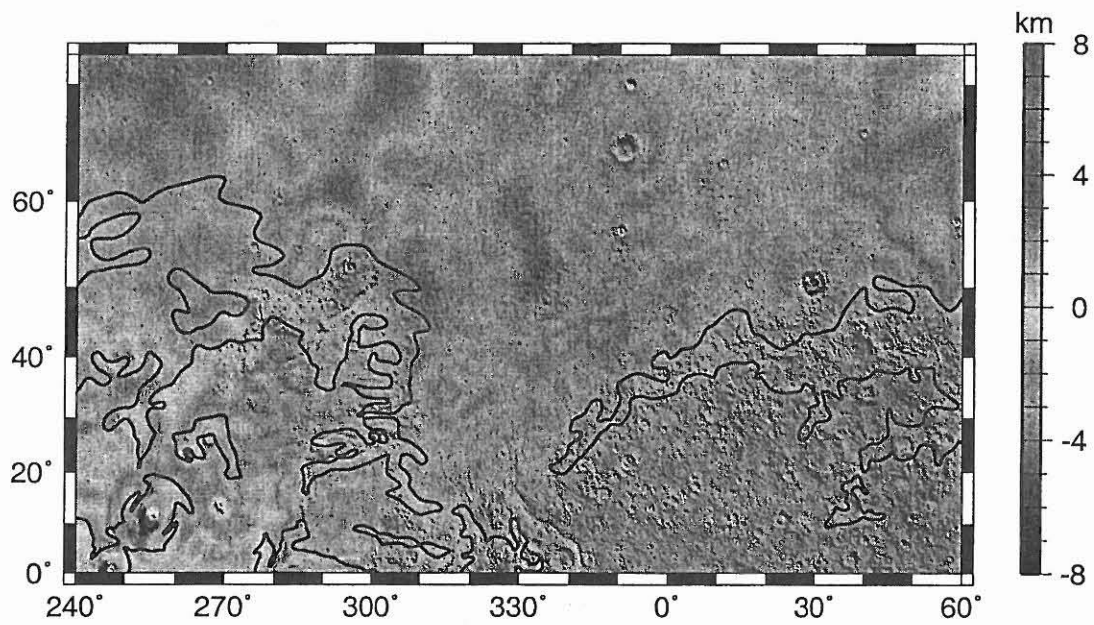


Figure 1: Isostatic topography, the residual topography above that which locally compensates moho relief, in color-shaded Mercator projection. Densities of 2900 and 3500 kg m^{-3} were assumed for the crust and mantle, respectively. Contours show steeper local gradients of terrain.

TECTONIC CONSEQUENCES OF DICHOTOMY MODIFICATION BY LOWER CRUSTAL FLOW AND EROSION. F. Nimmo, Dept. Earth and Space Sciences, University of California Los Angeles, Los Angeles, CA 90095-1567, nimmo@ess.ucla.edu

Abstract: The hemispheric dichotomy shows compressional lobate scarps ~100-500 km south of the dichotomy boundary, and extensional features along the boundary itself. Modification of the original boundary by lower crustal flow results in stresses which can explain the origin of both extensional and compressional features. Erosion would lead to extension to the south of the dichotomy, and compression to the north.

Introduction: The origin of the Martian hemispheric dichotomy is uncertain [1,2] but its present-day expression is probably due to the crustal thickness being higher in the south than the north [3]. The original surface expression of the dichotomy has been modified by both erosion [4] and impacts [5]. In the Eastern hemisphere of Mars, the dichotomy is characterized by a relatively steep scarp with a gentle rise further to the south. Prominent lobate scarps, interpreted as thrust faults, are found 100-500 km south of the dichotomy, near the crest of the rise [6]. Normal faults are observed along the boundary itself. Note that extensional features further out in the northern lowlands may have been buried by subsequent sedimentary or volcanic deposition. The age of deformation is Late Noachian to Early Hesperian [2,6].

Lower crustal flow: As noted by [3] and [7], the dichotomy may also have been modified by the tendency of the lower crust to flow outwards from areas of thickened crust. The rate of flow depends on the crustal thickness, rheology and temperature structure. Figure 1 shows an example of the evolution of the lower crust as a function of time due to lateral flow. Material is redistributed from the thick-crust to the thin-crust side.

The redistribution of lower crustal material will generate loads and thus modify the pre-existing topography. The change in topography depends on the effective elastic thickness T_e of the lithosphere. (Note that while the lower crustal flow model in Fig. 1 assumes isostasy i.e. $T_e=0$, a finite T_e will have little effect on the behaviour of lateral flow at the wavelengths under consideration here). Fig. 2a shows the final topography caused by the elastic response to the load due to lateral crustal flow. As expected, elevations are reduced on the thick-crust side of the dichotomy.

Fig. 2b shows the resulting surface stresses as a function of T_e . The reduction in elevation leads to compressional stresses on the thick-crust side of the dichotomy, and vice versa. The timing of the stresses depends on the rate at which lower crustal flow occurs. The lateral extent of the stresses depends on T_e , which was proba-

bly <15 km during the Noachian [8]. The magnitude of the stresses (~50 MPa) is relatively insensitive to elastic thickness. The corresponding elastic strain is ~0.05%, comparable to the value of 0.2% obtained by [9] from lobate scarp studies. The predictions of compression south of the dichotomy and extension further north are consistent with the observations.

Erosion: Erosion is likely to have modified the dichotomy surface topography. Fig 3 shows the effects of erosion, assuming that it can be modelled as a diffusion process. The redistribution of material from high to low elevations results in a load which will cause uplift on the thick-crust side and vice versa.

Fig 4a shows the load resulting from this mass redistribution, and the response of the lithosphere to this load. Isostatic rebound is not complete, because of the finite elastic thickness. Fig 4b shows the resulting surface stresses. The unloading and uplift of the thick-crust side results in extensional surface stresses of up to ~50 MPa. These results are not consistent with the geological observations, and suggest that erosional effects must be outweighed by effects leading to compression, such as lateral flow (see above) or global contraction.

Discussion: The mechanism proposed here can explain both the location and magnitude of the observed compressional and extensional features at the dichotomy boundary. It invokes local crustal flow, which is distinct from the global mantle flow models advocated by previous authors [2]. It also differs from the proposal by [6] that surface loading was responsible for the observed tectonic features. If this mechanism is correct, it implies that significant subsurface modification of the original dichotomy boundary has occurred, which will make it harder to test hypotheses of the dichotomy's origin. Conversely, it places limits on how much modification by erosion is likely to have happened.

References:

- [1] Frey, H.V. and R.A. Schultz, *Geophys. Res. Lett.* 15, 229-232, 1988. [2] McGill, G.E. and A.M. Dimitriou, *J. Geophys. Res.* 95, 12595-12605, 1990. [3] Zuber, M.T. et al., *Science* 287, 1788-1793, 2000. [4] Hynek, B.M. and R.J. Phillips, *Geology* 29, 407-410, 2001. [5] Frey, H.V. *Lunar. Planet. Sci. Conf. XXXIII*, 1727, 2002. [6] Watters, T.R., *J. Geophys. Res.* 108, 5054, 2003. [7] Nimmo, F. and D. Stevenson, *J. Geophys. Res.* 106, 5085-5098, 2001. [8] McGovern, P.J. et al. *J. Geophys. Res.* 107, 5136, 2002. [9] Watters, T.R. and M.S. Robinson, *J. Geophys. Res.* 104, 18981-18990, 1999.

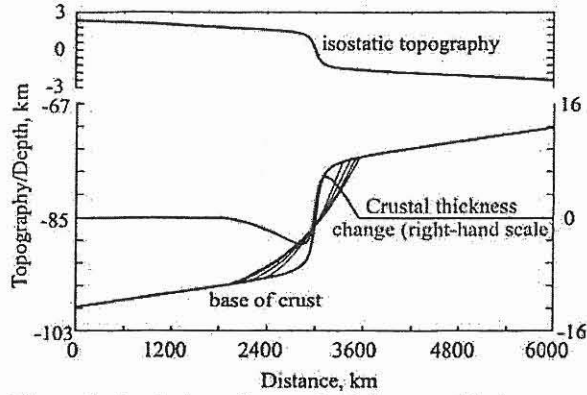


Figure 1. Evolution of crustal thickness with time, using lower crustal flow method of Nimmo and Stevenson (2001). Bold lines depict initial base of crust and resulting isostatic topography. Thin lines show evolution of base of crust with time, due to lateral flow. Red line shows change in crustal thickness; increase in thickness of lower crust generates an upwards load, and vice versa.

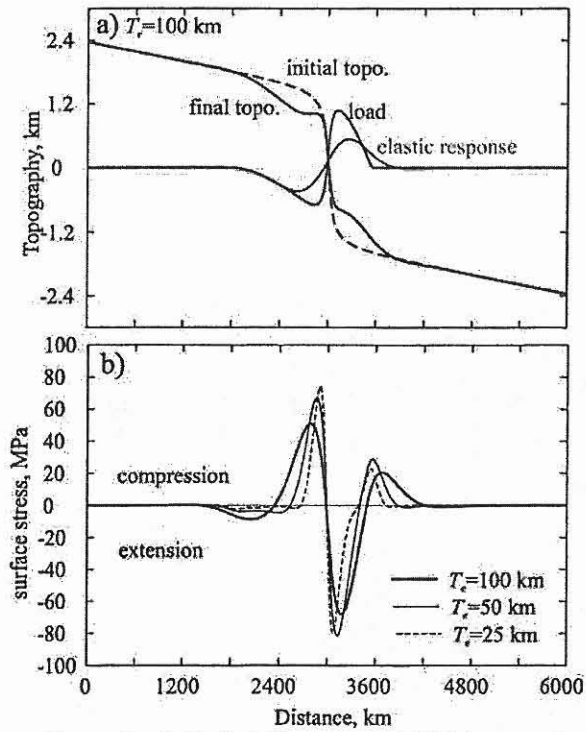


Figure 2. a) Dashed line shows initial topography from Fig 1a. Red line shows load generated by redistribution of lower crust (see Fig 1). Green line shows elastic response ($T_e=100$ km) to this load. Solid black line shows final topography once the elastic response is taken into account. b) Surface extensional stresses due to load shown in a). Stresses are compressional where crustal thickness has decreased.

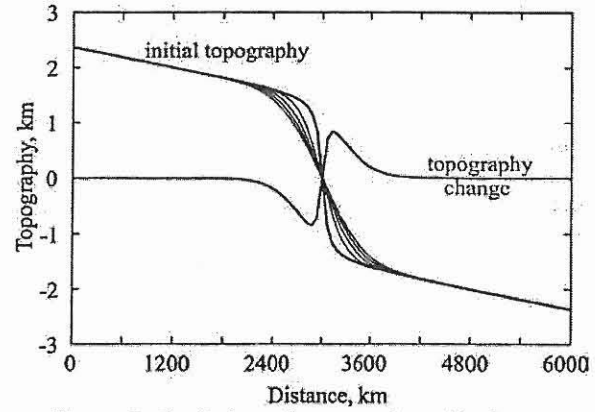


Figure 3. Evolution of topography with time, representing surface erosion by diffusion process. Bold line gives initial topography, red line gives change in topography. Reduction in topography results in an upwards load, and vice versa.

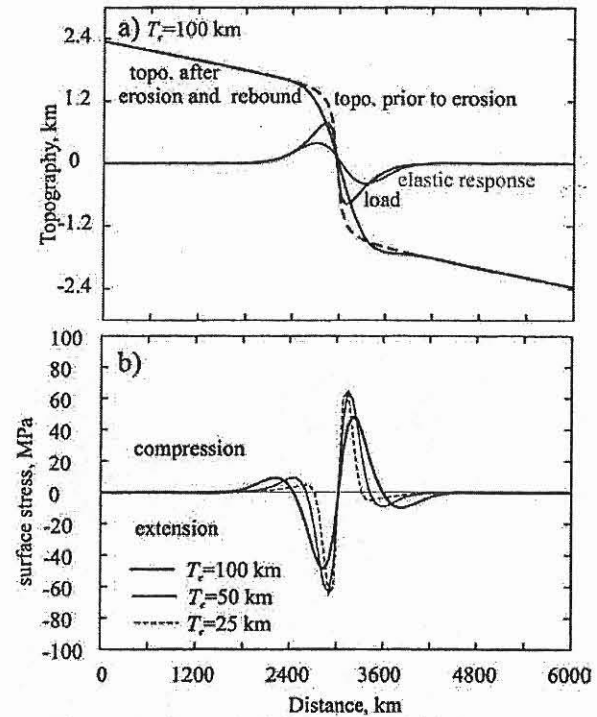


Figure 4. a) Dashed line shows initial topography from Fig 3a. Red line shows load generated by erosion (see Fig 3). Green line shows elastic response ($T_e=100$ km) to this load. Solid black line shows final topography once the erosional removal of topography and the elastic response are taken into account. b) Surface stresses due to load shown in a). Stresses are extensional where erosion has occurred.

GLACIAL MODIFICATION OF THE MARTIAN CRUST IN AEOLIS REGION, MARS. J. Nussbaumer,
Department of Mineralogy, Natural History Museum, London, UK, jurn@nhm.ac.uk.

Introduction: New Mars orbital data show evidence for widespread glaciation in Aeolis Region (Fig. 1). Geomorphic features like tunnel channels, and drumlins suggest a formation mechanism associated with subglacial high water pressures. Viscous flow features and moraines indicate ongoing sublimation and a rather young age for the retreating ice. These observations complement previous studies that report evidence for glaciation in southern Elysium Planitia.

Tunnel channels: Several subparallel broad- and flat-crested branches (Fig. 2a) with steep sides forms a radial and dendritic channel network. They are interpreted as a "tunnel channels", a subglacial drainage system. Their excavated positive relief (height ~40 m) indicate high pressure sedimentation [1]. The adjacent material was eroded by sublimation or aeolian activity. They are formed by subglacial meltwater flowing under high hydrostatic pressure and have been associated with large subglacial outburst floods on Earth [2, 3]. Sedimentation is thought to have taken place in a waning stage of the flood event, that fills the cavities with stratified sediments. MOLA data shows such crests are oriented perpendicular to the remains of an overlying unit (box in Fig. 1).

Drumlins: Longitudinal and streamlined accumulations (Fig. 2a) aligned parallel to former glacier flow directions, are located next to channel like forms and are interpreted as drumlin fields. In special cases, drumlin fields may reflect zones of formation behind former ice margins. Frozen margins could have blocked subglacial drainage, leading to elevated porewater pressures [4]. The general slope according to MOLA data is towards south. Their steep ends point in the up ice direction, the gentler slope is on the lee side. Their formation mechanism is controversial, however it always includes ice sheets. Terrestrial drumlins are concentrated in fields and form where basal shear stress is low and porewater pressures are high [5]. They were associated with catastrophic meltwater floods on Earth [6].

Viscous flow features: Sinuous glacier-like flow features, confined by compressional ridges (lateral moraines), are visible in Themis daytime IR images (Fig 3a). Lateral moraines are dumped to the adjacent terrain during ice recession. MOLA data shows a concave U-shaped cross-section which indicates glacial erosion. These flows or former glaciated valleys discharge into a basin showing a bright area in nighttime Themis IR images, indicating higher thermal inertia, suggesting the existence of solid surface material, which maintains day temperatures.

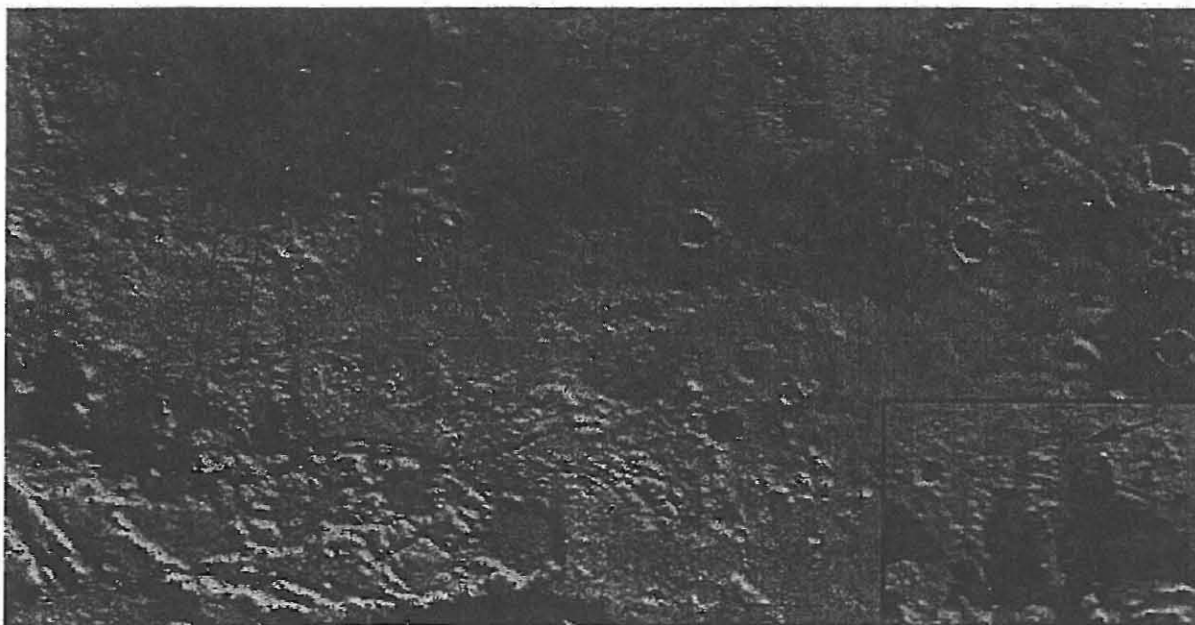


Fig. 1: MOLA Overview (128 x 256 pxl/deg.), boxes mark Fig. 2 (left) and Fig. 3 (right), image width is ~500 km, North is up.

Moraines: Sinuous lobate ridges are superposed on hummocky terrain, resembling the shape of nearby

higherstanding knobby deposits. These features are interpreted as end moraines and ground moraines, visi-

ble in Themis VIS images (Fig 3b). End moraines as a result of retreating ice are produced by dumping of debris, where the ice margin remains stationary during debris accumulation. Surficial features like round knobs may indicate ongoing sublimation processes. Ground moraines form hummocks and hills and represent the end products of debris-mantled ice ablation [7].

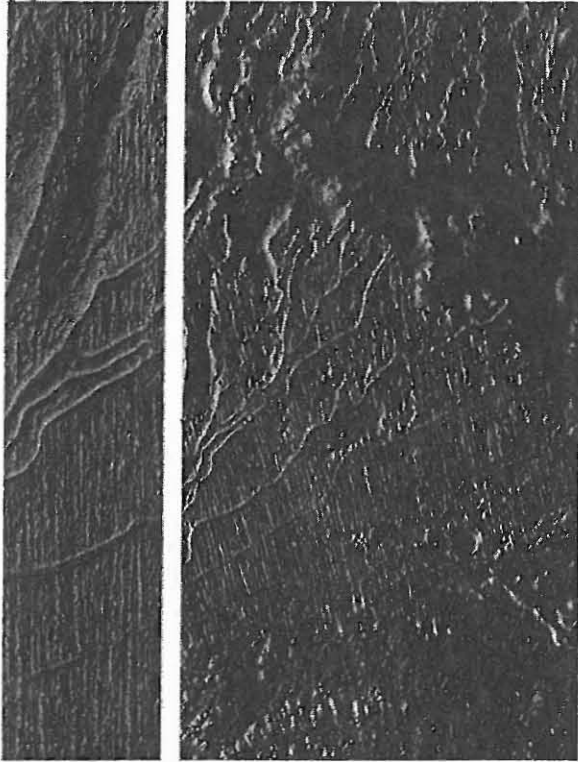


Fig. 2a: MOC e1800307 (left), 5,96 m/pxl, ~3km width, Tunnel channels and Drumlin fields.

Fig. 2b: Themis V05588002 (right), ~20 m/pxl, 18,4 km width, context image for Fig. 2a, shows branched channels.

Conclusions: The formation of equatorial ice sheets is essentially based on two different theories. Firstly, changes of Mars' tilt axis could be responsible for ice deposition in lower latitudes [8]. Secondly, water eruption from pressurized aquifers as a result of a growing cryosphere could form ice sheets as well [9]. Drumlin fields adjacent to tunnel valleys represent erosional forms associated with high water pressures [6]. Terrestrial analogies are found in permafrost regions, where freezing and pressurization of confined aquifers creates pingos and icing outbursts, also existent as cryovolcanism on icy moons.

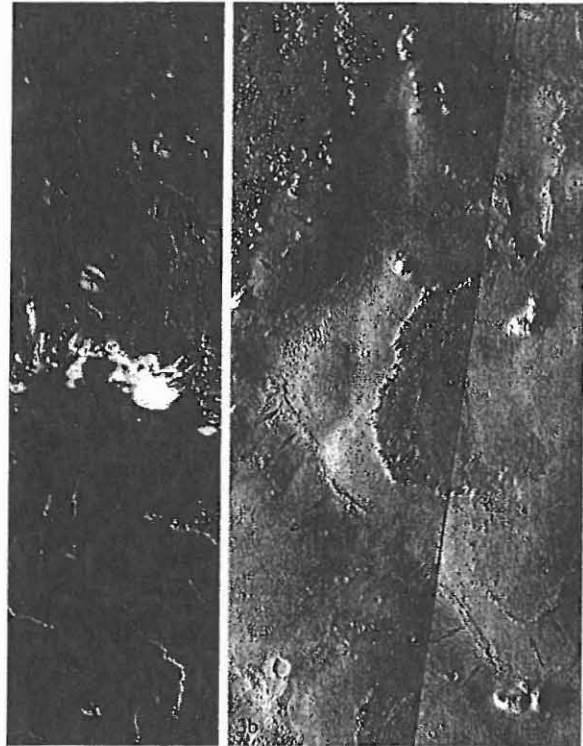


Fig. 3a: Themis I07684014 (left) showing Glacier-like viscous flows debouching into a bright basin, image width is 32 km, ~100m/pxl, box marks position of Fig. 3b.

Fig. 3b: Themis V06212002, V06574001(right), width is ~20 km, 20m/pxl res., shows moraine-like features (2), hummocky and knobby terrain (1) indicating ongoing sublimation.

References:

- [1] Russell, H. A. J. (2003) *Sedimentary Geology*, 160, 33–55. [2] Cutler, P. M. (2002) *Quaternary International*, 90, 23–40. [3] Beaney, C. L. (2002) *Quaternary International*, 90, 67–74. [4] Wright, H. E. (1957) *Geografiska Annaler* 39, 19–31. [5] Patterson, C. J. and Hooke, R. Le B. (1996) *Journal of Glaciology*, 41, 30–38 [6] Shaw, J. (2002) *Quaternary International*, 90, 5–22. [7] Harker, A. (1901) *Transactions of the Royal Society of Edinburgh*, 40, 221–225. [8] Mischna, M. et al. (2003) *J. Geophys. Res.*, 108, E6, pp. 16–1. [9] Gaidos, and Marion, G. (2003) *J. Geophys. Res.* E6 108, pp. 9–1.

Acknowledgements: This work is funded by the Marie Curie Association.

DEGREE-1 MANTLE CONVECTION AS A PROCESS FOR GENERATING THE MARTIAN HEMISPHERIC DICHOTOMY. James H. Roberts, *Department of Astrophysical and Planetary Sciences, University of Colorado, Boulder CO 80309-0391, USA, (jhr@anquetil.colorado.edu)*, Shijie Zhong, *Department of Physics, University of Colorado, Boulder CO 80309-0390, USA, (szhong@spice.colorado.edu)*.

Introduction

The crustal dichotomy is one of the most significant topographic and tectonic features on Mars [1]. The gradual pole-to-pole crustal thickness variations inferred from MGS topography and gravity data do not seem to support an exogenic origin, such as giant impacts [2]. We therefore seek to explain this as an endogenic feature, resulting from a degree-1 convection pattern in the mantle [3, 4].

We propose and test two hypotheses for how degree-1 mantle convection may lead to the crustal dichotomy [4]. In the first scenario, the planet starts with no crust at all. Partial melt occurs in a degree-1 plume, where upwelling material is above the solidus. This melt is then extracted to form crust above the plume. In the second scenario, a uniform crust overlies a mantle containing a single convection cell. The Martian crust is thought to be at least 50 km thick [3]. Early in Martian history, the base of such a thick crust may have been so warm as to be ductile. An upwelling mantle plume would erode the lower crust above it and move it laterally to be deposited at the base of the crust above the downwelling. As the interior cools, the crust would lose its mobility and this degree-1 pattern would be frozen in.

For either hypothesis to be tested, it is first necessary to have degree-1 convection in the mantle. We modeled stagnant lid convection in a primitive mantle to test the first hypothesis. In the second scenario, the warm, ductile lower crust may be decoupled from the mantle. The mantle is thus warm enough to be in the mobile-lid regime and we model it as such, overlain by a uniform crustal layer. We used finite-element convection code to solve the equations of mass, momentum, and energy in 2D axisymmetric and 3D spherical geometry [5,6]. The mantle was heated both from below and within and cooled from above. The viscosity was both temperature and pressure-dependent, following an Arrhenius Law. We used non-Newtonian activation parameters appropriate for a wet mantle [7] scaled to Newtonian rheology. We used depth-dependent thermal expansivity and diffusivity and considered the effects of adiabatic and frictional heating [8].

Stagnant-lid Convection in a Primitive Mantle

Many studies have been done to generate degree-1 convection in a stagnant-lid mantle [4,9-11], but all of them rely upon certain assumptions which may not be reasonable for a general Mars model. We sought to test these mechanisms while relaxing the assumptions to develop a more robust model of degree-1 convection.

Zhong and Zuber [4] achieved degree-1 convection using a layered-viscosity model, with an upper mantle 500 times less viscous than the lower mantle, capped by a high viscosity lid. The viscosity jump is a proxy for various possible mechanisms

including melting, phase change, pressure-dependent viscosity and non-Newtonian rheology. They did not attempt to seek minimum required viscosity jump for degree-1 convection. We wanted to relax the assumption that the mantle was layered, so we attempted to run their model using temperature and pressure-dependent viscosity in place of the layering, while preserving the overall viscosity contrast across the mantle. We were able to maintain a degree-1 pattern when we substituted pressure-dependence for much of the layering, but a jump in viscosity between the upper and lower mantle was still necessary. We were able to reduce the jump to a factor of 25 from a factor of 500 (Fig. 1), but could not eliminate it entirely and still maintain the convective pattern.



Figure 1: Degree-1 thermal convection pattern from a case with temperature-and depth-dependent rheology and a factor of 25 viscosity jump between the upper and lower mantle. Shown are 5% isosurfaces of residual temperature (yellow: relatively hot, blue: relatively cold)

Several studies [9-11] have utilized phase changes in the mantle as a mechanism for generating a degree-1 convective pattern. Harder and Christensen [9] and Harder [10] considered the endothermic spinel-perovskite phase change in an isoviscous mantle with a high viscosity lid. We successfully reproduced their results in 2D axisymmetric geometry, however, the inclusion of temperature-dependent viscosity destroys the single plume structure (Fig. 2). We have computed models with different phase change parameters, Rayleigh numbers and rheological parameters. We find that only when activation energy is unreasonably low (≤ 60 kJ/mol) we could produce degree-1 convection with the endothermic phase change. Furthermore, recent studies on the size of the Martian core [12] cast doubt as to whether the required pressure for this phase change is ever reached in the Martian mantle. Breuer *et al.* [11] considered the exothermic olivine-spinel transition, including the latent heat effects and obtained a single plume structure. Our experiments with this phase change failed to

produce a degree-1 pattern, indicating the limited role of the latent heating from the exothermic phase change. However, as Harder [10] pointed out, the calculations in [11] are in the mobile-lid regime. This, more than the physics of the exothermic phase change controls the convective pattern. Therefore, it is not surprising that we failed to achieve degree-1 in the stagnant lid regime.

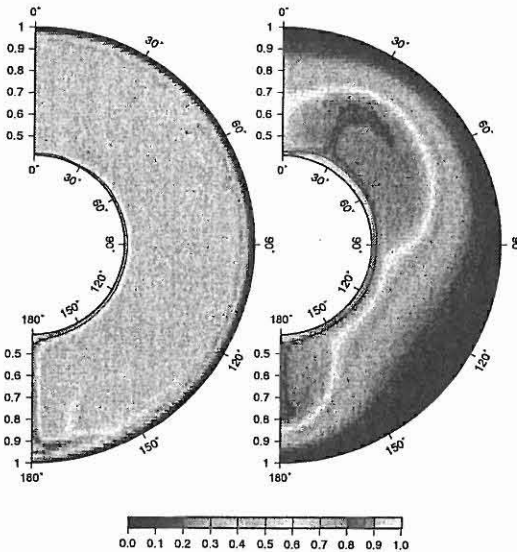


Figure 2: Comparison of two thermal convection cases including endothermic phase change. Location of phase transition indicated by the black curve near the CMB. Left: iso-viscous interior with high viscosity lid. Right: Temperature-dependent viscosity, activation energy of 180 kJ/mol.

Mobile-lid Convection

Mobile-lid convection, however, may be an appropriate choice for the second scenario. At the time of formation of the hemispheric dichotomy, the lower crust may have been so warm as to be decoupled from the mantle. We ran a series of calculations using the Moho temperature as the upper boundary

condition. The entire mantle was sufficiently warm that the mantle was in the mobile lid regime. However, we have not yet incorporated crust into these models. This produced degree-1 convection in some of the preliminary 2D models. With 3D spherical models, we achieve degree-1 structure with moderate temperature-dependent viscosity.

Discussions and Future Work

We find that although there are many ways of generating a degree-1 convective pattern in a stagnant-lid mantle, they rely upon certain assumptions that may not be reasonable for a realistic Mars. A layered viscosity structure is one way to get the desired convective pattern, but the actual mantle viscosity depends on temperature and pressure. If a viscosity jump is employed, there must be a physical reason for such a discontinuity. However a number of mechanisms may lead to a jump in viscosity. The exothermic phase change from olivine to spinel may lead to viscosity layering as often suggested for the Earth's mantle. Non-Newtonian mantle rheology may also be able to produce sharp viscosity transitions because of change in deformation mechanisms. We are currently exploring the roles of non-Newtonian rheology in producing sharp viscosity changes.

The mobile lid regime may be appropriate if the crust and mantle are sufficiently warm as to decouple the crust and the mantle, as one may expect for the early Mars. However, care must be taken to couple the convection models to the crustal conduction profile in a physically realistic way. We are currently working on a way to resolve this issue.

References

- [1] Smith et al. (1999) *Science* 284, 1495. [2] Zuber et al. (2000) *Science* 287, 1788. [3] Wise et al. (1979) *J. Geophys. Res.* 84, 7934. [4] Zhong and Zuber (2001) *Earth Planet. Sci. Lett.* 189, 75. [5] Zhong et al. (2000) *JGR* 105 11063. [6] Moresi and Solomatov (1995) *Phys. Fluids* 7, 2154. [7] Karato and Jung (2003) *Phil. Mag.* 83, 401. [8] Christensen and Yuen (1985) *J. Geophys. Res.* 90, 10,291. [9] Harder and Christensen (1996) *Nature* 380, 507. [10] Harder (2000) *Geophys. Res. Lett.* 27, 301. [11] Breuer et al. (1998) *GRL* 25 229-232. [12] Yoder et al. (2003) *Science* 300, 299.

CONTROL OF EXPOSED AND BURIED IMPACT CRATERS AND RELATED FRACTURE SYSTEMS ON HYDROGEOLOGY, GROUND SUBSIDENCE/COLLAPSE, AND CHAOTIC TERRAIN FORMATION, MARS. J.A.P. Rodriguez¹, S. Sasaki¹, J.M. Dohm², K.L. Tanaka³, H. Miyamoto², V. Baker², J.A. Skinner, Jr.³, G. Komatsu⁴, A.G. Fairén⁵ and J.C. Ferris⁶. ¹Department of Earth and Planetary Sci., Univ. of Tokyo, 7-3-1 Hongo, Bunkyo-ku Tokyo 113-0033, Japan (Alexis@space.eps.s.u-tokyo.ac.jp, sho@eps.s.u-tokyo.ac.jp), ²Department of Hydrology and Water Resources, Univ. of Arizona, AZ 85721 (miyamoto@geosys.t.u-tokyo.ac.jp, jmd@hwr.arizona.edu), ³Astrogeology Team, U.S. Geological Survey, Flagstaff, AZ 86001 (ktanaka@usgs.gov, jkskinner@usgs.gov), ⁴International Research School of Planetary Sciences, Università d'Annunzio, 65127 Pescara, Italy (goro@irsps.unich.it), ⁵Centro de Biología Molecular, Universidad Autónoma de Madrid, 28049 Cantoblanco, Madrid, Spain (agfairén@cbm.uam.es), ⁶U.S. Geological Survey, Denver, CO, 80225 (jcferris@usgs.gov).

Introduction. Mars is a planet enriched by ground-water [1,2]. Control of subsurface hydrology by tectonic and igneous processes is widely documented, both for Earth and Mars [e.g., 3]. Impact craters result in extensive fracturing, including radial and concentric peripheral fault systems, which in the case of Earth have been recognized as predominantly strike-slip and listric extensional, respectively [4]. In this work we propose that basement structures of Mars largely result from impact-induced tectonism, except in regions that are dominated by magmatic-driven activity such as Tharsis [e.g., 5] and/or possible plate tectonism during the extremely ancient period of Mars e.g., [6]. In many cases, impact-induced faults appear to have been reactivated and/or displaced by subsequent magmatic-driven groundwater-flow and collapse processes [7].

Fractured impact crater floors: These features are concentrated in the ancient cratered highlands along the margins of plain regions and within the lightly cratered plains near the canyon system of Valles Marineris [8]. Moats within some of these craters of varying diameters and relative ages surround plateaus and contain broken material (Fig. 1). The moats appear to be restricted to the margins of highly degraded crater rims. Only certain craters in a given region, however, display these characteristics. Schultz and Glicken [8] proposed that modification processes were localized by the impact structures and restricted to the crater interiors. They interpret this to be the result of heat generated by a tabular magmatic intrusion injected beneath the brecciated zone of an impact crater, which raises the temperature of the overlying material. Thawed materials would then subsequently escape through the peripheral fracture system surrounding the crater, or alternatively, a metastable state of liquification could occur, if the material is confined or the rate of thawing exceeds the rate of escape. The collapsed material within a moat marking a highly degraded impact crater rim forms ridges around a central plateau region (Fig. 1B). This suggests that the degradational processes may have been controlled by extensional concentric faults, possibly initiated during the inward collapse of the transient crater walls [4] and/or by concentric fractures produced by the uplift of the crater floor,

possibly resulting from the injection of a tabular magma body beneath the crater floor [8]. The water-enriched source region, which may have contributed to the formation of the features shown in Fig. 1A,B, has been destroyed, suggesting that the formation of the moat may have involved hydrologic processes. In addition, a depression that transects an impact crater (Fig. 1B) forms part of a longer valley, which terminates at the western margin of the Hydraspis Chaos (Fig. 1, V-B). This scenario may be explained by tabular intrusions being injected under crater floors and/or by hydrologic processes controlled by structures within impact craters [8].

Progressive highland subsidence and collapse: Rodriguez et al. [9] described the progressive highland subsidence and collapse of the Late Noachian subdued crater unit [10] in Xanthe Terra (Fig. 1). They propose that regional subsidence and collapse resulted from the release of pressurized groundwater in confined caverns. The release of water described in [9] served as an important, previously unproposed source of the water that carved the outflow channels. Terraced terrain marked by both chaotic terrain and channel bedforms (Fig. 2) may also indicate the release of large quantities of water and related collapse. These observations suggest that the plateau material was degraded and removed more efficiently from within craters than from the surrounding country rock (Fig. 3).

Crater-related fracture networks: Layered materials are pervasive on Mars [11] and may contain numerous buried impact craters of varying degradational states (Fig. 3). We propose that impact-induced fracture systems dominate the fracture population in the ancient highlands, away from volcano-tectonic regions [7]. Intermingling concentric and radial fracture systems from multiple impact crater events will result in complex crater fracture networks (CFN). Periods of rapid and/or modest surface burial, or periods of lesser bombardment and higher burial, will result in regions with relatively less abundant buried impact crater populations. As a consequence, the CFN will be less developed. On the other hand, heavy bombardment coupled with slow degradation and/or surface burial are expected to result in denser buried crater populations and highly developed

CFN. We propose that the highland plateaus are stratified into zones of variable fracture density. Fractures radial to impact craters will tend to converge near the buried craters' interior deposits. Since heat flow is hydrothermally transferred more rapidly and effectively along fracture planes, a consequence of this scenario is that pulses of heat, generated by magmatism, for example, will result in a highly anisotropic heat flow distribution, with higher heat flow and thus warming in areas of high fracture density. Valley networks dissecting the crater rims in the ancient highlands [1] suggests that crater interior deposits may have contained significant amounts of water-laden sediments. Therefore, buried impact craters are likely to be ice-enriched regions within the Martian permafrost [2]. Warming of the crater interior deposits might have resulted in melting of large volumes of water and intensive hydrothermal circulation and fracture enlargement, forming conduits that allowed subsurface distal migration of volatiles as well as escape to the surface. We propose that circulation within densely fractured regions will be highly effective at removing crater materials, possibly forming cavities, and resulting in the storage of large amounts of water within the subsurface conduit systems and porous media. Lateral interconnection will be enhanced by subsequent impacts. For example, impacted-induced basement structures and uplifted and overturned strata that dip away from the crater will interconnect regions with different permeability and volatile content. We propose that the distinct topographic levels visible in the plateau region of Fig. 2 can be explained by the successive collapse of densely fractured zones. The distribution of moderately vs. highly fractured zones, particularly if stratigraphically controlled, will determine the number of collapsed plateau levels in a given highland region. If collapse occurs to great depths, or the thickness of the collapse region is relatively thick, the plateau surface might respond by simple crustal warping and fracturing. On the other hand, if collapse occurs to shallow depths or the thickness of the collapse region is relatively thin, chaotic material may result. Evidence such as truncated impact craters preferentially preserved at distinct levels of subsidence (Fig. 2) and collapse features more common on crater floors (versus surrounding plateau material; Fig. 1) collectively add credence to our hypothesis that suggests preferential removal of subsurface crater interior deposits. Yet fracturing and collapse of crater floors were not localized to individual impact structures. Non-uniform groundwater and heat flow may explain why only certain craters display the characteristics described above for a given region. The formation of moats encompassing crater infill (e.g., Fig. 1) suggests that impact-induced fractures are more densely packed around the periphery of the crater rather than beneath the central fill.

Highland-lowland dichotomy: The highland-lowland transition regions are marked by a wide range of features indicative of subsidence and collapse. We propose that CFN may have been an important basement control on the lateral and vertical distribution of these topographic variations along the dichotomy boundary.

Fig. 1. A. THEMIS day-time infrared composite. 50 km in diameter impact crater with a moat around a central plateau (CA). North is at top. Lobate features (L). Impact crater with poorly developed moat (red arrow). A 30 km wide, 300 m deep depression transects the crater (blue pointer). B. Composite of MOLA DEM containing A.

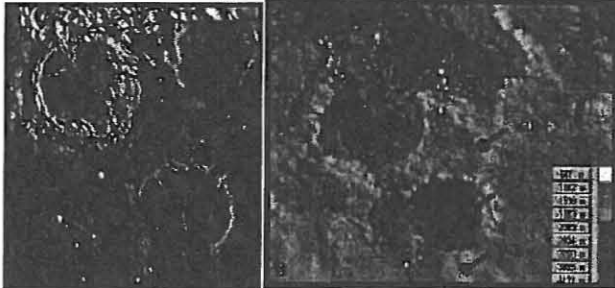


Fig. 2. MOLA based DEM. Image is 350 km wide. Noachian plateau region located to the north of Eos Chasma. Chaotic materials occur at several topographic levels (CL-A to E). Channel bedforms (blue arrows). Arcuate scarps (red pointers).



Fig. 3. THEMIS day-time infrared subframe showing Noachian plateau near Hydaspiis Chaos. Arcuate scarp 1000 m high exposes layered sequence.



- References:** [1] Carr M.H. (1996) *Water on Mars*, Oxford Uni. Press. [2] Clifford S.M. (1993) *GRL*, 19073-11016. [3] Rodriguez J.A.P. et al. (2003) *GRL* 30, 1304. [4] Osinski G.R. and J.G. Spray (2003) *Workshop on Impact Cratering*, #8010. [5] Anderson, R.C. et al. (2001) *JGR* 106, 20,563-20,585. [6] Baker, V.R. et al. (2002) *Geosciences* 7. [7] Dohm, J.M. et al. (2001) *JGR*. 106, 32,943-32,958. [8] Schultz H.P. and Glikson H. *JGR* (1979) 84, . [9] Rodriguez J.A.P. et al (2004) *LPSC XXXV*, #1676. [10] Rotto S. and Tanaka K.L. (1995) *USGS Map I-2441*. [11] Malin M. C. and Edgett K. S. (1999) *Fifth International Conference on Mars*, #6027.

OUTFLOW CHANNEL SOURCES, REACTIVATION AND CHAOS FORMATION, XANTHE TERRA, MARS. J.A.P. Rodriguez¹, S. Sasaki¹, J.M. Dohm², K.L. Tanaka³, H. Miyamoto², V. Baker², J.A. Skinner, Jr.³, G. Komatsu⁴ and A.G. Fairén⁵ and J.C. Ferris⁶. ¹Department of Earth and Planetary Sci., Univ. of Tokyo, 7-3-1 Hongo, Bunkyo-ku Tokyo 113-0033, Japan (Alexis@space.eps.s.u-tokyo.ac.jp, sho@eps.s.u-tokyo.ac.jp), ²Department of Hydrology and Water Resources, Univ. of Arizona, AZ 85721 (miyamoto@geosys.t.u-tokyo.ac.jp, jmd@hwr.arizona.edu), ³Astrogeology Team, U.S. Geological Survey, Flagstaff, AZ 86001 (ktanaka@usgs.gov, jkskinner@usgs.gov), ⁴International Research School of Planetary Sciences, Università d'Annunzio, 65127 Pescara, Italy (goro@irsps.unich.it), ⁵Centro de Biología Molecular, Universidad Autónoma de Madrid, 28049 Cantoblanco, Madrid, Spain (agfairen@cbm.uam.es), ⁶U.S. Geological Survey, Denver, CO, 80225 (jcferris@usgs.gov).

Introduction: The formation of outflow channels is classically attributed to the catastrophic discharge of groundwater [e.g.1,2]. Documented modes of confinement and release of groundwater, trapped within the Martian cryosphere include: catastrophic release of groundwater from confined aquifers [3], both catastrophic and non-catastrophic release of groundwater segregated from the permafrost into confined caverns [4], and catastrophic release of groundwater extracted from the permafrost by thermal convection [5]. Multiple events groundwater release resulted in the collapse of plateau materials [3,6,7], and the formation of chaotic terrains, which are mostly located at the head source regions of the outflow channels [6]. Crater counting of the outflow channel floors indicates a late Hesperian age [8], though earlier channeling events may have occurred [8,9,10,11]. Based on geologic mapping and geomorphic assessment using Viking-, Mars Global Surveyor-, and Mars Odyssey-based information of a highland region located east of Valles Marineris and bounded to the south, west, and north by Aureum, Hydraotes, and Hydaspis Chaos, respectively (hereafter referred to as the subsided plateau region--SPR; Figure 1), we propose new hypotheses, which can potentially explain the following unresolved issues: (1) sources for the large volumes of water required to carve the outflow channels, (2) mechanisms of outflow reactivation, which do not involve recharging of the head source region, and (3) an alternative mode of formation for chaotic terrains.

Highland subsidence: The SPR consists mostly of Late Noachian smooth to undulatory intercrater plains materials (unit, Npl2), which are marked by partly buried, mostly rimless and flat-floored impact craters [5]. The surface of the SPR is transected by northwest- and east-trending valley systems (E.G.: Figure 1, V-A). The contact with adjacent regions of the subdued cratered unit is gradational in places and sharp in others (Figure 1, SC, GC). Considerable changes in elevation occur over relatively short distances at contacts. For example, a maximum elevation difference of 2 km over a distance of 100 km is observed at the sharp boundary between SPR and the floor of valley A (Figure 1, SC, V-A). In the western part of valley-A (Figure 1, V-A), linear shallow scarps, (Figure 2B, S), scarp-bounded valleys (Figure 2B, V), and Graben-Horst systems (Figure 2B, GH) are visible. We propose that these features are the

manifestation of different degrees of relative displacement along normal fault planes, which possibly resulted due to ground subsidence [12].

Post-outflow chaotic terrains: South of the Hydaspis Chaos, the surface is heavily fractured with abundant scarps and graben systems in the northern region of the SPR. In this region the plateau margin breaks up gradually into chaotic material (Figure 3). The chaotic material clearly overlaps the surface of the outflow channel (Figure 3), which implies that it, at least in part, post-dates the surface of the adjacent outflow channel. These observations are not fully consistent with a strictly genetic association between chaotic regions and the outflow channels [e.g. 3, 6, 8], in which collapse of the ground formed the chaos, as water and debris were released catastrophically to form the associated outflow channels. Chaotic material possibly resting on top of outflow channel floors may result from aquifer discharges from levels above pre-existing channel floors.

Evidence for outflow reactivation: Elevation profiles of channel floor remnants (Figure 1, RM-A, B, C) taken from MOLA data reveal that these regions have the same maximum and minimum elevation values. These regions also display similar geomorphic characteristics and interpreted to result from contemporaneous surface flow activity during early and intermediate stages of excavation of the outflow channels [8]. A northern branch from the Hydraotes Chaos (Figure 1, HB-1) crosscuts the channel floor remnant C (Figure 3). Topographic and crosscutting relationships indicate that two more Hydraotes branches formed subsequently (Figure 1, HB-2, 3). The latest branch is in turn intercepted by the Tiu Vallis lower channel floor (Figure 1, TLC), as indicated by a marginal scarp contact. These observations indicate that reactivation of the flow from the Hydaspis source region has taken place.

Discussion: Our observations indicate that the warped and densely fractured surface of SPR resulted from ground subsidence. Ground subsidence possibly resulted from compensational sinking due to the removal of underground geologic materials by subsurface flow and/or by igneously induced segregation of the water phase within the permafrost into discrete regions, which was subsequently released to the Martian surface. In both cases, in multiple underground levels of caverns

[13] are likely to result. Subsurface structural control, which is consistent with the existence of caverns, is supported by well-defined SPR boundaries and geometric patterns of ground subsidence and collapse features that mimic the trends of adjoining valley systems and basement structures. In the vicinity of the Hydaspiis Chaos region, for example, the SPR is highly fractured, interpreted here to mark collapse of unstable regions of the SPR margin; the formation of the chaotic terrain postdates both the stage of plateau subsidence and the excavation of the adjacent outflow channels. In this particular case, we propose the following sequence of events (from oldest to youngest): (1) large volumes of water are locally stored in multiple levels of confined underground caverns [4], (2) subsequent release of water from these confined systems to the Martian surface combines with the transport of water from distal regions within the putative Tharsis aquifer [14] into the cavernous system, possibly routed through subsurface conduits [4] and/or fracture systems [13], and (3) the emergence of floodwaters from the Hydaspiis and other Chaotic regions in the circum-Chryse region carve the outflow channels. The Hydaspiis Chaos is mainly made up of a cluster of collapsed craters (Figure 1, CC). Since the lower elevations of the crater floors represent regions of relatively lower lithostatic pressure over the confined caverns, and the ground is densely fractured beneath the craters, they are regions where deconfinement is more likely to occur. In the proposed geologic scenario, as water drained away from the caverns, sinking and fracturing of the plateau surface would take place due to a decrease in the basal supportive hydrostatic pressure, ultimately resulting in the formation of the SPR. Reconfinement of the system might result from freezing of its surface region. Buildup of the hydraulic head and outflow reactivation might occur if the hydrostatic pressure increases, which could be caused by (1) thickening of the permafrost seal, (2) sinking of the cavern roof and/or (3) thermal heating of the region related to another pulse of Tharsis-driven magmatic activity [e.g., 14]. Reactivation could also be related to the deconfinement of lower cavernous levels as the confining pressure decreases due to the loss of water and debris from overlying preexisting confined caverns. After water fully drains away from the caverns, relatively shallow, late-stage collapse would occur over the unstable caverns with little or no volatile release. We propose that deconfinement of caverns resulted in the formation of extensive chaotic terrains and large-scale subsidence, features which mark the transition from highlands to lowlands, particularly in the eastern circum-Chryse region of Mars.

References: [1] Baker V.R. and D.J. Milton (1974) *Icarus*, 23, 27-41. [2] Baker V.R. (1982) *The Channels of Mars*, University of Texas Press, Austin. [3] Carr M.H. (1979) *JGR*, 84, 2995-3007. [4] Rodriguez J.A.P. et al. (2003) *GRL*, 30,

1304. [5] Ogawa Y. et al. (2003) *JGR* 108, 8046. [6] Carr M.H. (1996) *Water on Mars*, Oxford Uni. Press. [7] Lucchitta, B.K. et al. (1994) *JGR* 99, 3783-3798. [8] Rotto S. and K.L. Tanaka (1995) *USGS Map I-2441*. [9] Scott, D. H. (1993) *USGS I-Map* 2208. [10] Nelson, D. M., and R. Greeley, (1999) *JGR* 104, 8653. [11] Scott, D. H., and K. L. Tanaka, (1986) *USGS Map I-1802-A*. [12] Krassilnikov I. et al. (2003) *Vernadsky Microsymposium* 38, #051. [13] Rodriguez J.A.P. et al (2004) *LPS XXXV*, #.11 [14] Dohm J.M. et al. (2001) *JGR* 106, 32,943-32,958.

Figure 1. Context MOLA based DEM. North is up. White circle indicates the location of the MOC subframe in Figure 2. White rectangle indicates the location of the THEMIS image subframe in Figure 3. North at top.

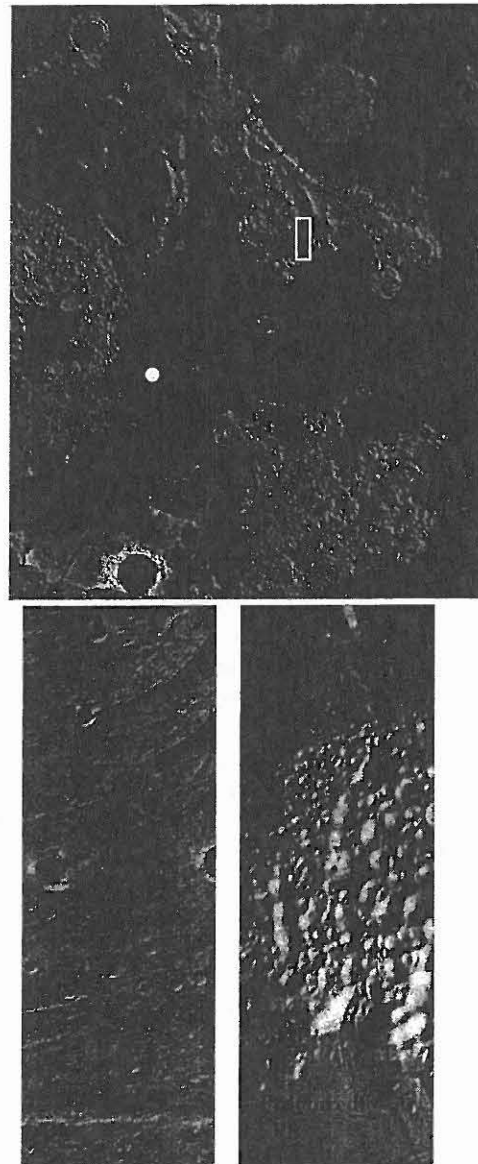


Figure 2. (Left) MOCNA image m1800610. Width is 2.77 km. North azimuth is 93. 12° **Figure 3.** (Right) THEMIS day IR I03883003. Width is 32 km. North is up.

MASS-WASTING OF THE CIRCUM-UTOPIA HIGHLAND/LOWLAND BOUNDARY: PROCESSES AND CONTROLS. J. A. Skinner, Jr.¹ (jskinner@usgs.gov) K. L. Tanaka¹, T. M. Hare¹, J. Kargel¹, G. Neukum², S. C. Werner², and J. A. P. Rodriguez³. ¹Astrogeology Team, U. S. Geological Survey, Flagstaff, AZ 86001; ²Institute for Geosciences, Freie Universitaet Berlin; ³Department of Earth and Planetary Science, University of Tokyo.

Introduction: Utopia Planitia forms a large (~3300 km diameter), plate-shaped depression interpreted as an ancient impact basin based on its regional gravitational expression [1] and its distribution of knobs, mesas, and partly buried craters [2]. Gravity studies indicate the basin may contain >10 km of material (~50x10⁶ km³) [8]. The southern and western boundary of the basin is rimmed by a ~400 km wide, arcuate exposure of the highland/lowland boundary (HLB) that extends >4000 km from Nepenthes to Protonilus Mensae (circum-Utopia HLB). The materials generally consist of fractured highland materials, degraded mesas and knobs, interposed slope materials, and smooth to undulating plains. These materials are variably interpreted as marginal marine features [4,5], lava flows [6], mass-wasting materials [2,3], and mud volcanoes [7]. However, these interpretations do not fully address the long-lived modification of the regional HLB and the massive infill of the Utopia impact basin.

We outline observations and offer hypotheses that suggest the circum-Utopia HLB has undergone long-term mass-wasting since the pre-Noachian formation of the Utopia impact basin. These processes are thermally driven, directly affect the ancient structural and stratigraphic framework of the circum-Utopia HLB, appear to be self-propagating, and are able to move massive volumes of material downslope.

Study Area: The circum-Utopia HLB was selected because it (1) was likely affected by various levels of geothermal heat, a mechanism to mobilize subsurface volatiles; (2) contains an excellent vertical and lateral exposure of highland and boundary plains materials, generally expressed as subdued "benches" that grade into lowland plains materials; (3) contains both extensional and contractional structural features; and (4) is proximal to a major structural and topographic basin.

Geologic Character. The circum-Utopia HLB ranges in elevation from approximately 0 to -3.5 km, though local rises and depressions exist outside of this elevation range. On average, the land surface slopes gently (<1.0°) toward the center of Utopia basin (approx. 50°N, 120°E [2]). However, some scarps, particularly in proximity to the highlands, locally exceed >30°. In general, the circum-Utopia HLB has relatively consistent contact elevations, which grade from cratered highland materials (Noachis unit; 0 to -1

km elevation) to dense knobs, mesas and local depressions (Nepenthes unit 1; ~ -2 km) to smooth, gently undulating plains (Utopia unit 1; -2 to -3 km) and finally, to isolated or coalesced, irregularly-shaped, shallow depressions (Utopia unit 2; -3 to -3.5 km). (Please refer to [3] and [7] for in-depth unit descriptions.) Notable deviations from the above elevation ranges occur in Nepenthes and Protonilus Mensae, where elevations of knobs and mesas are below -2 km. Crater counts indicate the boundary plains materials range in age from Early Hesperian to possibly Early Amazonian, with the youngest surfaces generally residing at the lowest elevations.

Structural Character. The circum-Utopia HLB contains both extensional and contractional tectonic features [10]. The most prominent extensional features are normal faults and graben circumferential to Isidis basin (Amenthes and Nili Fossae) that likely represent relaxation of Isidis impact structures. Less well-exposed fractures and graben are located sub-parallel to the HLB within Amenthes Fossae and west of Protonilus Mensae, along a highland massif identified by [2] and associated with the original Utopia impact basin. Though extensional features are currently confined to the higher-standing Noachis and Nepenthes units, subdued linear depressions with correlative trends to adjacent graben are evidence that these features are ancient and once extended through the entire boundary plains sequence. Mass-wasting processes associated with circum-Utopia HLB degradation have obscured these structures.

Contractional features include subdued ridges and broad arches [9], which occur both radial and circumferential to Utopia basin [10]. Radial features are generally prominent to subdued, linear ridges that are most prevalent in Utopia unit 2 while circumferential features are subdued, relatively short arches that are most prevalent in Utopia unit 1. The subdued nature of many contractional features is perhaps a result of poor surface exposure or a general subduing due to erosion or burial [7].

Hydrologic Character. Hypotheses that promote a global Martian groundwater table [e.g., 12] are likely inadequate due to the degree of structural development and topographic variability along the hemispheric dichotomy, as such features would impede the interconnectivity of a global aquifer system. Furthermore, recent Martian aquifer modeling by [13] indicates that

local to regional scale processes dominate groundwater migration, leading to relatively short flow paths. As such, we expect circum-Utopia HLB materials to have been affected by groundwater recharge, migration, and discharge via local or regional aquifers. The recharge of upgradient areas may have occurred through highland precipitation during occasional warm periods in the geologic past [14,15]. However, during colder periods when surface volatiles were unstable, external heating and cooling of subsurface volatiles may have driven the circum-Utopia hydrologic cycle. Without recharge, high elevation aquifers would desiccate, and may be susceptible to various mass-wasting processes.

Compared to other regions of Mars, the circum-Utopia HLB is notably lacking in channel-related features, though notable exceptions include the Elysium Fossae-sourced outflow channels [3] and sparse highland valley networks in northwestern Terra Cimmeria [15]. Hephaestus Fossae is the only channel-like feature observed within or immediately adjacent to the boundary plains, and is likely to have formed through groundwater discharge, downslope percolation, and cavernous collapse. While there is general lack of channel features, there is a relative abundance of mass-wasting morphologies and materials.

Mass-wasting of the circum-Utopia HLB: Mass-wasting applies to downslope movement of soil or rock under the direct influence of gravity. Such processes may be relatively "wet" (e.g., solifluction) or "dry" (e.g., debris slide). Mass-wasting processes may include ice-lubricated downslope creep, aquifer draining and collapse, mud volcanism-related flows, and slope-instability movements. Since the long-term effect of mass-wasting is planation to a regional base-level, resulting morphologies and materials are often self-destructive and difficult to identify. We note landform and material characteristics of the circum-Utopia HLB that implicate mass-wasting as a major contributor to the modification of the hemispheric dichotomy. Notable observations include (1) boundary plains subsidence related to graben locations, likely as a result of collapse and/or creep processes; (2) surface blisters in boundary materials adjacent to the Elysium rise, likely due to the upwelling of thermally mobilized ground ice; (3) channels and pits of Hephaestus Fossae that are related to groundwater discharge and rapid downslope percolation back into the regolith, possibly across aquifers; (4) lobate depressions of Utopia unit 1, which may have formed via subsidence following aquifer draining or desiccation; (5) small, pitted cones and thin flows occurring in Utopia unit 1, perhaps related to late-stage activity from overpressurized aquifers [7]; (6) the relative smoothness of the Utopia unit 2, perhaps as the result of long-lived downslope processes;

and (7) subdued, chaos-like depressions within Nepenthes and Protonilus Mensae. The latter observation is significant, since the chaos-like morphologies are conspicuously located near the base of highland scarps and are positioned at near-equivalent distances from the estimated center of the Utopia impact basin.

Implications: Based on our observations, we offer several hypotheses that outline how mass-wasting has pervasively modified the circum-Utopia HLB since the pre-Noachian formation of Utopia basin. First, circum-Utopia structure and stratigraphy provides a horizontal and vertical framework within which lateral mass-wasting processes may propagate. Ground volatile migration was likely obstructed, and thus concentrated, at such subsurface horizons, many of which may be directly related to the Utopia impact. Second, since regional structure and stratigraphy were likely established early in Mars' history [16], the degradation of the circum-Utopia HLB was a long-lived, pervasive and self-propagating process that operated at various intensities. Third, mass-wasting intensity was variously affected by interactions between climate and regional geothermal gradients. Thermal effects include both "top-down" effects (those associated with climate variations) and "bottom-up" effects (those associated with endogenic heating). Interplay between these two effects has driven long-term mass-wasting of the circum-Utopia HLB. Fourth, ground volatile migration was regional and resulted from long-term recharge and discharge of local to regional aquifers rather than pole-to-pole hydrostatic pumping [12,15].

Future Work: Our careful application and interpretation of crater counts to identify resurfacing events along the circum-Utopia HLB will improve understanding of HLB degradation. We continue to examine top-down (climatic) and bottom-up (geothermal) interactions as they relate to mass-wasting processes and landforms, and plan field studies in high-latitude permafrost and volcanic regions of Earth to examine additional relevant settings and processes.

References: [1] Sjogren (1979) *Science*, 203, 1006-1010. [2] McGill (1989) *JGR*, 94, 2753-2759. [3] Tanaka et al. (2003) *JGR*, 108, E4. [4] Parker et al. (1989) *Icarus*, 82, 111-145. [5] Parker et al. (1993) *JGR*, 98, 11061-11078. [6] Wilhelms and Baldwin (1989) *LPSC* 19. [7] Tanaka et al. (2003), *JGR*, 108, E12. [8] Banerdt (2004) *LPSC Abstract* #2043. [9] Watters *JGR*, 93, 10236-10254. [10] Thomson and Head (2001) *JGR*, 106, 23209-23230. [11] Schultz (2000) *JGR*, 105, 12035-12052. [12] Clifford and Parker (2001) *Icarus*, 154, 40-79. [13] Grimm and Harrison (2003) *LPSC Abstract* #2053. [14] Craddock and Maxwell (1993) *JGR*, 98, 3453-3468. [15] Carr (2002) *JGR*, 107, E12. [16] Schultz et al. (1982) *JGR*, 87, 9803-9820

SUBSURFACE STRUCTURE OF THE ISMENIUS AREA AND IMPLICATIONS FOR EVOLUTION OF THE MARTIAN DICHOTOMY AND MAGNETIC FIELD. S. E. Smrekar¹, C.A. Raymond¹, and G.E. McGill², ¹Jet Propulsion Lab, California Inst. of Technology, M.S. 183-501, 4800 Oak Grove Dr., Pasadena, CA 91109; ssmrekar@jpl.nasa.gov; ²Univ. of Massachusetts, Dept. of Geosciences, Amherst, MA 01003.

Introduction: The Martian dichotomy divides the smooth, northern lowlands from the rougher southern highlands. The northern lowlands are largely free of magnetic anomalies, while the majority of the significant magnetic anomalies are located in the southern highlands. An elevation change of 2-4 km is typical across the dichotomy, and is up to 6 km locally [1,2]. We examine a part of the dichotomy that is likely to preserve the early history of the dichotomy as it is relatively unaffected by major impacts and erosion. This study contains three parts: 1) the geologic history, which is summarized below and detailed in McGill et al. [5], this volume, 2) the study of the gravity and magnetic field to better constrain the subsurface structure and history of the magnetic field (this abstract), and 3) modeling of the relaxation of this area (Guest and Smrekar, [6], this volume). Our overall goal is to place constraints on formation models of the dichotomy by constraining lithospheric properties. Initial results for the analysis of the geology, gravity, and magnetic field studies are synthesized in Smrekar et al. [7].

Geologic History: Our study area (50°-90°E) is characterized by steep scarps, a fairly rapid change in crustal thickness [3,4], and large magnetic field anomalies in the adjacent lowlands. The area includes a series of 10 graben with slopes of 13° to 21° bounding the rim of the plateau with >3.5% horizontal strain. A topographic bench separates the highlands from the lowlands. The northeastern edge of the bench is defined by the abrupt disappearance of topographic knobs and parallels graben along the dichotomy boundary to the south. These observations support the interpretation that the boundary marks a buried fault, with the lowlands dropped down to the north. Additionally, crater counts indicate that the basement material in the lowlands is likely similar in age to the highlands material [8]. Finally, the 2.5 km of relief at the dichotomy could not have been a result of erosion. Given the similarity in age between the highlands and the bench, erosion would have had to have occurred in the Early Noachian. The scarp separating the highlands and the bench cuts Middle Noachian deposits, and could not have survived early bombardment. Nor could erosion have occurred subsequently as 2.5 km of erosion would have erased all but the largest craters.

Gravity and Magnetic Field Data: The free air and Bouguer gravity both have anomalies with a

similar frequency and amplitude variation as that of the magnetic field anomalies. In order to gain more insight into the geologic evolution and subsurface structure in this area, we examine the hypothesis that both the magnetic and gravity anomalies are due to the same source regions. Our modeling of the admittance signature of this area [7] indicates that the highlands regions are isostatically compensated, as is found elsewhere [9-11]. To determine what additional density anomalies remain once both topographic and isostatic effects are modeled, we remove the effect of a 50 km thick crust to produce the isostatic anomaly. Modeling the isostatic anomaly along a profile (50°E, 33°N to 75°E, 49.5°N) perpendicular to the buried fault and dichotomy boundary we find that each of the two main peaks in the isostatic and magnetic field anomalies are offset by approximately 200 km and have a lower peak to the south (Fig. 1). For an intrusion 100 kg/m³ denser than the surrounding crust, a layer roughly 30 km thick is needed to match the observed gravity anomalies. The more dense the intrusion, the thinner the required layer.

We next model the total magnetic field along the same profile, examining a range of possible paleopole positions consistent with prior estimates [12,13]. In each model the intensity is held constant. The position and thickness of each block is varied to fit the observed data. All of the models in Figure 2 provide a reasonably good fit to the data, except for the model with a 0° paleopole inclination (Fig. 2b). For an inclination of -30°, gaps in the magnetic field are aligned with the locations of the isostatic gravity anomalies (Fig. 2c). For a 30° magnetic inclination (Fig. 2d) the isostatic anomalies are aligned with magnetized crustal blocks.

One possible interpretation of the large positive isostatic anomalies is that they are due to subsurface magmatic intrusions. Both Martian meteorites [e.g. 14] and estimates of volcano densities from gravity studies [9,10,15-17] are consistent with the presence of high-density intrusions. Although no volcanism is visible at the surface, there is a plausible mechanism to produce intrusions in this location. King and Anderson [18] model the effects of a transition in lithospheric thickness on a convecting system and find that localized upwelling is produced at the transition. The extension across the boundary may also be related to the volcanism.

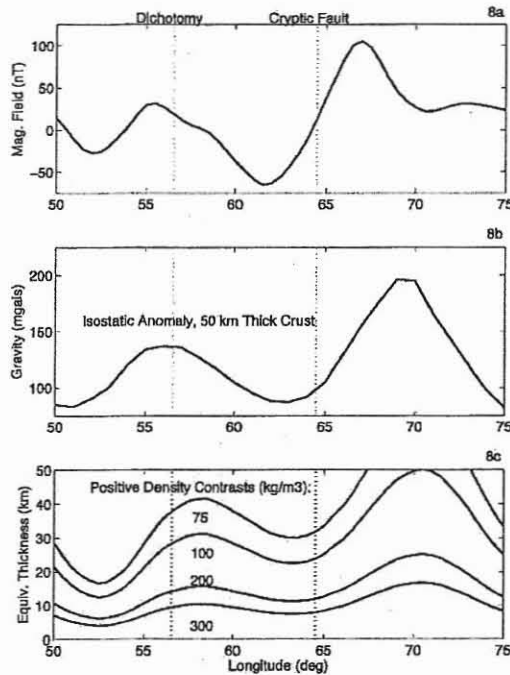


Figure 1. Profiles through the magnetic field (a), and the isostatic gravity anomaly (b), and thicknesses of layers with that would produce an equivalent gravity anomaly (c).

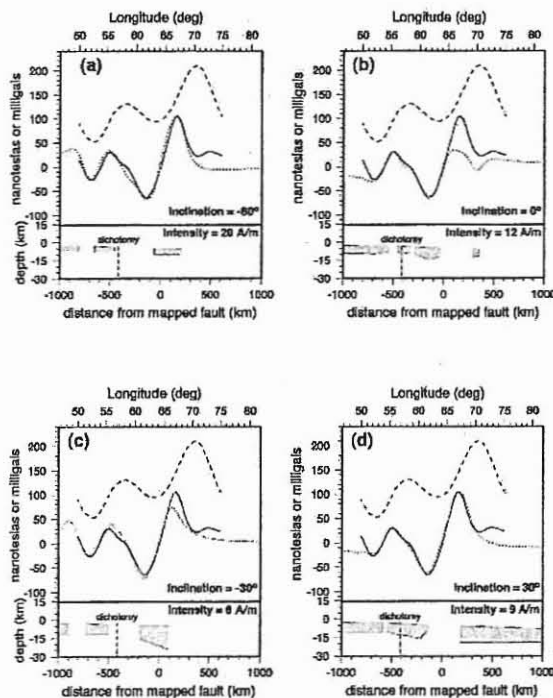


Figure 2. Model fits (dotted lines) to the observed magnetic field in nT (dashed lines) along with the isostatic gravity anomaly in mgals (dashed lines). The source blocks are shown at the bottom of each panel as a function of distance from the buried fault and depth. Intensity and field

inclination assumed for each model are indicated on the figure.

In the magnetic field model shown in Fig. 2c, the gaps in the magnetic field would be caused by magmatic intrusions that both demagnetized the crust and emplaced high-density bodies at depth. An intriguing aspect of this model is that the magnetized crust stops at approximately the location of the buried fault. In an alternate model (Fig. 2d), in which there is a common source for the gravity and magnetic anomalies, the intrusions would have been emplaced in the presence of a magnetic field. An interesting implication of this model is that the plains to the north of the magnetic anomalies are magnetized.

Preliminary Conclusions and Follow-on Work

The modeling results offer interesting possible interpretations but are non-unique. The next step is to develop a 3D model of the gravity and magnetic field for those anomalies associated with the dichotomy boundary and down dropped block. Objectives include better defining the extent of magnetized material at depth, placing narrower bounds on paleopole position, and determining if there is strong evidence for either correlation or anticorrelation of the gravity and magnetic anomaly source regions. Results will be used to test two alternative hypotheses: 1) magnetic anomalies in the lowlands along the boundary represent highlands crust that has been dropped down via extension across the boundary, and 2) the lowlands are in fact magnetized at a low level. We will continue our study of the dichotomy by examining the geology, gravity, and magnetic field data for additional areas of the dichotomy. Our initial examination of the boundary to the east, in the Amenthes area, indicates a pattern of gravity and magnetic field anomalies with similar magnitude and frequency content.

Ref: [1] Frey H.A. et al. (1998) *GRL*, 25, 4409-4412. [2] Smith D.E. et al. (1999) *Sci.*, 284, 1495-1503. [3] Zuber M.T. et al. (2000) *Sci.*, 287, 1788. [4] Neumann, G.A., et al. (2004) *JGR*, in press. [5] McGill G.E. et al. (2004) this conf. [6] Guest, A. & S.E. Smrekar, (2004) this conf. [7] Smrekar et al. (2004), sbmted. [8] Frey (2004) *LPCS XXXV*, Abst# 1382. [9] McGovern P.J. et al. (2002) *JGR* 107, doi: 10.1029/2002JE001854. [10] McKenzie D. et al. (2002) *EPSL* 196, 1. [11] Nimmo F. (2002) *JGR* 107, doi:10.1029/2000JE001488. [12] Cain J. C. et al. (2003) *JGR*, 108, doi: 10.1029/2000JE001487. 1151-1154. [13] Hood L.L. & Zakharian A. (2001) *JGR*, 106, 14601-14619. [14] Britt D.T. & G.J. Consolmagno (2003) *Meteor. Planet. Sci.* 38, 1161. [15] Arkani-Hamed (2000) *JGR* 105, 26,712. [16] Kiefer W.S. (2002) *Trans. Am. Geophys. Un.*, Fall Mtg, Abst# P71B-463. [17] Kiefer W.S. (2003) *LPS XXXIII*, Abstract #1234. [18] King S.D. (1998) *EPSL*, 160, 289.

ENDOGENIC MECHANISMS FOR THE FORMATION OF THE MARTIAN CRUSTAL DICHOTOMY: HYPOTHESES AND CONSTRAINTS. Sean C. Solomon, Department of Terrestrial Magnetism, Carnegie Institution of Washington, 5241 Broad Branch Road, N.W., Washington, DC 20015 (scs@dtm.ciw.edu).

Introduction. The southern uplands and northern lowlands of Mars differ markedly in average elevation [1] and crustal thickness [2,3]. This crustal dichotomy, recognized following the first global observations of the planet by Mariner 9, has variously been attributed to internal [e.g., 4,5] and external [e.g., 6,7] processes, but no single hypothesis for its formation has heretofore been fully persuasive. This paper offers a review of proposed endogenic formation mechanisms for the dichotomy, as well as the geophysical and geochemical constraints [8] that these hypotheses must satisfy.

Formation Hypotheses. Excavation and ballistic transport by one [6] or several [7] large impacts have been suggested as an explanation of the crustal dichotomy. Beyond the portion of the dichotomy boundary clearly influenced by the Hellas, Utopia, and Isidis basins, however, there is no confirming evidence from topography for these suggestions [1,2], and no simulations of impacts of such scale have been carried out to test whether the observed pattern of crustal thickness variations [2,3] can be produced.

Endogenic mechanisms proposed for the formation of the crustal dichotomy fall into three classes: those associated with the evolution of an early magma ocean, those associated with an early episode of lithospheric recycling, and those associated with long-wavelength patterns of solid-state mantle flow.

A magma ocean has been postulated as a mechanism to accommodate early differentiation of core, mantle, and crust on Mars and the early establishment of distinct isotopic reservoirs [e.g., 9,10]. The crustal thickness dichotomy may have arisen from the heterogeneous evolution of such a magma ocean during the crustal formation process. Alternatively, crystallization of a magma ocean may have led to gravitationally unstable mantle layering, because the late-stage silicates that crystallized at shallow mantle depths were denser than earlier cumulates that crystallized near the base of the magma layer. Overturn of an unstable mantle may have thickened the crust over downwelling regions and thinned the crust elsewhere [9].

An early episode of lithospheric recycling, or even some variant of plate tectonics, is theoretically possible for Mars [11]. Crust generated at spreading centers at later times might be expected to be thinner than earlier formed crust if the mantle cooled

appreciably during the intervening time, a possible explanation for the crustal dichotomy if the crust of the northern hemisphere is substantially younger than that of the south [11]. If plate recycling was occurring during the formation of the comparatively thicker crust of the southern hemisphere, then such recycling would tend to shut down after the surface area of such crust grew beyond a critical fraction of the planet's surface [12].

Some models of mantle convection, after solidification of any early magma ocean, predict a strongly long-wavelength (harmonic degree 1) component of flow for layered mantle viscosity structures [13]. Such flow models might have led to thicker crust over the hemisphere dominated by upwelling and melt generation, or alternatively thinner crust over that hemisphere if flow-induced crustal thinning was more important than the effect of magmatic additions to crustal volume [13].

Constraints on Formation. Hypotheses for the formation of the crustal dichotomy must, of course, account for the present structure of the crust [2,3], as well as the preservation of crustal thickness variations against the tendency of the lower crust to flow in response to stress differences arising from variations in topography at the surface and crust-mantle boundary [2,14]. Any documented differences in major element composition between the crust of the northern and southern hemispheres would be pertinent, but available remote sensing information is subject to multiple interpretations [15,16].

The constraint most able to discriminate among competing hypotheses is the time of formation of most of the crust. A variety of lines of evidence point to crustal formation very early in Martian history, as early as the first 50 My after solar system formation [8].

The most complete simulations of the final stages of terrestrial planet formation to date can account for planets with masses and semimajor axes similar to those of Earth and Venus, but any final body at the orbit of Mars tends to be too large [e.g., 17,18]. While this difficulty may point to an unusually low initial density of disk material in the vicinity of Mars's orbit [17], it may instead indicate that Mars is a surviving embryo that escaped either accretion or ejection [18]. The latter outcome would imply that Mars was nearly fully formed before the final stage of formation of the larger inner planets. Rapid

accretion of Mars would have converted into heat a sufficient quantity of kinetic energy to melt a substantial fraction of the Martian interior and drive global differentiation.

Although surface units in the northern lowlands of Mars are Hesperian to Amazonian in age, numerous partially buried impact craters and basins have been identified from their topographic signatures [19]. Comparison of the density of such features at crater diameters greater than 50 km establishes that the formation of much of the present Martian crust in both hemispheres was complete by the Early Noachian [19].

Isotopic anomalies in Martian meteorites provide strong evidence in support of the inference that global differentiation of core, mantle, and crust on Mars occurred very early in solar system history. The presence of ^{182}W , a product of the decay of ^{182}Hf (9-My half life), at levels in all Martian meteorites in excess of that for primitive chondritic meteorites [19-21] is indicative of core formation within 10-15 My of the formation time of the oldest solar system objects [20].

Martian meteorites also contain abundances of ^{142}Nd , the decay product of ^{146}Sm (103-My half life), comparable to or in excess of terrestrial values [22]. Nakhilites show elevated levels of both ^{142}Nd and ^{182}W , while for shergottites the abundance of ^{142}Nd varies while the ^{182}W abundance is approximately constant [23]. These relationships suggest that the source regions for nakhilites were isolated early (while ^{182}Hf was still extant), whereas the source regions for the shergottites were apparently established while ^{146}Sm was extant but after all ^{182}Hf had decayed, i.e., at least 50 My after solar system formation [22].

Several additional lines of evidence support the inference that both the mantle source regions of Martian meteorite magmas and much of the Martian crust were established by 4.5 Ga, i.e., about 50 My after solar system formation. Relationships among isotopes of Pb [24], Sr [25], Os [26], and Nd [27] in Martian meteorites have been interpreted as consistent with large-scale silicate fractionation at about 4.5 Ga and little to no remixing of crust and mantle thereafter. The 4.5-Ga age of ALH84001 [28] also indicates that a stable crust had formed by that time. Such a rapid formation time for the crust and meteorite source regions supports the hypothesis that these regions formed by the differentiation of a global silicate magma ocean that dated from the earliest phase of Martian history [9,10].

A 4.5-Ga age for much of the volume of crustal material on Mars is thus supported by a variety of

indicators, including isotopic systematics of Martian meteorites, expectations from planetary accretion models, and the density of impact craters at the surface and discernible beneath younger infilling deposits. The crustal dichotomy, because of its global scale, must be comparable in age.

Assessment of Hypotheses. Plate recycling is probably too slow a process to have formed most of the crust by 4.5 Ga. Hypotheses for the formation of the dichotomy invoking mantle convection patterns subsequent to global differentiation encounter similar difficulties with timescale. An age for most of the crust, including the dichotomy structure, of about 4.5 Ga is most consistent with formation by silicate differentiation of a global magma ocean.

A still open question is the mechanism for producing different average crustal thicknesses on opposite hemispheres by magma ocean differentiation processes. Such an outcome for an early silicate magma ocean is seen on the Moon as well [29, 30], however, and the longest-wavelength crustal thickness variations are those most likely to have survived any early episode of lower crustal flow [2,14].

References. [1] Smith D. E. *et al.* (1999) *Science*, 284, 1494. [2] Zuber M. T. *et al.* (2000) *Science*, 287, 1788. [3] Neumann G. A. *et al.* (in press) *JGR*. [4] Mutch T. A. (1976) *The Geology of Mars*, Princeton. [5] Wise D. U. *et al.* (1979) *JGR*, 84, 7934. [6] Wilhelms D. E. and Squyres S. W. (1984) *Nature*, 309, 138. [7] Frey H. and Schultz R. A. (1988) *GRL*, 15, 229. [8] Solomon S. C. *et al.* (submitted) *Science*. [9] Hess P. C. and Parmentier E. M. (2001) *LPS*, 32, 1319. [10] Elkins-Tanton L. *et al.* (2003), *MAPS*, 38, 1753. [11] Sleep N. H. (1994) *JGR*, 99, 5639. [12] Lenardic A. *et al.* (2004) *JGR*, 109, E02003. [13] Zhong S. and Zuber M. T. (2001) *EPSL*, 189, 75. [14] Nimmo F. and Stevenson D. J. (2001) *JGR*, 106, 5085. [15] Bandfield J. L. *et al.* (2000) *Science*, 287, 1788. [16] Wyatt M. B. and McSween H. Y. Jr. (2002) *Nature*, 417, 263. [17] Chambers J. (2001) *Icarus*, 152, 205. [18] Lunine J. I. *et al.* (2003) *Icarus*, 165, 1. [19] Yin Q. *et al.* (2002) *Nature*, 418, 949. [20] Kleine T. *et al.* (2002) *Nature*, 418, 952. [21] Schoenberg R. *et al.* (2002) *GCA*, 66, 3151. [22] Harper C. L. *et al.* (1995) *Science*, 267, 213. [23] Foley C. N. *et al.* (2004) *LPS*, 35, 1879. [24] Chen J. H. and Wasserburg G. J. (1986) *GCA*, 50, 955. [25] Borg L. E. *et al.* (1997) *GCA*, 61, 4915. [26] Brandon A. D. *et al.* (2000) *GCA*, 64, 4083. [27] Borg L. E. *et al.* (2003) *GCA*, 67, 3519. [28] Nyquist L. *et al.* (2001) *Space Sci. Rev.*, 96, 165. [29] Warren, P. H. (1985) *Ann. Rev. Earth Planet. Sci.*, 13, 201. [30] Neumann G. A. *et al.* (1996) *JGR*, 101, 16841.

TRIGGERING THE END OF PLATE TECTONICS BY FORCED CLIMATE CHANGES.

M. G. Spagnuolo¹, J. Dohm². ¹Departamento de Geología. Facultad de Ciencias Exactas y Naturales. UBA. maurospag@yahoo.com, ²Department of Hydrology and Water Resources, University of Arizona, Tucson, AZ, 85721 (jmd@hwr.arizona.edu)

Introduction: Several investigators have suggested that plate tectonics was an active process [1,2], recently proposed for extremely ancient Mars [3-6]. Based on the assumption that accretion and subduction were active processes in the extremely ancient past, and plate tectonism ended in the formation of the southern cratered highlands [7], we propose that the cratered highlands represents a supercontinent that formed through plate tectonism and that it had a significant influence on the subsequent evolution of the planet, which includes catastrophic global climate change. This work brings together some exogenic- and endogenic-derived evidences to propose a new global dynamic model.

Driving to a Martian Pangea: Assuming a phase of very ancient plate tectonism, as recorded in the ancient terrains where mountain ranges and other extremely large structures (including fault-controlled basins) [3-5] are recognized, and considering that the presence of magnetic anomalies [8] has been explained either by extensional (probably sea floor spreading) [9] or convergent systems associated with the accretion of oceanic plateaus [3-5], we propose that during lithospheric recycling, which includes the formation of hemispheric dichotomy, a supercontinent was configured. This megacontinent, also known as the southern cratered highlands, should have resulted from accretion of lithospheric plates which is in agreement with a smooth difference in crustal thickness across the dichotomy boundary [10]. The collision of plates also would build up a higher topographic relief in analogous fashion as orogenic belts in Earth.

A Megacontinent and Its Influence in Global Climate: After the formation of the Hemispheric dichotomy and emplacement of a Megacontinent, exogenic conditions should have changed dramatically. We propose that the particular geography of this huge supercontinent resulted in catastrophic global climate change. The global climate change would include the development of ice sheets and glaciers due to a higher relief, an associated increase in the planet's albedo, and subsequent global cooling, as has occurred repeatedly in the Earth when supercontinent configurations took place; such supercontinent-related activity has been suggested for a glacial period following the collision of India with Asia (resulting in

the Himalayan rise). Taking into account the smaller size of the planet when compared to the Earth, this self-sustained process of cooling would be of high proportion.

Cool weather, no water. No water, the end of plate tectonics: We think that together with fast subduction of hydrated slab peridotite, which removed oceanic water to the interior [3], the increase in the cryosphere caused an initial hydrospheric loss (IHL), where liquid water was removed from the global system. Some authors have suggested that subduction cannot take place in an anhydrous environment due to the absence of silicates, which allows one plate to slide under another one [11]. Eventual planetary cooling (endogenic and exogenic) would result in the termination of plate tectonics around 3.9 [3,4], leaving a supercontinent frozen in time. As plate tectonics transitioned into a stagnant lid (superplume [3,12]) phase of planetary evolution, Mars became less efficient at releasing its internal heat energy, and thus the planet would necessarily heat up [13]. In Earth, supercontinents are unstable and ultimately break into separate plates to allow independent motion [14] following the Wilson cycle. But in Mars, this internal heating and volatile elements, which were added to the interior during subduction [3], would lead to immense episodic outpourings of lava and volatiles such as at Tharsis [15], equivalent of 1.5 bar CO₂ atmosphere and a 120 m thick global layer of water [16]. These MEGAOUTFLO-induced outbursts [3,17] would result in transient climatic, atmospheric, and hydrospheric changes [3,18]

Conclusions: The hemispheric dichotomy could be a consequence of a supercontinent formation due to plate tectonics. This established "megacontinent" was responsible for a catastrophic global climate cooling of Mars. This global cooling, together with internal processes, would cause an IHL where liquid water would be removed from the surface. This could favor the end of plate tectonics that preceded an internal heating phase.

References: [1] Sleep N.H. (1994) *JGR*, 99, 5639-5655 [2] Nimmo, F., and Stevenson, D.J. (2000) *JGR*, 105, 11969-11979. [3] Baker, V.R., Maruyama,

- S., Dohm, J.M. (2002) *Electronic Geosciences* 7, (<http://link.springer.de/service/journals/10069/free/conferen/superplu/>). [4] Dohm, J.M. Maruyama, S., Baker, V.R., Anderson, R.C., Ferris, J.C., and Hare, T.M. (2002a) *LPSC XXXIII* abstract 1639. [5] Fairén, A.G., Ruiz, J., and Anguita, F. (2002) *Icarus* 160, 220-223. [6] Fairén, A.G., and Dohm, J.M. (2004) *Icarus* 168, 277-284. [7] Lenardic A., Nimmo, F., and Moresi, L. (2004) *JGR*, 109, E02003, doi:10.1029/2003JE002172. [8] Acuña, M.H. and 13 colleagues (2001) *JGR* 106, 23,403-23,417. [9] Connerney, J.E.P., Acuña, M.H., Wasilewski, P.J., Ness, N.F., Rème, H., Mazalle, C., Vignes, D., Lin, R.P., Mitchell, D.L., and Cloutier, P.A. (1999) *Science* 284, 794-798. [10] Zuber, M.T. (2001) *Nature* 412, 220-227. [11] Ragenauer-Lieb, K., Yuen, D., and Branlund, J. (2001) *Science* 294, 578-580. [12] Dohm, J.M., Maruyama, S., Baker, V.R., Anderson, R.C., and Ferris, J.C. (2002). *Superplume International Workshop, Abstracts with Programs*, 406-410. [13] Stevenson, D. J., (2001) *Nature* 412, 214-219. [14] Wilson, J.T., and Burke, (1973) *Eos Trans AGU*, 54, 238 (abstract) [15] Dohm, J.M., Ferris, J.C., Baker, V.R., Anderson, R.C., Hare, T.M., Strom, R.G., Barlow, N.G., Tanaka, K.L., Klemaszewski, J.E., and Scott, D.H. (2001) *JGR* 106, 32,943-32,958. [16] Phillips, R. J., Zuber, M.T., Solomon, S.C., Golombek, M.P., Jakosky, B.M., Bandert, W.B., Smith, D.E., Williams, R.M.E., Hynek, B.M., Aharonson, O., Hauck, S.A. (2001) *Science* 291, 2587-2591. [17] Baker, V.R., Strom, R.G., Gulick, V.C., Kargel, J.S., Komatsu, G., Kale, V.S. (1991) *Nature* 352, 589-594. [18] Jakosky, B.M. and Phillips, R.J. (2001) *Nature* 412, 237-243.

MARS IMPACT ENERGY ANALYSIS IN SUPPORT OF THE ORIGIN OF THE CRUSTAL DICHOTOMY AND OTHER ANOMALIES. G. R. Spexarth, Representing Self, 14510 Cobre Valley Dr, Houston, TX 77062. spexarth@houston.rr.com

Introduction: By analyzing Mars from an engineering perspective, a violent and cataclysmic past is unveiled. This paper looks at multiple anomalies of Mars, shows how they may be inter-related, and describes a very possible scenario, supported by analysis, that could have led to a violent and sudden destruction.

Impact Energy: The energy of impact for the 2300 km Hellas Basin, located in the southern hemisphere of Mars, is calculated to be 5.33×10^{26} Joules. This is over 1200 times more energy than the K/T Impact that extinguished 75% of life on earth [1], and Mars is only 1/8 the volume of Earth. This is an enormous amount of energy for Mars to absorb.

This paper shows that the energy input to the Mars system by the Hellas impact is sufficient enough to strain the lithosphere until rupture, thus forming the Tharsis Montes and initiating the Valles Marineris, both of which are located 180 degrees away from the Hellas Basin (Fig-1).

By analyzing the lithosphere of Mars as a thin-wall pressure vessel, it is shown that the amount of energy required to rupture the lithosphere ranges from 36% to 84% of the total Hellas impact energy. This assumes that the lithosphere thickness is between 110-260km [2]. Based on this analysis, there was sufficient energy in the Hellas impact to rupture the planet's lithosphere. Prior to rupture, the lithosphere would deform due to excessive yielding, thus forming the Tharsis Montes.

Tharsis Montes: It is proposed that this rupture initiated radial fractures that are identified as originating at the center of the Tharsis Montes (Bulge) [3]. The Tharsis volcanoes and Valles Marineris are aligned 60-degrees radially from each other (Fig-2). It is shown that 60-degree radial fractures (six-sided petals) are a typical feature formed when thin-walled pressure vessels rupture due to a build-up of excessive internal pressure (Fig-3) [4], [5]. These radial fractures could have been the source of extensive volcanism observed in the Tharsis region, as well as the initiation of the Valles Marineris as a rupture in the lithosphere.

Northern Lowlands: In addition, the Northern Lowlands are 5 km below datum ("sea level") and the Tharsis Bulge is 10 km above datum [6]. It is proposed that the Northern Lowlands are a direct result of the lithosphere deforming to create the Tharsis Bulge. The increase of arc-length required to form

the Tharsis Bulge is shown to correspond directly to the reduction of elevation and arc-length of the Northern Lowlands.

Rate of Rotation: The rotational rate of Mars is slower than predicted when compared to the angular momentum of the rest of the terrestrial planets [7], [8]. It is shown that only 8% to 18% (depending on the thickness of lithosphere assumed) of the total impact energy from the Hellas Basin would be required to reduce the rotational spin of Mars by 20%.

Magnetic Field: It is also suggested that this sudden reduction of Mars' rotation, as well as pressure waves originating from the Hellas impact and passing through the possible liquid iron core, would disrupt the rotation of the liquid core, and in turn, significantly affect the dynamo process. Unless specific conditions are met, the planetary dynamo is non-regenerative [9]. Therefore, the planetary magnetic field would remain at a depleted level, and Mars would be in the present state that we find it in today.

Atmosphere: Without a magnetosphere to protect the planet from the Sun's solar wind, the atmosphere of Mars would be etched away and blown into space and leave it with the minimal amount of atmosphere that it has today [10].

Conclusion: This paper proposes, and provides evidence for, an alternate geological past for Mars. Detailed structural analysis supporting this theory is provided herein. However, ultimately, Mars must be explored in order to unlock its secrets and fully understand the implications of its history.

References: [1] Sharpton, V. L. and Grieve, R. A. F. (1990), *Global Catastrophes in Earth History*, pp. 301-318. [2] Willemann, R. J. and Turcotte, D. L. (1982), *JGR*, Vol-87, No. B12, pgs (9793-9801). [3] Carr, M. H., (1974), *Tectonism and Volcanism in the Tharsis Region of Mars*, *Jour. Geophys. Res.*, V. 79, pg 3943-3949. [4] Whitney, J. P. (1993), *NASA-JSC 32294*. [5] Friesen, L. J. (1985), *NASA-JSC 27081*. [6] Cattermole, Peter (1992), *Mars, The Story of the Red Planet*. [7] Mars Orbiter Laser Altimeter (MOLA), NASA/GSFC, <http://ltpwww.gsfc.nasa.gov/tharsis/mola.html>. [8] Chabai, A. J. (1977), *Influence of Gravitational Fields and Atmospheric Pressures on Scaling of Explosion Craters*, *Impact and Explosion Cratering*, pgs. (1191-1214). [9] Russell, C. T. (1986) *Solar and Planetary Magnetic Fields*. [10] Luhmann, Janet G., (1996), *Solar Wind Effects on the Atmospheres of*

the Weakly Magnetized Bodies: Mars, Titan, and the Moon, NASA Contractor Report 202224.

[11] Hancock, G. (1998), The Mars Mystery.

Figures:

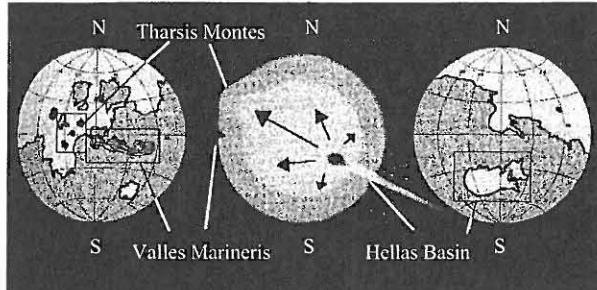


Figure-1. Formation of the Tharsis Montes and Valles Marineris due to the Hellas Impact. [11].

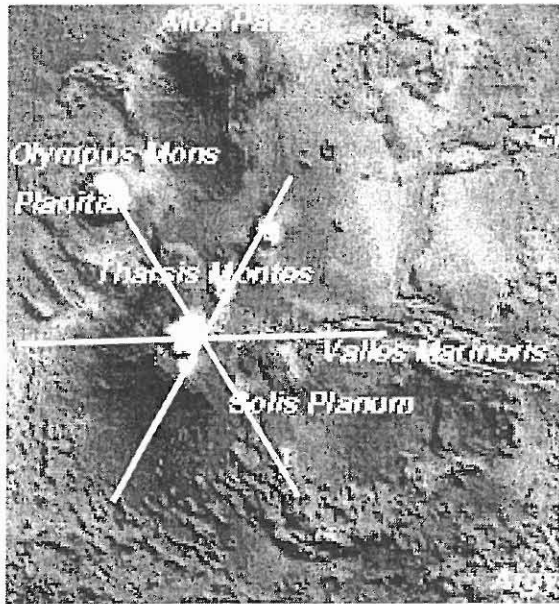


Figure-2: Six-sided star patten observed in the Tharsis region. This pattern is typical during rupture of thin-walled pressure vessels. [7] (radial lines added by author) (formation best observed on color map)



Figure-3: Six-sided star pattern observed in the rupture of thin-walled pressure vessels in a laboratory experiment [4], [5].

TOPOGRAPHIC AND GEOMORPHIC MODIFICATION HISTORY OF THE HIGHLAND/LOWLAND DICHOTOMY BOUNDARY OF MARS: I NOACHIAN PERIOD. K.L. Tanaka, Astrogeology Team, U.S. Geological Survey, Flagstaff, AZ 86001; ktanaka@usgs.gov.

Introduction. Formation of the Martian hemispheric highland/lowland boundary (HLB) may be the earliest recorded landscape-producing event on the planet [e.g., 1]. The boundary traverses a somewhat sinuous path that encircles about one-third of the planet's surface, separating the -2000 to -6000 m lowlands from highlands that average several thousand meters higher in elevation. The HLB has a regional slope that averages $\sim 1^\circ$ across a few hundred kilometers [2]; however, it varies in detail from a relatively abrupt scarp (e.g., Isidis, Elysium, and Amazonis Planitiae), to an abrupt top scarp having lower, beveled ledges or benches (e.g., Utopia basin), to a gentle slope (parts of northwest Arabia and northeast Tempe Terrae, and southeastern Elysium Planitia).

Both impact and tectonic origins for the dichotomy remain in vogue to account for the low topography, thin crust, and low remanent magnetization of the northern lowlands [e.g., 3]. Either type of origin likely produced extensive fault and fracture systems and rock units, which have long-since been obscured by subsequent geologic activity. However, ancient, impact-related structure and rock units, perhaps highly altered, may be preserved at depth. Here I discuss the earliest geomorphic modification of the highland/lowland topographic boundary as recorded in the extant Noachian surface geology; a companion abstract describes younger, Hesperian and Amazonian modification.

Early Noachian impacts. Among the most profound modifications of the HLB are huge impacts. Utopia basin forms a circular depression about 3300 km in diameter containing a positive free-air gravity anomaly and thin crust consistent with an impact origin [4-6]. However, finer-scaled structures and deposits pertaining to its origin are not clearly recognized. The southern and western margins of Utopia basin account for about one-fourth of the HLB. Curiously, it transitions smoothly into adjacent sections of the HLB north of Arabia Terra and south of Elysium Planitia, so it is unclear whether the formation of Utopia basin had a relatively moderate or substantial effect on the original outline of the HLB.

Another huge impact may account for the broad (nearly 2,000 km across) lowland embayment of Chryse Planitia, which has some poorly preserved indications of a circular basin structure, including massifs along the western basin flank [7]. Isidis basin forms the best-preserved but smallest of the major Early Noachian impacts that have modified the HLB. It forms a basin ~ 1200 km in diameter that partly overlaps the southwest margin of Utopia basin. A broad, low (a few hundred meters high) shoulder separates the basins. Isidis basin preserves a strong positive gravity anomaly [5] and is partly ringed by arcuate troughs (Nili and Amenthes Fossae) and high-standing massifs (Libya Montes).

Noachian resurfacing. Mars Orbiter Camera images at high resolution (a few meters/pixel) reveal that the heavily cratered terrain that comprises the oldest, most widespread rocks of the HLB appear to be pervasively layered, where fresher exposures occur [e.g., 8]. The layered highland rocks likely result from a complex history and interplay of geologic processes. Layer origins likely include: (a) thousands of local to regional crater ejecta blankets, (b) blankets of ash and perhaps volcanic flows, particularly in and near the Tharsis rise, which overlies the HLB and began forming in the Noachian [9-10], (c) alluvium and paleolake sediments within inter- and intra-crater plains formed by fluvial dissection of high topography [e.g., 11-12], and (d) eolian dust mantles from atmospheric fallout from dust storms [9, 13]. These deposits may have become mildly to highly consolidated and indurated through compaction and/or chemical cementation. They also may have been saturated or supersaturated with both groundwater and ground ice during or after deposition. Depending on the climatic conditions during the Noachian and local/regional thermal regimes, these widespread aquifers may have resulted in a variety of Earth-like polar/sub-polar hydrogeologic settings, such as fluvial, glacial, and periglacial environments. Derived erosional materials could have contributed to sedimentation, particularly along and below the HLB and among massifs such as at Libya Montes and the montes west of Chryse Planitia and Mareotis Fossae. Noachian oceans have also been proposed within the northern lowlands [14], but the geomorphic evidence is not compelling [15-17].

Along with deposition, erosion of the landscape may have been extensive during the Noachian, as evidenced by impact craters in various stages of degradation. Impact gardening no doubt pulverized surface rocks ubiquitously to depths of meters or more depending on the size of impactors, target material properties, and local to regional net rates of resurfacing [18-19]. The comminuted material produced by impacts may have been susceptible to other erosive processes or become trapped in depressions. Potentially, repeated pulverization and grinding of originally intact materials such as igneous rocks, impact melt, and cemented deposits, could have led to an extensive megaregolith a couple kilometers thick over much of the surface [18]. Fluvial erosion of Noachian rocks may have been prominent in many areas and perhaps ubiquitously [20-21]. In some cases, paleolake discharges led to catastrophic floods and deep dissection, such as Ma'adim Vallis [12]. Locally, erosion by mass wasting processes, particularly where ground ice and water were present, may have been extensive.

Noachian tectonism. Tectonic modification of the HLB likely resulted from stresses generated by global cooling and contraction and early growth of Tharsis,

which included lithospheric loading [22], upwelling and dynamic support [e.g., 23], and modification of the gravity field [24]. Surface modification would include formation of wrinkle ridges, grabens, normal faults, and alteration of slope-directed erosive processes including fluvial dissection [22, 24, 25]. However, the Early to Middle Noachian tectonic record mostly either is not well preserved or is difficult to isolate from more distinctive, younger structures, many of which may represent rejuvenated, older structures.

Summary. Noachian modification of the HLB appears to have been extensive. Gross reshaping took place due to the Utopia impact and a likely Chryse impact. These features may have greatly enlarged the extent of the northern plains by producing embayments reaching across hundreds to a few thousand kilometers in width and breadth. Isidis basin in turn modified the margin of Utopia basin thereby extending a further embayment of lowlands. A variety of resurfacing processes, include impacts, volcanism, fluvial and other erosive processes likely resulted in burial of the primordial crust by a megaregolith that may be kilometers thick. Tectonism likely has affected the HLB to some degree, but much of its record during the Noachian may have been erased or obscured by later activity.

References. [1] Frey H.V. (2004) LPSC XXXV, #1382. [2] Frey H.V. et al. (1998) GRL 25, 4409. [3] Nimmo F. and Tanaka K.L. (2005) Ann. Rev. Earth Planet. Sci., submitted. [4] McGill G.E. (1989) JGR 94, 2753. [5] Smith D.E. et al. (1999) Science 286, 94. [6] Zuber M.T. et al. (2000) Science 287, 1788. [7] Schultz P.H. et al. (1982) JGR 87, 9803. [8] Malin M.C. and Edgett K.S. (2001) JGR 106, 23,429. [9] Tanaka K.L. (2000) Icarus 144, 254. [10] Hynek B.M. et al. (2003) JGR 108, 5111. [11] Malin M.C. and Edgett K.S. (2000) Science 290, 1927. [12] Irwin R.P. and Howard A.D. (2002) JGR 107, doi:10.1029/2001JE001818. [13] Haberle R.M. et al. (2003) Icarus 161, 66. [14] Clifford S.M. and Parker T.J. (2001) Icarus 154, 40. [15] McGill G.E. (2001) GRL 28, 411. [16] Tanaka K.L. et al. (2003) JGR 108, 8043. [17] Carr M.H. and Head J.W. III (2003) JGR 108, 5042. [18] MacKinnon D.J. and Tanaka K.L. (1989) JGR 94, 17,359. [19] Hartmann W.K. (2001) Icarus 149, 37. [20] Grant J.A. and Schultz P.H. (1990) Icarus 84, 166. [21] Craddock R.A. and Maxwell (1993) JGR 98, 3453. [22] Tanaka K.L. et al. (1991) JGR 95, 15,617. [23] Kiefer W.S. (2003) Meteorit. Planet. Sci. 38, 1815. [24] Phillips R.J. et al. (2001) Science 291, 2587. [25] Anderson R.C. et al. (2001) JGR 106, 20,563.

TOPOGRAPHIC AND GEOMORPHIC MODIFICATION HISTORY OF THE HIGHLAND/LOWLAND DICHOTOMY BOUNDARY OF MARS: IL HESPERIAN AND AMAZONIAN PERIODS. K.L. Tanaka, Astrogeology Team, U.S. Geological Survey, Flagstaff, AZ 86001; ktanaka@usgs.gov.

Introduction. Modification of the highland/lowland boundary (HLB) on Mars is a long, complex story involving a large portion of the planet as well as the entire span of recorded geologic history of the planet. The Noachian history is described in a companion abstract and involves much of the first-order form and relief of the HLB and characterization of the materials forming the ancient crust. This abstract addresses how the HLB was subsequently modified during the Hesperian and Amazonian Periods. Recent geologic mapping and topical studies based largely on Mars Orbiter Laser Altimeter elevation data [1] have contributed to new perspectives on this history [e.g., 2].

End of Noachian to Amazonian HLB erosion and mass wasting. Modification of the HLB beginning near the end of the Noachian is better preserved in the geomorphologic record than earlier activity. The character of modification varies by region as delineated in the following subsections.

Utopia basin. Among the most pronounced HLB modification is the apparent two-level, two-stage degradation observed between Lyot crater and south-southwest of Elysium Mons, except where disrupted by Isidis basin [2, 3]. The upper level ranges mostly from -1800 (or higher) to -2900 m and the lower level from -3100 to -3500 m. South of Lyot crater along the southern margins of Deuteronilus Mensae, the upper, older contact apparently deepens to -3600 m. Upper-level collapse occurred from about the end of the Noachian into the Early Hesperian (N(5)-165), whereas the lower level is Late Hesperian (N(5)-90). Generally, the elevations of these contact levels decrease radially from the center of Utopia basin and may reflect an overall, gradually deepening zone in which undermining and collapse of the Noachian strata took place. Also, local evidence for possible sedimentary volcanism and groundwater discharge of possibly Late Hesperian and Amazonian age indicates local resurfacing within lowland rocks [2-4].

These observations are consistent with stratigraphic control of mass wasting for a giant impact into flat-lying beds. Strata surrounding the crater are gently uplifted and buried near the crater rim by overturned beds and by radially thinning ejecta, resulting in strata that dip away from the impact structure, accounting for horizons in which mass wasting and collapse occur [5]. In addition, the buried substrate may include dense impact fracture networks that could also lead to development of caverns and collapse features [6].

Chryse basin. Several sinuous valley systems dissect the highland margins (Xanthe Terra) of Chryse Planitia, which may account for Late Noachian (N(5)-230) deposits as well as middle Hesperian deposits (N(5)-120) on the basin floor [2]. Outflow channel dissection and

deposition and chaos formation generally appears to be Late Hesperian (N(5)-90). This activity could have erased evidence of earlier outflow discharges. Low knobs are plentiful in eastern Chryse Planitia, suggestive of shallow mass wasting during the Hesperian. Similar to Utopia basin, the putative Chryse impact structure may have resulted in strata susceptible to collapse that dip away from Chryse Planitia. This is indicated by the floor levels of chaos, which decrease in elevation from -4100 m at the northern margin of the chaos in Simud Vallis to -5000 m in Hydraotes Chaos, across a radial distance of ~800 km from the margin of the proposed impact basin.

Northwest Arabia Terra. Between Chryse basin and Deuteronilus Mensae, Arabia Terra dips gradually into the northern lowlands and includes one to two relatively low boundary scarps generally a few hundred meters high. The Vastitas Borealis Formation (VBF) obscures the HLB below -4000 m. Within Arabia Terra and the VBF, especially in the Cydonia region, sets of irregular collapse depressions disrupt surface materials [2]. The lowland depressions include dense fields of knobs and local, high-standing mesas. The floors of these plains depressions along the HLB decrease in elevation northeastward away from Chryse basin from -3500 m southwest of Mawrth Vallis to -4600 m at Cydonia Colles/Labyrinthus. Nearby depressions in Arabia Terra reach depths of -4900 m. Depressions surrounding Acidalia Mensa, which appears to be a low-lying plateau of Noachian material, bottom out at -4700 to -5000 m. The base elevations of these features also could be related to collapse controlled in part by the Chryse impact-basin structure and strata gently dipping northeastward, and/or to the regional surface slope.

Tempe Terra. The northern margin of Tempe Terra forms the northernmost part of the HLB. The eastern margin of this plateau generally slopes gently into Acidalia Planitia and appears to be terraced and extensively graded by fluvial channel systems, probably Late Noachian in age. Collapse structures are not evident, except near Kasei Valles. In contrast, northwestern Tempe has an abrupt margin 1 to 2 km high ringed by a band of large, dispersed knobs that are embayed by flows from Alba Patera. Mareotis Fossae defines the western margin of Tempe and forms rugged plateaus marked by broad troughs, reflecting both extensional tectonics and mass-wasting processes. This margin is proximal to Alba Patera and other volcanic centers, and thus geothermal activity was likely pronounced periodically at Mareotis Fossae.

Elysium and Amazonis Planitiae. Much of this part of the HLB is buried and embayed by Amazonian materials, including the Medusae Fossae Formation and lava flows associated with the Elysium and Tharsis rises. The HLB tends to form an abrupt scarp hundreds of meters to

more than a kilometer high, below which Late Noachian to Early Hesperian ridged plains material embays the HLB. The plains material could have diverse origins including volcanic flows, fluvial sediments, or mass-wasting deposits. Farther north, inliers of chiefly Noachian materials and perhaps some ridged plains material crop out extensively as dense patches of knobs and moderately degraded cratered terrain. The scarp is locally dissected by channel systems, including Mangala and Ma'adim Valles. However, a gentle slope and scattered knobs characterizes much of the HLB west of Ma'adim Vallis, with a dense knob field southwest of Apollinaris Patera. Locally, the flows overlying the HLB are marked by grabens generally radial to and wrinkle ridges concentric to Tharsis. Sporadic discharges across and below the HLB formed Mangala Valles and other valley systems west and southeast of the Elysium rise during the Late Hesperian through the Late Amazonian [7].

Isidis basin. Three distinct zones of the HLB border Isidis, including the rugged, dissected Libya Montes along the south margin, the gently sloping Syrtis Major Planum consisting of lava flows along the west margin, and the sloping knobby cratered terrain along the north margin. Local collapse structures form along the HLB, including shallow depressions that mark the west and lowest margin of Isidis Planitia. The Early Amazonian VBF deposit that covers the basin floor slopes gently southwestward and has been attributed to tectonic tilting in response to loading in the northern plains [8].

Amazonian subpolar modification. Following emplacement of the VBF, a large section of lowlands north of Alba Patera appears to have been degraded as suggested by knobs north of Milankovic crater that grade into a scarp to the east that gradually disappears at ~290°E. The base of the knobs and scarp decrease in elevation from west (~3900 m) to east (~4400 m). North of the center of this boundary are mounds and depressions of Scandia Cavi (down to ~5300 m). The mounds and depressions have been attributed to sedimentary volcanism [2], although a glacial origin also has been suggested [9]. These features occur north of Alba Patera and may represent an Early Amazonian phase of HLB-style resurfacing out in the northern plains caused by geothermal and/or climatic heating.

Discussion. Hesperian and Amazonian modification of the HLB was dominated by collapse and mass-wasting processes that likely involved ground water and ice. The resulting features have base elevations that correspond with distinct stratigraphic controls and possible geothermal activity.

The most profound stratigraphic control appears to be potential horizons extending hundreds of kilometers from the margins of the Utopia and putative Chryse impact basins as defined by base elevations of collapse features. The depressions decrease in elevation by hundreds of meters to more than a kilometer across radial distances of several hundred kilometers away from the basin margins, which is consistent with circum-basin

stratigraphy formed by impacts into flat-lying strata. The Utopia HLB includes two levels of degradation. The upper one is oldest and coincides with Early Hesperian degradation that forms remnant knobby lowland inliers of Noachian materials common over most of the exposed HLB. The widespread occurrence of this degradation, following the apparent shutdown of widespread valley network dissection, may be related to climate induced processes, such as the formation of a thick cryosphere and perhaps initial development of high pore-water pressures in confined, sub-permafrost aquifers. The younger, lower level is Late Hesperian and coincides with the crater age of the Chryse outflow channels and chaos. The discharge of large volumes of water may have induced climate change [e.g., 10] or resulted in infusion of relatively warm water into lowland rocks.

Origin of the VBF is commonly attributed to a northern plains ocean [e.g., 11]. However, a puzzle is that the VBF embays the outflow channels and has a significantly lower crater density than the outflow materials. It appears that when the VBF formed, it intensely degraded pre-existing craters, including those formed after the outflow channels. One scenario worth entertaining is that the lower boundary plains material, exposed along the Utopia HLB, reflects the margin of a water-rich debris ocean [8] that later underwent melting and periglacial reworking to form the VBF.

Potential geothermal modifications include (1) backwasting of the HLB, (2) ground-water discharges perhaps accompanied by ground ice melting in regions surrounding the Elysium and Tharsis rises to form collapse structures and outflow channels, and (3) subpolar plains discharges north of Alba Patera. Many of the features are hundreds of kilometers from apparent surface manifestations of volcanism, which indicates that heat may have been transferred through radiating dikes or by hydrothermal circulation of ground water along fracture systems radial to the Tharsis and Elysium rises.

This collective view points to stratigraphic, structural, hydrologic, climatic, and geothermal controls for the modification of the HLB during the Hesperian and Amazonian. Many of the suggested scenarios can be tested and then reworked and refined as needed by further, more detailed mapping of strata, structure, and landforms and more detailed crater counting to achieve more precise historical reconstructions.

References. [1] Smith D.E. et al. (1999) *Science* 284, 1495. [2] Tanaka K.L. et al. (2003) *JGR* 108, 8043. [3] Skinner J.A. Jr. et al. (2004) this volume. [4] Tanaka K.L. et al. (2003) *JGR* 108, 8079. [5] Rodriguez J.A.P. et al. (2003) *GRL* 30, 1304. [6] Rodriguez J.A.P. et al. (2004) *LPSC XXXV*, #1792. [7] Scott D.H. et al. (1986-87) *USGS Maps I-1802A-C*. [8] Tanaka K.L. et al. (2001) *Geology* 27, 427. [9] Fishbaugh K.E. and Head J.W. III (2000) *JGR* 105, 22,455. [10] Baker V.R. et al. (1991) *Nature* 352, 589. [11] Parker T.J. et al. (1989) *Icarus* 82, 111.

LONG WAVELENGTH TOPOGRAPHY OF THE DICHOTOMY BOUNDARY IN NORTHERN TERRA CIMMERIA: EVIDENCE FOR FLEXURE OF THE SOUTHERN HIGHLANDS

T. R. Watters¹, P. J. McGovern² and R. P. Irwin¹, ¹Center for Earth and Planetary Studies, National Air and Space Museum, Smithsonian Institution, Washington, D.C. 20560 (twatters@nasm.si.edu); ²Lunar and Planetary Institute, 3600 Bay Area Blvd., Houston TX 77058.

Introduction: In the eastern hemisphere of Mars, the dichotomy boundary is expressed by a significant change in elevation (>2 km) (Fig 1). The dichotomy boundary in this hemisphere is also marked by tectonic features [1]. Fault-controlled fretted valleys or extensional troughs are found in the lowlands [2] and lobate scarp thrust faults are found in the adjacent highlands [3]. Extensional and compressional deformation along the dichotomy boundary appears to have occurred during the late Noachian to early Hesperian [2, 4]. This suggests that tectonism played a role in shaping the present-day dichotomy boundary in the eastern hemisphere. The population of ancient buried impact basins in the northern lowlands suggests that the lowlands crust and the crustal dichotomy formed in the early Noachian [5]. A number of lines of evidence suggest that the slopes of the ancient dichotomy boundary are still preserved [6]. Thus, the present-day boundary in the eastern hemisphere may be the result of late Noachian-early Hesperian tectonic modification of the ancient highlands-lowlands crustal boundary.

Long Wavelength Topography: The long wavelength topography along the length of a ~2100 km section of the dichotomy boundary in northern Terra Cimmeria has been examined (Fig. 1). This study area includes the ~200 km long section of the boundary initially studied by Watters [1]. We find that the dichotomy boundary along much of its length consists of an arching ramp flanked by a broad rise. Topographic profiles across the boundary show that the broad rise is followed by a relatively steep ramp that slopes downward into the lowlands (Fig. 2). Slopes reach a maximum on the ramp and the scarp that marks the dichotomy boundary and are gently sloping away from the boundary on the back rise.

Flexure Model: Lithospheric flexure results in long wavelength topography with a distinct deflection profile. The downward deflection of the lithosphere is accompanied by a flanking upwarp or bulge [see 7, 8]. This deflection profile is very similar to profiles of the dichotomy boundary in northern Terra Cimmeria. We model lithospheric flexure of an elastic plate overlying an incompressible fluid subjected to an end load and a bending moment [1]. The model universal flexure profile is valid for any two-dimensional elastic flexure of a semi-infinite lithosphere under an end load [7]. The height of the bulge or rise w_b and the half-width of the rise $x_b - x_0$ can be directly measured from topographic profiles. The flexural parameter is

related to the half-width of the rise by $x_b - x_0 = (\lambda/4)$ [7]. Two well-preserved areas of the dichotomy boundary in northern Terra Cimmeria have been modeled. The topography of the dichotomy boundary in western Terra Cimmeria (Fig. 1) is best fit by $x_b - x_0 = 120$ km and $w_b = 600$ m (Fig. 3) [1]. The long wavelength topography of the boundary in eastern Terra Cimmeria is very similar. Here a good fit is obtained by $x_b - x_0 = 120$ km and $w_b = 350$ m (Fig. 4). The model fits correspond to an elastic thickness of ~30 km, assuming the mean density of the highland of $2900 \text{ kg}\cdot\text{m}^{-3}$, a density of the martian mantle of $3400 \text{ kg}\cdot\text{m}^{-3}$ and a Young's modulus of the lithosphere of $E = 100$ GPa. Flexure of the highlands may be the result of late Noachian-early Hesperian vertical loading from the emplacement of volcanic material in the northern lowlands [1].

Broken or Continuous Lithosphere: The shape of the deflection of the highlands may provide insight into the nature of the transition between the elastic lithosphere of highlands and lowlands (i.e., broken or continuous). This may have important implications for the origin of the crustal dichotomy. The most pronounced difference between the deflection of a continuous or infinite elastic plate and a broken or semi-infinite plate supporting a line load is in the height of the bulge w_b . For a given load, w_b for a broken plate is greater than that of a continuous plate (Fig. 5) [see 7, 8]. The slope of the downward deflection or ramp is also less for the continuous plate (Fig. 5). The good fits obtained for the profiles of the dichotomy boundary (Fig. 3, 4) favor a broken or weak contact between the highlands and lowlands lithosphere. A discontinuous lithosphere could have been formed in an early stage of plate tectonics [9], making the dichotomy boundary in the eastern hemisphere analogous to a terrestrial passive margin [1]. However, a continuous highlands-lowlands lithosphere can not be ruled out. Finite element modeling that accounts for the crustal and mantle structure in the area of the dichotomy boundary shows that it may be possible to explain the long wavelength topography and the height of the bulge with a continuous lithosphere [10].

References: [1] Watters T.R. (2003a) *Geology*, 31, 271-274. [2] McGill G.E. and Dimitriou A.M. (1990) *J. Geophys. Res.*, 95, 12595-12605. [3] Watters T.R. (2003b) *J. Geophys. Res.*, 108, doi: 10.1029/2002JE001934. [4] Watters T.R. and Robinson M.S. (1999) *J. Geophys. Res.*, 104, 18981-

18990. [5] Frey H.V. et al. (2002) *Geophys. Res. Letts.*, 29, 22-1—22-4. [6] Irwin R.P. and Watters T.R., this volume. [7] Turcotte D.L. and Schubert G. (2002) Cambridge Univ. Press, Cambridge. [8] Watts A.B. (2001) Cambridge Univ. Press, Cambridge. [9] Lenardic A., Nimmo F. and Moresi L. (2004) *J. Geophys. Res.*, 109, doi: 10.1029/2003JE002172. [10] McGovern P.J. and Watters T.R., this volume.

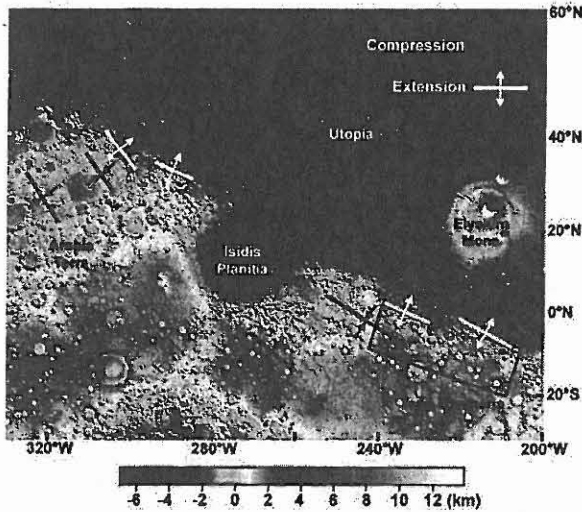


Figure 1. Location of extensional (troughs) and compressional (lobate scarps) tectonic features along dichotomy boundary in the eastern hemisphere overlaid on a color-coded digital elevation model (DEM) combined with a shaded-relief map derived from MOLA $1/32$ degree per pixel resolution gridded data. Black box shows the approximate location of the study area in northern Terra Cimmeria.

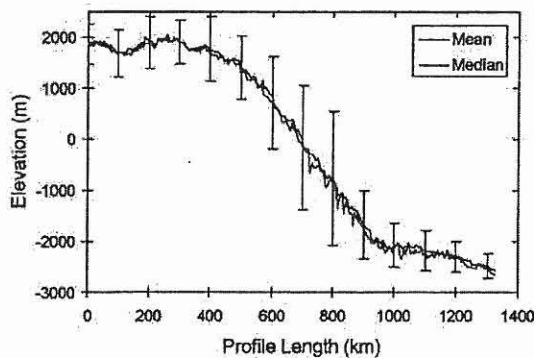


Figure 2. Long wavelength topography of the dichotomy boundary in northern Terra Cimmeria. Topographic profiles are the mean and median of 41 profiles spaced at approximately 50 km intervals covering the area of the boundary shown in Fig. 1. The error bars are 1 standard deviation. Vertical exaggeration is $\sim 160:1$.

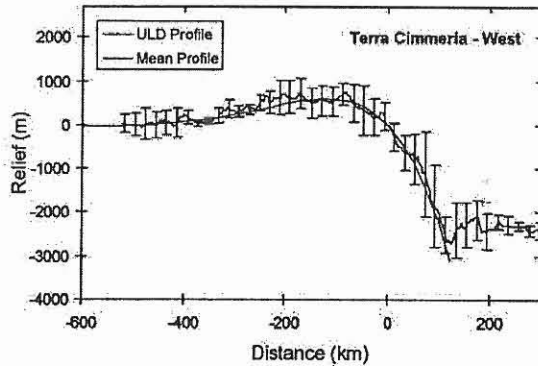


Figure 3. Topographic profile across dichotomy boundary in western Terra Cimmeria compared to a universal lithospheric deflection (ULD) profile. Topographic profile (blue curve) is the mean of the 7 profiles with ± 1 standard deviation error bars. ULD profile (red curve) was obtained for $x_b - x_0 = 120$ km and $w_b = 600$ m. Vertical exaggeration is $\sim 85:1$.

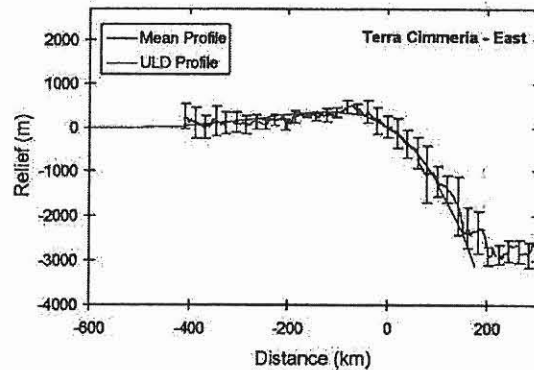


Figure 4. Topographic profile across dichotomy boundary in eastern Terra Cimmeria compared to a ULD profile. Topographic profile (blue curve) is the mean of the 4 profiles with ± 1 standard deviation error bars. ULD profile (red curve) was obtained for $x_b - x_0 = 120$ km and $w_b = 350$ m. Vertical exaggeration is $\sim 85:1$.

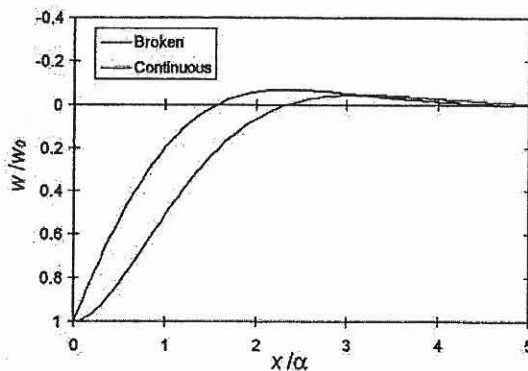


Figure 5. The deflection of a continuous and broken elastic lithosphere under load. The x-axis is the ratio of the deflection w to the maximum amplitude of the deflection w_0 and α is the flexural parameter.

EFFECT OF THE DICHOTOMY ON MANTLE PLUME LOCATIONS M. J. Wenzel¹, M. Manga², and A. M. Jellinek³, ¹Department of Earth and Planetary Science, University of California, Berkeley, CA 94720; mjwenzel@seismo.berkeley.edu, ²Department of Earth and Planetary Science, University of California, Berkeley, CA 94720; manga@seismo.berkeley.edu, ³Department of Physics, University of Toronto, Toronto, Canada; markj@physics.utoronto.ca

Introduction: Martian crustal thickness is dichotomous [1]. As the crust is expected to be enriched in heat-producing elements, the temperature at the base of the thicker crust of the southern highlands will be higher than at the base of the northern lowlands. This is analogous to an insulating lid on part of the mantle. It is also possible the martian mantle is compositionally layered [2]. These two effects strongly influence mantle dynamics, including the location and longevity of upwelling plumes [3]. We perform a series of analogue laboratory experiments to examine these effects.

Experimental methods: We perform the experiments in a glass-walled, aluminum-floored tank of aspect ratio ~ 4 . The top boundary condition is set to be at a constant temperature by an inset glass tank, filled with well-stirred ice water. To simulate the thicker highland crust, for some experiments 60% of the floor of the inset tank is covered with a 1.27-cm thick acrylic insulating lid. The effective thermal conductivity of the insulated side is $\sim 40\%$ of that of the side with no insulating lid, equivalent to a crust about twice as thick under the southern highlands [1]. Working fluids are aqueous corn syrup solutions with highly temperature-dependent viscosity, with food dye added to the lower layer. Two opposite sides of the tank are insulated with 5.1-cm-thick polystyrene foam blocks. The two remaining sides are left open so that we can photograph and videotape the experiment. The experiments take one of two forms: (1) bottom heating and top cooling, or (2) secular cooling simulating internal heating. In the experiments with bottom heating, the fluids and the tank are initially at room temperature; the base of the tank is a hollow aluminum heat exchanger, through which hot water is pumped. In contrast, in the experiments with secular cooling the tank base is insulated. The fluids and the tank base are separately warmed and the fluids are then poured into the tank. We then bring the ice bath into contact with the top of the fluid, which results in thermal convection. The system cools over time as heat is lost to the ice bath. We quantify heat transfer during convection with timeseries of temperature and heat flux, measured with thermocouples and heat flux sensors on the tank roof and floor and thermocouple probes within the convecting interior.

Results: In the case with no insulating lid, the plume spacing is predicted from linear stability theory to be $L = C(\nu/\alpha)^{1/3}$, where C is a constant, ν is the ratio of viscosity in the fluid interior to that in the thermal boundary layer, and Ra is the Rayleigh number (e.g., [4]). The number of plumes (n) in the convecting layer is a proxy for the spacing: $L \sim n^{-1/2}$. The prediction then is that $n \sim Ra^{2/3}$. We count the number of plumes visible in the shadowgraph videos and plot n as a function of Ra in Figure 1. The flow is transient by the nature of the secular cooling experiments, and scatter is greatest at earlier times (high Ra). Nevertheless, a clear trend is defined, with a slope in $\log(Ra)$ - $\log(n)$ space of 3, not 1.5 as predicted by theory. One effect of compositional layering is that the topography on the interface stabilizes the locations of upwelling plumes. We argue that the presence of compositional layering slows the reorganization of flow that accompanies a decrease in Ra . The result is that the number of plumes is higher than would otherwise be predicted at a given point in the planet's evolution.

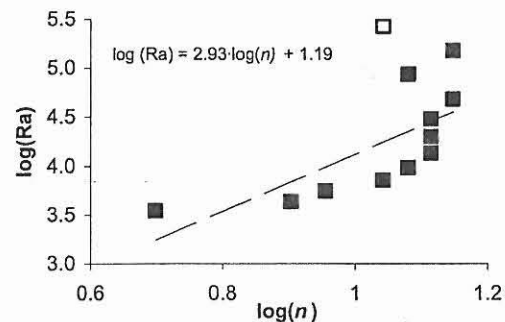


Figure 1: $\log(Ra)$ v. $\log(n)$. Best-fit line excludes first point (open symbol). Slope of ~ 3 is different from predicted slope of 1.5.

In the case with both an insulating lid and layered convection, a strong hot upwelling forms under the lid and persists for the equivalent of many billions of years [3]. If the mantle upwelling leads to melting, volcanic material will be emplaced as crust over the upwelling. The thickening of the crust will reinforce the difference in insulation that localizes the upwell-

ing—that is, there is a positive feedback between crustal thickness and mantle upwelling.

References: [1] Zuber M. T. et al. (2000) *Science*, 287, 1788-1793. [2] Elkins-Tanton, L. T. et al. (2003) *Meteoritics and Planet Sci.*, 38, 1753-1772. [3] Wenzel, M. J. et al. (2004) *GRL*, 31, L04702. [4] Jellinek, A. M., and Manga, M., *Rev. Geophys.*, in press.

On The Dynamic Origin Of The Crustal Dichotomy and Its Implications For Early Mars Evolution. Shijie Zhong, James H. Roberts and Allen McNamara, Department of Physics, University of Colorado, Boulder, Colorado 80309, USA (szhong@anquetil.colorado.edu).

Introduction: The crustal dichotomy and Tharsis Rise are the most important large-scale tectonic features on the Martian surface [1]. An understanding of their formation has important implications for understanding thermal evolution of Mars and the Martian gravity anomalies, tectonics, volcanism, and volatiles losing history [2,3]. Both endogenic and exogenic processes were proposed for the formation of the crustal dichotomy. In this study, we focus on endogenic processes. Two different endogenic processes were proposed: crustal erosion derived from degree-1 mantle convection [4] and plate tectonics [5], both proposed before the MGS missions.

With the MGS high resolution data, there are a number of studies on the nature of Martian crust, crustal dichotomy and Tharsis rise that should be considered in any attempts to unravel the formation of crustal dichotomy and the evolution of early Mars. 1) The discovery of abundant buried ancient impact craters in the northern plains indicates that the crust of the northern hemisphere is of the middle Noachian or as old as that of the southern hemisphere, if not older [6]. 2) The topography and gravity anomalies suggest a pole-to-pole gradual and smooth variation of crustal thickness [7]. 3) The topography and gravity anomalies suggest that Martian crust is on average >50 km thick and is thicker than the elastic plate (or the layer that is capable of supporting long-term geological loads) [7,8]. Not only the surface but also the bulk of the crust may have been produced quite early on (in the first 0.5 Ga), according to the thermal evolution modeling [9]. 4) Significant tectonic deformation occurred along the crustal dichotomy in late Noachian and early Hesperian [10]. 5) The surface tectonics suggest that the bulk of the Tharsis rise was formed by the late Noachian [11,4], similar to the formation time of crustal dichotomy. Modeling the Tharsis topography and gravity indicates that the Tharsis rise is mostly supported by surface loads on elastic plate with little or no dynamic contribution from a plume [12].

Among the two proposed endogenic processes (i.e., crustal erosion and plate tectonics) for crustal dichotomy formation, a necessary process is the degree-1 mantle convection in which hot upwellings preferentially occurs in one hemisphere while cold downwellings are in other hemisphere. Such a degree-1 mantle convection is also required for a plate tectonic process to explain the formation of crustal dichotomy, although this was never explicitly stated before (why does it occur only in the northern hemisphere?). However, the physical conditions under which mantle convection forms degree-1 structure are not well understood [13,14,15]. Furthermore, even if degree-1 mantle convection is achieved, it is unclear how degree-1 mantle convection could lead to crustal dichotomy and how crustal dichotomy

could be preserved through the Martian geological history [15]. In addition to crustal dichotomy, the formation of the Tharsis rise also needs a largely degree-1 mantle convection or a one-plume convection that operated during late Noachian period, following the formation of crustal dichotomy [12]. Although the Tharsis rise is centered at the dichotomy boundary not below either of the hemispheres, the similarity in mantle dynamics is intriguing.

There are two goals of this study: 1) to critically review all the published mantle dynamic models for degree-1 mantle convection and to explore new and more realistic mantle parameter space for degree-1 mantle convection; 2) to synthesize surface observations and mantle dynamic models for a coherent picture for the early evolution of Mars.

Degree-1 mantle convection: Two different mechanisms have been proposed for degree-1 or one-plume mantle convection for Mars: 1) one-plume convection derived from exothermic or endothermic phase changes that was initially proposed for a dynamic support for the Tharsis rise [13,14], and 2) degree-1 convection caused by layered viscosity proposed to explain the formation of crustal dichotomy [15].

The effects of exothermic phase change on one-plume convection [14] were questioned in [16] that showed that the actual effects seen in [14] are caused by the moderately high viscosity lithosphere. There are two potential problems with the endothermic phase change models: 1) existence of such an endothermic phase change given the recent estimate of core size [17], and 2) the published models with phase changes were done with only moderate depth-dependent viscosity and no temperature-dependence. Our calculations with the endothermic phase change, while reproducing one-plume structure with no temperature-dependent viscosity, fail to produce one-plume structure with more realistic temperature-dependent viscosity [18]. The models with layered viscosity structure that produced degree-1 convection used a temperature- and pressure-dependent viscosity, but the models were done in 2-D axisymmetric models [15]. It is important to examine the effects of 3-D geometry on the flow.

We have recently explored the layered viscosity models in 3D spherical geometry with temperature- and pressure-dependent viscosity and pressure-dependent thermal expansion coefficient and thermal diffusivity [18]. Our calculations showed that degree-1 convection remains with 3D layered viscosity models. However, it appears that a smoothly varying viscosity with depth is not as effective as a step function like increase of viscosity in producing degree-1 convection. This suggests that either non-Newtonian viscosity or viscosity change caused by the olivine-spinel phase change may be essential.

Two end-member models for Martian mantle convection are the stagnant-lid convection and plate-tectonic style convection [5,19]. However, while the evidence for early plate tectonic process on Mars is still elusive, the application of stagnant-lid convection may also be problematic. It is well known that stagnant-lid convection in its original form often leads to small-wavelength structures [20], which is in sharp contrast with crustal dichotomy and Tharsis rise that are both of very long wavelength. We propose that for early Mars the crust may play an active role in controlling heat transfer and mantle structure, if the crust was indeed >50 km thick. The key components of our proposal are that the lower crust for early Mars may be sufficiently weak to serve effectively as free-slip boundary condition for the mantle and that the thickened crust increases the mantle lithospheric temperature so that the mantle lithosphere may be able to deform. The net effect for mantle convection is that mantle lithosphere may be mobile with only moderate viscosity contrast with respect to the underlying asthenosphere. In this scenario, the crust may be the limiting factor for heat transfer. If the lower crust is sufficiently weak that convection can take place there (i.e., crust convection), then crust may transfer heat efficiently out of the mantle. If crust convection cannot happen, then heat has to transfer conductively through the crust.

We have computed 3D spherical models with free-slip top boundary and moderate temperature-dependent viscosity that approximate the effects of the crust. We found that degree-1 convection may be produced within certain model parameter space. In particular, when large internal heating is included, the lithospheric viscosity becomes sufficiently large compared with the interior viscosity and degree-1 convection is achieved.

Degree-1 mantle convection and crustal dichotomy and Tharsis rise: Two possible scenarios were proposed in [15] to link degree-1 mantle convection and crustal dichotomy. 1) The southern hemisphere with thickened crust was formed above the upwellings of degree-1 convection due to melting and the significant fraction of the crust was created during the formation of the dichotomy. 2) The southern hemisphere was formed above the downwellings of degree-1 convection due to shear coupling between the mantle and crust that produces crustal convergence towards the southern hemisphere, and the bulk of the crust may be produced uniformly before degree-1 mantle convection occurs. The first scenario may imply that the southern hemisphere with newly produced crust is younger than the northern hemisphere. That this scenario permits an old northern hemisphere is consistent with the old crust age as suggested in [6]. The second scenario implies that the northern hemisphere is younger (but not much younger) than the southern hemisphere, as the crustal thinning there would lead to some amount of volcanisms in the northern hemisphere. Therefore, it seems that the relative ages of the two hemispheres are important in distinguishing these two scenarios.

With either scenario, as long as the degree-1 mantle convection is active for sufficiently long time, to maintain crustal dichotomy does not seem to be a problem. This is because mantle convection can have significant effects on crustal relaxation.

Finally, given the relatively short time span between the formation of crustal dichotomy and Tharsis rise and the fact that they both should be related to degree-1 mantle convection, it is interesting to consider how degree-1 mantle convection may shift its centers. We will speculate the role of melting in degree-1 mantle convection.

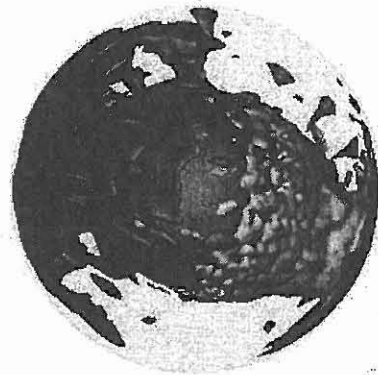


Figure 1. Degree-1 convection from models with moderate temperature-dependent viscosity [21].

- References:** [1] Smith et al. (1999) *Science* 286, 94-97. [2] Solomon & Head (1990) *JGR* 95 11073-11083. [3] Phillips et al. (2001) *Science* 291 2587-2591. [4] McGill & Dimitriou (1990) *JGR* 95 12595-12605. [5] Sleep (1994) *JGR* 99 5639-5655. [6] Frey et al. (2002) *GRL* 29 1387. [7] Zuber et al. (2000) *Science* 287 1788-1793. [8] McGovern et al., (2002) *JGR* 107. [9] Hauck & Phillips (2002) *JGR* 107 5052. [10] Watters (2003) *Geology* 31 271-274. [11] Anderson et al. (2001) *JGR* 106 20563-20585. [12] Zhong & Roberts (2003) *EPSL* 214 1-9. [13] Harder & Christensen (1996) *Nature* 380 507-509. [14] Beruer et al. (1998) *GRL* 25 229-232. [15] Zhong & Zuber (2001) *EPSL* 189 75-84. [16] Harder (2000) *GRL* 27 304-307. [17] Yoder et al (2003) 300 299-303. [18] Roberts & Zhong, this volume. [19] Leonardic et al. (2004) *JGR* 109 E02003. [20] Ratcliff et al. (1997) *Physics D*. [21] McNamara & Zhong (2004) in preparation.

NOTES

NOTES

NOTES
